APTAMER-BASED DETECTION AND CHARACTERIZATION OF OVARIAN CANCER

By

DALIA LÓPEZ-COLÓN

A DISSERTATION PRESENTED TO THE GRADUATE SCHOOL
OF THE UNIVERSITY OF FLORIDA IN PARTIAL FULFILLMENT
OF THE REQUIREMENTS FOR THE DEGREE OF
DOCTOR OF PHILOSOPHY

UNIVERSITY OF FLORIDA

2011

To my daughter, Dalianis, my inspiration
To my mother, my pillar of strength

ACKNOWLEDGMENTS

I would like to thank my advisor, Dr. Weihong Tan of the Chemistry Department, University of Florida for his guidance and constructive comments throughout my PhD career. I would also like to especially thank Dr. Rebecca Sutphen of the College of Medicine, University of South Florida. She has been of tremendous help in my research work, as she has provided me with guidance and advice on our collaborated efforts. I am also grateful to my entire Ph.D. research committee members, including Dr. Ben Smith, Dr. Satya Narayan, Dr. Gail Fanucci and Dr. Nicole Horenstein for their support and constructive comments that have helped me to refine this dissertation.

I thank the support staff at the Department of Chemistry, University of Florida, for their silent contribution during my research work. My special thanks go to Ms. Lori Clark, Dr. Kathryn Williams and the staff at the editorial office and ETD office for their continuing help with numerous tasks during the preparation and submission of this dissertation.

During all this years, the Tan group has been like a family away from home. Both old and new members have contributed greatly to my academic advancement. I would like to thank Dr. Karen Millians and Dr. MariCarmen Estevez for their unconditional help, their friendship and support during the early stages of my graduate studies. I am also grateful to Elizabeth Jimenez, Dimitri Van Simaeys, Basri Gulbakan and Meghan O'Donoghue for their continuous friendship and support. Special thanks must be given to the most extraordinary member of the Tan group, Dr. Kwame Sefah, as he has not only trained and guided me throughout my PhD career, but has also been a true friend throughout all these years. I am equally thankful to the entire Tan group members for their friendship, support and encouragement throughout the years.

I thank my friends outside the Tan lab for their friendship and support. To my puertorrican friends, Emelyn Cordones, Sheila Sanchez, Jose Valle, Mariselis Luna, Evelyn Lopez and Rafael Ruiz, thank you so much for your honest friendship and support. To my Zumba ® friends, Madel Sotomayor, Sandy Highsmith, Michelle Lucas, Mimi Zarate, Marisol, Cecilia Mejias, Nicole Alibrandi, Eric Ocane and Enrico Eastmond, for their unconditional friendship. You all made my life brighter and my problems insignificant. I feel very blessed to have you in my life.

I would like to give special thanks to my family for their unconditional support throughout my PhD career. I thank my parents for, without them, I would not be here. Thank you for believing in me, and for supporting me. I thank my cousin, Evelyn Navarro Colon, for her support and friendship during one of the hardest parts of my life. I thank my cousin, Evelyn Lebrón, for her friendship, and her advice during many difficult moments. I also thank my aunts, Magali Estrada and Gloria Lopez, for your unconditional support. Finally, I thank the rest of my family, as, one way or another, each one has helped me throughout my Ph.D. career.

Last but not least, I thank God for putting on my path so many wonderful persons. I have been blessed by having so many great friends and a supportive family. I thank God for giving me the strength to continue on my path even when I encountered moments of adversity.

TABLE OF CONTENTS

page

LIST OF TABLES

LIST OF FIGURES

LIST OF ABBREVIATIONS

2D-PAGE	two-dimensional polyacrylamide gel electrophoresis
CA125	carbohydrate antigen 125
BRCA	breast cancer gene
CD	cluster of differentiation
CTC	circulating tumor cell
Cy5	cyanine derivative 5
Cy5.5	cyanine derivative 5.5
DNA	deoxyribonucleic acid
dNTP	deoxyribonucleotide triphosphate
DPBS	Dulbecco's phosphate buffered saline
EPCAM	epithelial cell adhesion molecule
FBS	fetal bovine serum
FITC	fluorescein isothiocyanate
FL1	channel one on the flow cytometer, emission of 525nm (FITC)
FL4	channel three on the flow cytometer, emission >610 (PE)
FSC	Forward Scatter
HBOC	Hereditary Breast-Ovarian cancer syndrome
HNPCC	Hereditary nonpolyposis colon cancer
HPLC	high-performance liquid chromatography
IC50	half maximal inhibitory concentration
IDT	Integrated DNA Technologies
MRI	magnetic resonance imaging
mRNA	messenger ribonucleic acid
MS	mass spectrometry

NP	Nanoparticle
Nucleotide	nt
PAGE	polyacrylamide gel electrophoresis
PBS	Phosphate buffer solution
PCR	polymerase chain reaction
QD	quantum dot
RNA	ribonucleic acid
SELDI-TOF	surface-enhanced laser desorption/ionization time-of-flight
SELEX	systematic evolution of ligands by exponential enrichment
siRNA	small interfering RNA
SSC	Side Scatter
ssDNA	single stranded deoxyribonucleic acid
TVS	Transvaginal ultrasound

Abstract of Dissertation Presented to the Graduate School
of the University of Florida in Partial Fulfillment of the
Requirements for the Degree of Doctor of Philosophy

APTAMER-BASED DETECTION AND CHARACTERIZATION OF OVARIAN CANCER

By

Dalia Lopez Colon

August 2011

Chair: Weihong Tan
Major: Chemistry

Whereas ovarian cancer presents only 3% of the new cases of cancer in women, it is the 5th deadliest malignancy overall in the United States. Due to a lack of effective methods to screen for ovarian cancer, 75% to 80% of ovarian cancers are diagnose in stage III or stage IV. At these stages, the 5-year survival is only 15-20% as compared to an 80-90% survival rate for ovarian cancer diagnosed at early stages of the disease. Therefore, detection of the ovarian cancer tumor at an early stage will improve the outcome for ovarian cancer patients. For this purpose, we selected a panel of aptamers for the detection and characterization of ovarian cancer.

Aptamers are single-stranded nucleic acids (DNA or RNA) capable of recognizing a specific target with high affinity and specificity. Aptamers are selected from a random pool containing about 10^{15} distinct sequences. During the selection process, unbound sequences are washed away, while sequences binding to the target are eluted, PCR amplified and used for subsequent rounds of selection. This cycle is repeated until the pool has been fully enriched for the target. The enriched pool is then sequenced and potential aptamer sequences are identified by looking at sequence homology.

In this work, we have identified six aptamer sequences capable of binding to the epithelial ovarian adenocarcinoma cell line CAOV3. From these sequences, DOV-2a, DOV-3, DOV-4 and DOV-6a were further characterized. These aptamers showed binding affinities between 30-130 nM. Furthermore, the aptamers specificity was tested with other cancer cell lines. DOV-4 showed no binding to normal immortalized lung epithelial cells, while DOV-2a showed no binding to the ovarian benign cysts cell line. The selected ovarian cancer aptamers were further characterized to identify the target in the cell membrane. The aptamer binding was assayed after trypsin, proteinase K and glycosidase treatment. Finally, the aptamers were used to develop an ovarian cancer detection assay using whole blood. The assay developed allows the detection of 500 ovarian cancer cells spiked in 1 mL of whole blood with little pretreatment of the blood sample.

CHAPTER 1
BACKGROUND AND SIGNIFICANCE

Ovarian Cancer

Ovarian cancer is a malignancy in which normal ovarian cells begin to grow in an uncontrolled, abnormal manner and produce tumors in one or both ovaries. It is considered a disease of postmenopausal women, as the peak age of development of ovarian cancer is between the ages of 75-79. Tumors can develop from germ cells, stromal cells or the connective tissue within the ovaries that generate reproductive hormones, as well as from the epithelia ovarian lining. Epithelial ovarian cancers are the most common type of ovarian malignancies, accounting for more than 80% of the ovarian cancer (*1*).

Ovarian cancer is the fifth most common cause of cancer-related death in women, and it is the most lethal gynecologic malignancy (*2*). This disease is characterized by few early symptoms, typical presentation at an advanced stage and poor survival statistics. According to the American Cancer Society, there were an estimated 21,880 newly diagnosed cases of ovarian cancer and 13,850 deaths in 2010 (Figure 1-1) (*3*). This dismal outcome is due, in part, to the inability to detect ovarian cancer at an early, curable stage. More than two-thirds of patients with ovarian cancer have widespread metastatic disease at initial diagnosis, with a 5-year survival rate of 15-20%. Conversely, at early stages, the long-term survival rate is approximately 90% (*4-7*). These statistics provide a compelling basis for development of an effective early detection strategy.

There is currently no effective screening strategy for ovarian cancer. The only currently used clinical biomarkers, CA125 (*8-10*) and the recently marketed Ova1 test

(*11*, *12*) are not used for general population screening, but only as adjunct tests at the time of clinical symptoms or diagnostic work-up of a pelvic mass. Unfortunately, not only is it currently impossible to reliably detect ovarian cancer early, it is not even possible to accurately diagnose it. Even among women presenting with clinical symptoms suggesting the possibility of ovarian cancer, using all available biomarker and imaging tools, it is currently not possible to accurately distinguish women with ovarian cancer from those who do not. Thus, a staggering 80% of women who undergo surgery for suspected ovarian cancer do not, in fact, have cancer, but benign disease that could be managed far less invasively, avoiding significant anxiety, distress, morbidity and associated costs (*11*,*12*). This is an issue of major public health impact, given that the American College of Obstetrics and Gynecology estimates that 5-10% of all women in the U.S. will undergo such surgery during their lifetime (*13*).

Causes of Ovarian Cancer

The molecular events responsible for the initiation and propagation of ovarian cancer are still unknown. Nonetheless, several theories have been postulated as an attempt to explain the physiological processes that give rise to the malignant transformations leading to ovarian cancer. The most accepted theory is the Incessant Ovulation Theory (*14*). This theory suggests that the ovarian surface epithelium undergoes malignant transformations due to continuous ovulation and repair. During her lifetime, a woman’s ovarian epithelium undergoes recurrent trauma as monthly ovulations break the ovarian surface to release an ovule. As the ovarian surface is ruptured, ovarian epithelial cells undergo rapid proliferation to repair the damage. With each, menstrual cycle, the possibility of having mutations accumulate due to errors during the repair process increases, thus leading to an increased risk of ovarian cancer

with age (i.e. the risk of ovarian cancer is a function of the total number of ovulatory cycles). This theory is supported by the observation that reduction of ovulation cycles by pregnancy, lactation and use of birth control reduces the risk of ovarian cancer.(*15*)

The second theory postulated to explain the initiation of ovarian cancer is the Pituitary Gonadotropin Hypothesis. This theory postulates that the ovarian epithelium is stimulated by high levels of follicle-stimulating hormone (FSH) or leutenizing hormone (LH) to proliferate in excess, leading to accumulation of deleterious mutations and to eventual malignant transformation. Both hormones are known to result in the production of estrogen, which stimulates the ovarian epithelium to form inclusion cysts. Furthermore, FSH is known to activate many oncogenes. This theory is also supported by the observation that reduction of ovulation cycles by pregnancy, lactation and use of birth control reduces the risk of ovarian cancer, as well as the observation that infertility and polycystic ovarian syndrome increase the risk of ovarian cancer, while it decreases with the use of progesterone-only birth control (*4*).

Risks of Ovarian Cancer

As mentioned above, the molecular events that give rise to the malignant transformation of the ovarian surface epithelial cells are unknown. Yet, several risk factors have been associated with epithelial ovarian cancer (*15*). Some of the risk factors are:

- Nulliparity
- Early menarche
- Late menopause
- Increasing age
- Family history
- Personal history of breast cancer
- Ethnic background

Women having a larger number of menstrual cycles (ovulation) seem to be at higher risk of ovarian cancer. Thereof, nulliparity (not having conceived), early menarche, late menopause and increasing age are considered risk factors of ovarian cancer (*16*). Woman who have not given birth are at double risk of developing ovarian cancer. The protective effect of pregnancy increases with the number of births. This effect is hypothesized to be caused by a reduction in the number of ovulations. It has also been hypothesized that malignant cells are shed during pregnancy. Ethnic background and race also play a role in ovarian cancer. Although the reason why different races present different risk of ovarian cancer are unknown, it has been observed that white women have the highest incidence of ovarian cancer, while black and Hispanic women have the lowest risk. Inherited germline mutations, genetic predisposition and personal history of breast cancer also increase the risk of ovarian cancer. Inherited germline mutations are the most important and best understood risk factor for ovarian cancer, as risk of ovarian cancer increases from 1.4% in the normal population to 15-60% on woman having a family history of ovarian cancer. These factors will be discussed individually in the following sections (*5*, *17*).

Hereditary Breast-Ovarian Cancer syndrome (HBOC): Breast Cancer gene (BRCA) mutations

Hereditary genetic disorders account for about 10% of all ovarian cancer cases. The most common genetic disorder in ovarian cancer is the Hereditary Breast-Ovarian cancer syndrome, which is characterized by BRCA1 and BRCA2 mutations, accounting for 90% of all cases of hereditary ovarian cancer. Mutations on the BRCA genes increase the risk of ovarian cancer to 60-70% (*18*). BRCA1 and BRCA2 are involved in signaling of DNA damage, activation of DNA repair, induction of apoptosis and cell cycle

checkpoints (*19*). Thus, cells having aberrant or non-functional BRCA have increased aneuploidy (abnormal chromosome number), centrosome amplification and chromosomal aberrations, making them susceptible to further mutations. The HBOC syndrome is particularly common in woman of Ashkenazi ancestry, as 35-40% carry the BRCA1 or BRCA2 mutation, as compared to a 10% occurrence on the general population (*4*, *5*).

Lynch syndrome or Hereditary Nonpolyposis Colon Cancer (HNPCC)

Patients with Lynch syndrome account for 10% of all cases of hereditary ovarian cancer (1-2% of all cases). This syndrome is characterized by defects on the mismatch-repair mechanism (mutations on repair genes such as MSH2, MSH6 and MLH1), thus resulting in genetic instability and susceptibility to accumulate multiple mutations, which can lead to malignant transformation of the cell (*4*).

Ovarian Cancer Subtypes

Ovarian cancer is a very heterogeneous disease. In general, ovarian cancer tumors can originate from three different cell types: Germ cells (5-10%), stromal cells or the connective tissue within the ovaries that generate reproductive hormones (10-15%) and the epithelial ovarian lining (>80%). Most ovarian cancer patients present cancer of epithelial origin; therefore, this introduction will focus on epithelial ovarian cancers and its subtypes. Epithelial ovarian cancer is divided into several subtypes: serous, mucinous, endometrioid, clear cell carcinoma, squamous cells, mixed epithelial tumors, Brenner tumors- transitional cell-, undifferentiated carcinomas and unclassified tumors (*1*, *4*, *5*). Figure 1-2 shows the four major histologic subtypes for epithelial ovarian carcinoma: serous, endometrioid, mucinous and clear cell (*7*). Although, these subtypes derive from the same cell type, poorly developed differentiated mesothelial cells forming

the ovarian surface epithelium, they resemble tissues from the female reproductive track in morphology. For instance, serous carcinomas resemble cells from the fallopian tube epithelium, while endometrioid carcinomas resemble endometrial glands. Each tumor subtype is further classified as benign, malignant or borderline; and described as low- or high-grade malignancy. Research based on genetic and biomarker profiling of ovarian cancer, as well as mRNA expression, has shown that each subtype has a unique molecular signature (*20*, *21*). This indicates that each ovarian cancer subtype represents a distinct disease and should be treated as such in the context of detection, treatment and prognosis. Therefore, proper histological classification is highly important as each subtype has a different behavior and response to therapy.

Staging and Treatment

Ovarian cancer staging involves the determination of the degree of disease spread on the patient. Most ovarian cancers are staged at the time of surgery (Laparotomy), when tissue samples are obtained from different parts of the pelvis and abdomen for diagnosis and staging (*5*, *22*). Exploratory laparotomy's goal is to assess the tumor histology and staging, as well as complete or partial tumor removal (cytoreduction). Also, during the exploratory laparotomy, biopsies of at-risk tissues are taken (systematic sampling) to ensure metastasis has not occurred. Staging is imperative as ovarian cancers have a different prognosis at different stages and require a different treatment. The accuracy of the staging may determine the survival of the patient (*4*).

As shown on Figure 1-3, ovarian cancer is divided into four stages depending on how far has the cancer spread beyond the ovary. During the first stage of disease, the cancer is limited to one or both ovaries (Figure 1-3 A). Patients with stage 1 ovarian cancer undergo total abdominal hysterectomy (removal of the uterus) and bilateral

salpingo-oophorectomy (removal of both ovaries and the fallopian tubes), omentectomy (removal of the omenetum or abdominal lining), with tumor removal as initial therapy. A biopsy of lymph nodes and other tissues in the pelvis and abdomen is performed to ensure the disease has not spread. When ovarian cancer presents in young women, hysterectomy is avoided. Also, if the disease is confined to one ovary, the patient undergoes unilateral salpingo-oophorectomy (removal of the affected ovary and fallopian tube), leaving the healthy ovary intact. In all cases, the tumor is classified into the corresponding histological subtype, and classified as low grade or high grade. Patients with low-grade ovarian cancer do not undergo any further treatment, but remain under observation. If the tumor is high grade, the patient may receive combination chemotherapy (i.e. intravenous chemotherapy with carboplatin plus taxane).

During stage two, the cancer has spread into the pelvic region (fallopian tubes, uterus), but has not yet reached the abdominal organs (Figure 1-3B). Patients diagnosed with stage 2 ovarian cancer undergo hysterectomy and BSO with removal of as much of the tumor as possible. Lymph nodes and other tissues in the pelvis and abdomen that are suspected of harboring cancer are biopsied as well. After the surgical procedure, treatment may be one of the following: 1) combination chemotherapy with or without radiation therapy or 2) combination chemotherapy.

Stage 3 ovarian cancer patients present metastasis into the abdominal organs (Figure 1-3C). Treatment is the same as for Stage II ovarian cancer. Following the surgical procedure, the patient may either receive combination chemotherapy possibly followed by additional surgery to find and remove any remaining cancer.

Finally, stage four ovarian cancer presents metastasis to distant organs, including the lungs, liver and lymph nodes (Figure 1-3D). Experts agree that aggressive or radical surgery should be performed to remove as much of the tumor as possible, reaching optimum cytoreduction (no visible residual disease). After surgery, the patient is treated with combination chemotherapy (intravenous chemotherapy with carboplatin plus a taxane) (*7*).

Symptoms of Ovarian Cancer

Ovarian cancer has long been known as the silent killer, as most woman report not having symptoms during early stage ovarian cancer. Yet, ovarian cancer does present a series of nonspecific symptoms. These symptoms are typically attributed to other diseases, leading to a delay on ovarian cancer diagnosis. Ovarian cancer symptoms include (*4*, *23*):

- Bloating
- Difficulty eating or feeling full quickly
- Pelvic or abdominal pain
- Abnormal menstrual cycles
- Constipation
- Increased gas
- Indigestion
- Lack of appetite
- Nausea and vomiting
- Sense of pelvic heaviness
- Swollen abdomen or belly
- Unexplained back pain that worsens over time
- Vaginal bleeding
- Vague lower abdominal discomfort
- Weight gain or loss
- Excessive hair growth
- Increased urinary frequency or urgency

Current Detection Methods

Epithelial ovarian cancer usually presents no symptoms until the disease has spread outside the ovaries. This is largely due to the anatomical position of the ovaries deep inside the pelvis, offering little interference with nearby structures until the tumor has grown significantly or metastasis has ensued (*4*). Therefore, the need for a screening method for the early detection of ovarian cancer is imperative. To this end, many ovarian cancer biomarkers have been identified (*5*, *24*). Unfortunately, the diagnostic and prognostic tumor biomarkers in use today are not adequate in distinguish benign from malignant ovarian neoplasma. They also fail to differentiate among the various histological and clinically aggressive forms of ovarian cancer (*25*, *26*). To date, there are no screening tests for epithelial ovarian cancer available to the general population. However, women with a high risk of developing epithelial ovarian cancer are tested in two possible ways: transvaginal sonography and serum biomarker testing (*27*).

Transvaginal sonography (TVS) is a type of sonogram used to non-invasively image the ovary size and shape in detail, facilitating the detection of ovarian cancer tumors. Although the technique has a reported specificity of about 98%, it does not provide adequate sensitivity as an early detection tool as it is incapable of distinguishing cancerous from benign masses. Therefore, tumors detected using this technique need to be surgically evaluated to make the final diagnosis (*28-31*). Furthermore, TVS can only detect tumors, which cause an increase in the size of the ovary. Therefore, this technique cannot be used to identify early stage serous ovarian cancer, as this histology is characterized by rapid spread of the disease to other pelvic sites prior to ovarian enlargement. Transvaginal sonography cannot absolutely diagnose cancer.

Early detection of disease based on serum biomarker testing is ideal as it presents a non-invasive, cost effective, easily administered and non-subjective method. The most commonly used biomarker for clinical screening and prognosis in patients with ovarian cancer is ovarian cancer antigen 125 (CA-125) (*7*). CA125 is a transmembrane glycoprotein of the mucin family, which is typically elevated in epithelial ovarian cancer patients. CA-125 serum levels directly correlate with the protein production in the tumor, indicating that the tumor is undergoing active growth. Although present in the fallopian tubes, endometrium and endocervix, it is not expressed my normal ovarian epithelia. CA-125 is detected at low levels (<35 U/mL) in the serum of normal individuals, but its value is elevated in about 80% of women with advanced stage epithelial ovarian cancer. However, it is only elevated in 50% to 60% of women with stage I disease (*10*, *32*, *33*). Forty percent of patients with early-stage ovarian cancer will have a negative CA-125 test result. At the same time, CA-125 is elevated by other gynecological conditions, including pelvic inflammation, endometriosis and ovarian cysts. The high rate of false-positive results with CA-125 screening may lead to unnecessary follow-up testing and invasive procedures. Therefore, the only role f or CA-125 testing is in monitoring disease progression and recurrence and in assessing the effects of treatment for ovarian cancer. Similarly, TVS, although sometimes used for screening or early detection, is not a reliable tool for diagnosing ovarian cancer (*7*). Therefore, it is imperative to create a new and reliable screening method for the early detection of ovarian cancer.

Early Diagnosis

The potential benefits of earlier diagnosis of ovarian cancer are evident in current 5-year survival statistics: 80% to 90% for stage I tumors, 65% to 70% survival with

stage II disease, 30% to 60% for tumors diagnosed in stage III and 20% or less when diagnosed with stage IV ovarian cancer. Unfortunately, at present, 75% to 80% of ovarian cancers are detected in stage III or stage IV, and the prognosis is poor (*7*).

Experts agree that development of a targeted screening strategy for effective early detection of ovarian cancer is: 1) likely to require complementary approaches, and 2) that an efficient plan for development is to first focus on methodology to accomplish accurate diagnosis (e.g., distinguish, among women with clinically suspected ovarian cancer, between those who have it and those who do not) before applying the methods to screening (i.e., can the methods for identification of ovarian cancers associated with clinical symptoms also detect cancers before clinical symptoms develop?). This suggests development of methods that are based on: 1) inherited characteristics of disease risk that are present before development of disease, and 2) characteristics of cancer cells present at the earliest stages of disease.

Aptamers

Aptamers are probes capable of specifically binding to biomarkers expressed by targeted tumor cells, and represent a feasible alternative for ovarian cancer early detection and diagnosis. Aptamers are short single-stranded oligonucleotides (<100 bases, RNA or DNA) selected from large combinatorial pools of sequences by SELEX (Systematic Evolution of Ligands by Exponential Enrichment) for their capacity to bind to many types of different targets, ranging from small molecules to proteins or nucleic acid structures.(*34-39*) They have a definite tertiary structure that confers them the selectivity towards their target (*40-42*).

Aptamers Characteristics

Aptamers present the same high specificity and affinity for their targets as antibodies. With respect to antibodies, aptamers present several advantages for *in vivo* applications. First, aptamers do not appear to trigger an immune response, which is one of the major limitations of antibodies for *in vivo* use (*43-47*). Second, their smaller size could promote a better tissue penetration (*48-51*). Third, aptamers may be chemically synthesized for relatively low prices, allowing better batch-to-batch reproducibility and easier incorporation of chemical modifications, therefore conferring plasmatic resistance to their degradation or improved pharmacokinetic (*52-55*). Finally, aptamers are easily developed in a short time as compared to antibodies. Also, multiple aptamers against the different targets in the cell membrane may be developed at the same time. This is a very important advantage as using multiple aptamers for the detection of a certain type of cell may decrease the false positive and false negative results. Many aptamers are now being developed against biomedical relevant extracellular targets, such as membrane receptor proteins, hormones, neuropeptides and coagulation factors (*56*, *57*). Furthermore, one aptamer has recently been approved by the FDA and several more are now in clinical trials (*58-62*).

Systematic Evolution of Ligands by EXponential Enrichment (SELEX)

Aptamers are selected from a random library of about 10^{15} different sequences by the Systematic Evolution of Ligands by EXponential enrichment (SELEX). Each sequence on the random library contains a stretch of 30-45 random bases (N) flanked by to primer sequences. Because there are four different bases, the pool has a theoretical number of 4^N different sequences. For a library containing 30 random bases, the pool can contain 4^{30} or 1.1×10^{18} different sequences. Nonetheless, preparing a

DNA library with a larger number of random bases improves the library variety. Another fact that needs to be considered is the library concentration used for selection. In order to ensure the pool used for selection indeed contains 10^{15} different sequences, a minimum concentration of 10^{15} molecules/$6.02x10^{23}$ molecules/mole or 1.66 nmoles must be used.

Once the library is prepared, the selection process is started. For the first round of selection, between 2-20 nmoles of the synthetic library are incubated with the target. A few of the sequences will bind to the target, while most of the sequences will not. Unbound sequences are then removed from the pool. Meanwhile, the bound sequences are eluted and PCR amplified to be used as pools for subsequent rounds. This process is repeated between 10-20 times until the pool is fully enriched for the target. Since some molecules can have similar motifs, a negative selection step can be incorporated into the selection process to ensure that the pool will recognize only the target. For this purpose, a counter selection step is added to the selection process. The counter selection step can be performed before or after incubating the target with the pool. During the counter selection step, the pool is incubated with a negative target and the unbound sequences are recovered. The rest of the selection process is continued as described above (*63*).

Aptamer-Target Interactions

Aptamer-target recognition is mainly governed by the three-dimensional structure adopted by the aptamer sequence. This interaction, which involves the formation of many weak and specific interactions with the target, confers the aptamer it’s specificity and selectivity. In solution, the aptamer adopts the most stable conformation at that temperature, salt concentration and pH. Once the aptamer encounters its target,

hydrogen bonding, Van der Waals, stacking (for flat ligands) and electrostatic interactions are formed between both species (*64*). Electrostatic interactions are especially important when the aptamer target carries a positive charge, as charge complementarity creates the perfect environment for the target to bind. Furthermore, the aptamer three-dimensional structure is believed to undergo an “induced fit” change in conformation, which further improves the interaction between the aptamer and its target (*41*, *65*, *66*). When the aptamer’s target is a small molecule, the aptamer structure folds to form a binding pocket for the target. On the other hand, when the aptamer is binding to a bigger molecule, such as a protein, the aptamer itself adopts a structure, which will allow it to bind “fit” into the protein’s binding pocket. The aptamer binding affinity to it’s target typically falls in the nanomolar to sub-pico-molar range.

Cell-SELEX

The SELEX method has been applied for the selection of aptamers against whole cells. The process of selecting aptamers for whole cells has been termed cell-SELEX and is shown in figure 2-4. Cell-SELEX exploits differences on the membrane of different cells, for example between diseased and normal cells, to generate a panel of aptamers that is capable of differentiating between the two cells. During the selection process, the target cells are incubated with the random unselected library (around 10^{15} sequences). Some sequences on this library will bind to the cell, while most will not. Unbound sequences removed by washing the cells with washing buffer. Meanwhile, bound sequences are recovered by heating the cells at 95 ^{o}C, followed by centrifugation. These sequences can then be incubated with a counter selection cell line. During counter-selection, sequences binding to common markers in the cell membrane are removed, leaving only those sequences selective for the target cell line.

After recovering of the unbound sequences, the selected pool is PCR amplified and used as starting library for subsequent rounds. The selection process is then repeated until the pool has been fully enriched for the target cell line, while showing no binding to the counter-selection cell line.

Rationale

Disease cells differ from normal cells in many degrees. First, disease cells, such as cancerous cells, undergo mutations in their genome, which can add, remove or change one or more bases on the DNA strand. These mutations are then carried over to mRNA expression, resulting in changes on the mRNA sequence. Changes in mRNA sequence can result in changes in the protein sequence during translation, or can result in early termination of protein synthesis. Changes in protein sequence may, in turn, cause changes in protein conformation and/or loss of protein activity. The protein itself may undergo changes in post-translational modifications, such as glycosylation, methylation, phosphorylation, etc. Furthermore, the protein expression level may also be affected by the disease. Therefore, many changes at the genomic, and protein level exist which can be exploited to select aptamer probes capable of differentiating between normal and diseased cells.

Generation of a panel of aptamers

Since the selection process is performed against the whole cell, multiple aptamers binding to different markers in the cell membrane can be selected at the same time. Moreover, because these molecular markers are unknown at the time of selection, the selected aptamers can be used as tools for the identification of new disease-related membrane markers for that particular disease. Therefore, the result of the selection is a panel of aptamers that can selectively bind to the target cell and not to normal cells.

This panel of aptamers can then be employed for the detection, diagnosis and profiling of the disease.

The most significant feature of using a panel of markers for disease detection, diagnosis and profiling is the reduction of false positive and false negative results. Because of disease heterogeneity, every patient can present a different expression level and even expression pattern of membrane markers. If only one or few of these markers are used for monitoring of disease, the probability of that particular marker having a different expression pattern between two patients is high. On the other hand, if a larger number of markers is used during diagnosis, the overall error in diagnosis is greatly decreased as the probability of having every single marker changing between different patients is much smaller. Therefore, using cell-SELEX to generate a panel of aptamers for the early detection of ovarian cancer is a feasible and valuable alternative for disease diagnosis.

Aptamers in Cancer Research

Aptamers have been used for the detection, imaging and targeted therapy of cancer. Table 1 lists some of the cancer types used for the *in vitro* selection of aptamers. Several functional aptamers have recently been selected, and their function has been monitored by fluorescence microscopy. Xiao *et al.* demonstrated that sgc8, an aptamer selected against T-cell leukemia (CEM), is internalized into the endosome by observing its colocalization with transferring (a serum glycoprotein known to be internalized via receptor-mediated endocytosis) (*67*). Li *et al*. used a Cy5-labeled aptamer against angiogenin to monitor the internalization of angiogenin in real-time by human umbilical vein endothelial cells (HUVEC) and human breast cancer cells (MCF-7). By monitoring the fluorescent signal from the aptamer by confocal microscopy, the

authors demonstrated that the aptamer-angiogenin conjugate was internalized into intracellular organelles (*68*). Similarly, an aptamer selected against the mouse transferring receptor was used to deliver streptavidin-Cy5 or α–L-iduronidase (lysosomal enzyme which is deficient in lysosomal storage disease or LSD) into enzyme-deficient mouse fibroblasts. The aptamer successfully delivered the streptavidin-cy5 into the cell, as observed by confocal microscopy. The aptamer was also successful in delivering α–L-iduronidase, as the deficient cell line showed no glycosaminoglycan accumulation after treatment (*69*).

In clinical settings, aptamer probes can be used for disease diagnosis, in particular for the detection of leukemia cells in blood by fluorescence microscopy and flow cytometry. Aptamers selected against T-cell leukemia cells (CEM), Burkitt's lymphoma (Ramos), non-Hodgkin's B cell lymphoma (Toledo) and Acute Myeloid leukemia (HL60) (*70-73*) have been shown to recognize leukemia cells in patient samples, showing great promise for their use in profiling for these diseases (*74*). Furthermore, leukemia cells (Toledo, Ramos and CEM) were sorted, enriched and detected from a mixture of cells by using a PDMS microfluidic device design containing aptamers for each cell type immobilized in different regions of the device. These cells where shown to be 96% pure, viable, and capable of growing at the same speed as cultured cells. Once immobilized in the PDMS device, each cell line can be individually recovered for further analysis or can be analyzed *in situ* (*73*).

Their use as imaging probes has also been explored. Recently, the Missailidis group published two papers on the use of a ^{99m}Tc-labeled anti-MUC1 (cell-surface mucin glycoprotein) aptamer (AptA) as an *in vivo* imaging and radiopharmaceutical

probe. In the first report, a new ^{99m}Tc cyclene-based chelator was synthesized to improve the stability of the ligand-metal complex. Furthermore, commercially available chelators were used to create a multi-aptamer complex, which showed increased tumor retention and circulation time, while maintaining rapid penetration and low immunogenicity (*75*). In the second report, two anti-MUC1 aptamers (AptA and AptB) where conjugated to MAG2 and labeled with ^{99m}Tc, and their *in vivo* biodistribution was assessed. Furthermore, the aptamers were modified on the 3'-end with an inverted thymidine to provide resistance to nuclease degradation. Both aptamer conjugates showed accumulation in the tumor site and rapid blood clearance (*76*).

Poly(D,L-lactic-co-glycolic acid)-block-poly(ethylene glycol) (PLGA-b-PEG) nanoparticles conjugated to the A10 RNA aptamer, which targets the prostate-specific membrane antigen (PSMA), have been developed to target PSMA positive cells *in vivo*, but their potential as imaging probes was not explored (*77*, *78*). Aptamers have also been used as optical imaging probes *in vivo* (*79*, *80*). Cy5-labeled TD05, an aptamer selected against the IgM heavy chain expressed in Ramos cells (B cell lymphoma), was administered by tail-vein injection into tumor-bearing BALB/c nude mice, and whole-body fluorescence imaging was used to determine the temporal biodistribution of the Ramos cells. The aptamer probe was shown to circulate through the animal, producing signals in all tissues min after injection. After 4 hours post-injection, the non-specific signal observed in non-target tissues faded, while the tumor signal remained even after 6 hours post-injection. To demonstrate the specificity of the aptamer probe, a control aptamer, Cy5-Sgc8a, and free Cy5 dye were also administered, and they cleared from the system, showing no signal in the tumor site after 3.5 hours post-injection. To further

demonstrate the specificity of the TDO5 aptamer, the aptamer binding to tumors produced from two cell lines, Ramos cells (target cell line) and CEM (non-target cell line, T cell leukemia), was compared. The Cy5-labeled TDO5 aptamer accumulated only in Ramos tumors, with minimum non-specific accumulation in CEM tumors. Therefore, these results demonstrate that dye-labeled aptamers selected by *in vitro* cell-SELEX are useful probes for *in vivo* optical imaging, with good specificity, sensitivity and biostability (71). Furthermore, these probes can be further explored as reporting probes for monitoring *in vivo* cell function and distribution. However, more research is needed to further demonstrate the potential of dye-labeled aptamers for *in vivo* studies.

Nanoparticle-based contrast agents have shown great promise, because they can be easily modified with targeting moieties, such as aptamers, as well as with drugs or other reporting molecules, such as organic dyes, for the development of multimodal nanoparticles. For example, Hwang *et al*. developed magnetic fluorescent nanoparticles (cobalt-ferrite nanoparticles coated with a silica shell containing rhodamine) conjugated to gallium-67 (^{67}Ga) and the nucleolin aptamer AS1411. The aptamer-nanoparticle conjugates were administered by intravenous injection into tumor-bearing nude mice, and their biodistribution was analyzed. The conjugates showed rapid blood clearance and accumulation in the tumor site as observed by scintigraphic images and MRI. Furthermore, accumulation of the conjugate was corroborated by fluorescence imaging of the tumor after organ extraction. However, the conjugate was also shown to accumulate in the liver and intestine (*79*).

Aptamers have been successfully employed for the *in vitro* and *in vivo* imaging of live cells, thus providing many potential applications in biomedicine. These probes are

easily synthesized and conjugated to numerous nanomaterials, such as silica, gold and magnetic nanoparticles and quantum dots, providing them with many characteristics attractive for their use as imaging and drug delivery probes. However, their application is mainly restricted by the limited number of aptamer probes currently available. Therefore, effort is needed on the development of new aptamers capable of detecting other diseases, as well as probes that will allow the monitoring of disease progression. Furthermore, incorporation of nuclease resistant nucleotides into the aptamer design to increase their lifetime in blood could greatly extend their use for *in vivo* studies. In conclusion, aptamers show great promise as detection, characterization and targeted therapy probes in both academic and clinical settings, and these applications will increase in number as new nanomaterials capable of conjugating to aptamers become available.

Overview of Dissertation

The scope of the research work presented here involves the development of aptamer probes capable of binding and recognizing ovarian cancer. The project was initiated by applying the cell-SELEX technology to select a panel of aptamers against ovarian cancer cells. The selected aptamers were further characterized to determine their binding affinity and selectivity against other cancer cells. Furthermore, preliminary studies were performed to determine the type of molecule in the cell membrane the aptamers recognize. Once characterized, the best aptamer was used to develop a FACS-based cancer detection method from whole blood.

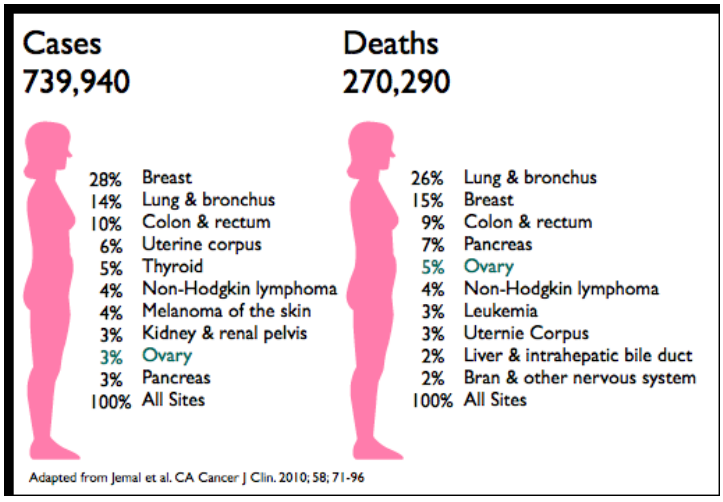

Figure 1-1: Ten leading cancer types for the estimated new cancer cases and deaths for women, 2010

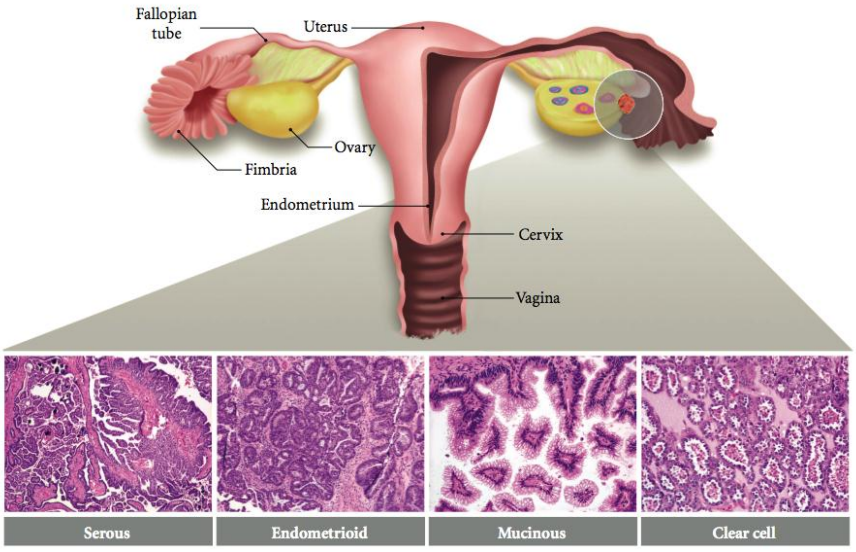

Figure 1-2: The major histologic subtypes of ovarian carcinoma. Serous carcinomas resemble fallopian tube epithelium, endometrioid carcinomas resemble endometrial glands, and mucinous carcinomas resemble endocervical epithelium. Photographs show representative tumor sections stained with hematoxylin and eosin. The shaded circle represents the general anatomical location from which ovarian carcinomas are thought to arise. The pink and blue entities within the cross-sected ovary represent maturing ovarian follicles (Adapted from Karst, A. M., and Drapkin, R. (2010) Ovarian cancer pathogenesis: a model in evolution, *Journal of oncology 2010*, 932371)[1]

[1] Copyright © 2010 Alison M. Karst and Ronny Drapkin. This is an open access article distributed under the Creative Commons Attribution License, which permits unrestricted use, distribution, and reproduction in any medium, provided the original work is properly cited.

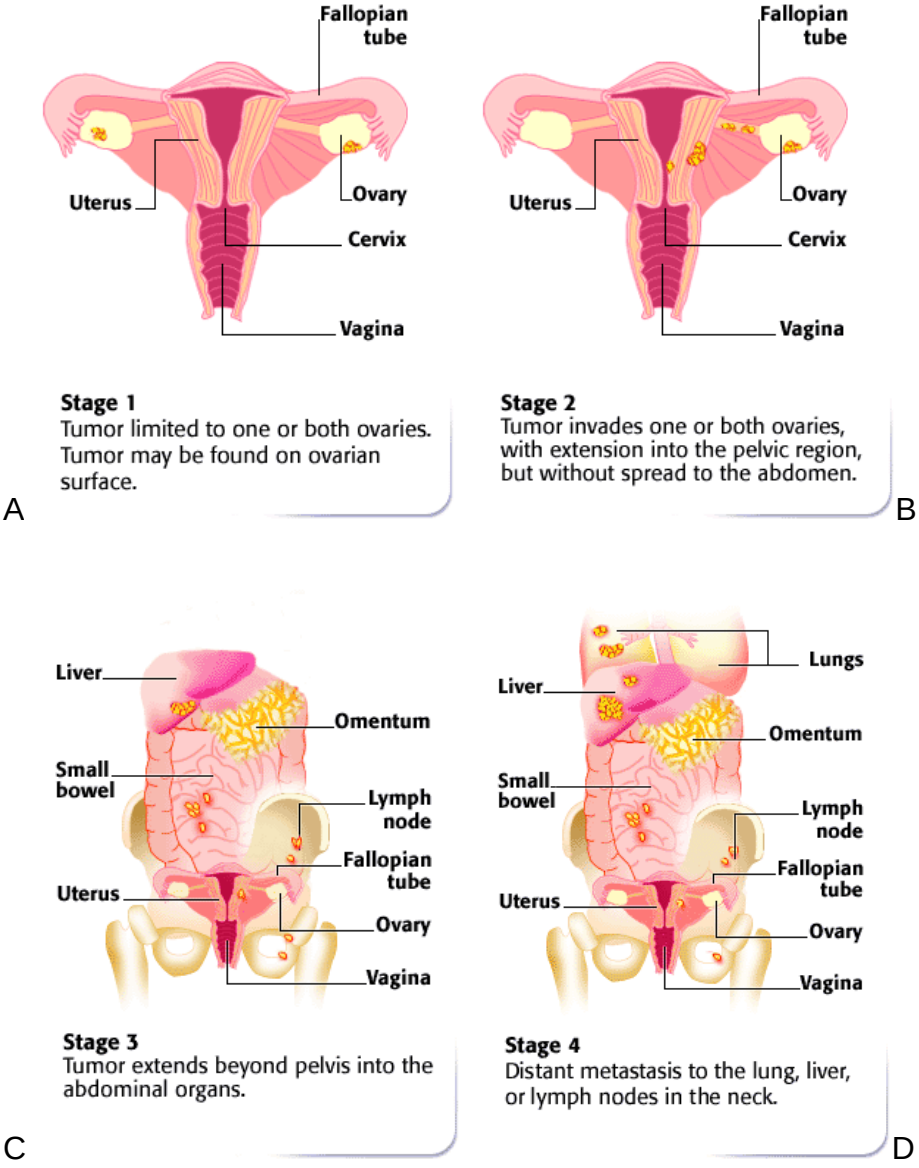

Figure 1-3: Stages of ovarian cancer: A) Stage 1 ovarian cancer B) Stage 2 ovarian cancer C) Stage 3 ovarian cancer D) Stage 4 ovarian cancer (Adapted from www.ovarian-cancer-facts.com)

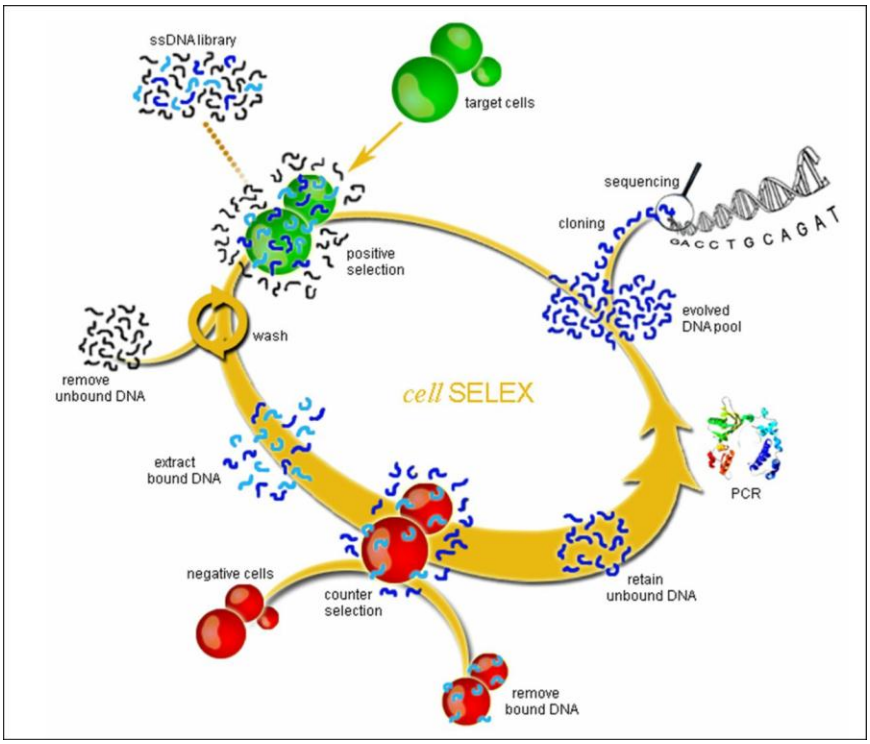

Figure 1-4: Schematic of cell-based aptamer selection (cell-SELEX). Briefly, ssDNA pool is incubated with target cells. After washing, the bound DNAs are eluted by heating in binding buffer. The eluted DNAs are then incubated with control cells (negative cells) for counter-selection. After centrifugation, the unbounded ssDNAs in supernatant are collected, and then amplified by PCR. The amplified DNAs are used for the next round of selection. The selection process is monitored using fluorescent analysis by flow cytometry. The final pool is cloned and then sequenced (Adapted from Shangguan, D., Li, Y., Tang, Z., Cao, Z. C., Chen, H. W., Mallikaratchy, P., Sefah, K., Yang, C. J., and Tan, W. (2006) Aptamers evolved from live cells as effective molecular probes for cancer study, *Proceedings of the National Academy of Sciences of the United States of America 103*, 11838-43).[2]

[2] Copyright © by the National Academy of Sciences

Table 1-1: List of aptamers selected for cancer cell lines

Cancer type	Aptamer	Applications
Ovarian cancer (CAOV3 and TOV-21G)	Multiple: TOV-1 to TOV-10, DOV-1 to DOV-6a	Imaging by flow and confocal microscopy (*81*)
Lung cancer (H69-SCLC and A549-NSCLC)	Multiple	Imaging by flow, confocal microscopy and histology (*82*)
Colon cancer (DLD-1, HCT116,)	Multiple	Imaging by flow, confocal microscopy (*83*, *84*)
Burkitt's Lymphoma (Ramos)	Multiple: TDO5	Imaging by flow and confocal microscopy, in vivo imaging, targeted therapy (*85*)
T cell leukemia (CEM)	Multiple: SGC8	Imaging by flow and confocal microscopy, in vivo imaging, targeted therapy, drug delivery (*86*, *87*)
Glioblastoma (U251)	Multiple	Imaging by flow and confocal microscopy
Liver Cancer (IMEA)	Multiple: TLS11a	Imaging by flow and confocal microscopy (*37*, *47*, *74*, *88-90*)
Prostate cancer	Multiple: PSMA	Imaging by flow, confocal microscopy, in vivo imaging, targeted therapy, drug delivery (*46*, *91*)

CHAPTER 2
SELECTION OF OVARIAN CANCER APTAMERS BY CELL-SELEX

Introductory Remarks

DNA aptamers that target cell surface markers on the ovarian cancer cell membrane with high affinity and specificity will expand the repertoire of molecular probes and offer opportunity for molecular targeting. Furthermore, they offer the opportunity for extensive research on the molecular aspect of the disease. Molecular markers that can be used to predict therapy effectiveness, residual disease detection and long term prognosis will benefit clinical therapy in maximizing survival and minimizing toxicity. Aptamer probes selected against these molecular markers can be used as a panel to profile ovarian cancer cells and to construct molecular profiles of ovarian cancer. These profiles can be used to classify ovarian cancer into subgroups with favorable or unfavorable prognosis within genetically defined subclasses. These molecular differences possess great significance in aiding the understanding of the biological processes and mechanisms of the disease (*92-97*).

Cell-based selection of high affinity aptamers for ovarian cancer involved several rounds of incubation of the live target cell with a randomized pool of DNA sequences (library). After the incubation, washing buffer was used to remove the unbound sequences. Following this step, the bound sequences were eluted, amplified by PCR and used as the enriched library pool for subsequent selection. The entire process involved (i) cell-based SELEX, (ii) flow cytometric analysis, and (iii) sequencing and alignment of the selected pool (*46*, *47*, *72*, *74*).

Materials and Methods

Instrumentation and Reagents

DNA primers and libraries were synthesized using an ABI 3400 DNA/RNA synthesizer (Applied Biosystems, Foster City, CA). All the reagents needed for DNA synthesis were purchased from Glen Research. Varian Prostar reverse phase HPLC system was used to purify all DNA sequences. PCR was performed on Biorad Thermocycler and all reagents were purchased from Fisher Scientific. The enrichment of the selected pool monitoring, characterization of the selected aptamers and identification of the target protein assays were performed with flow cytometric analysis using a FACScan cytometer (BD Immunocytometry Systems).

Design of the DNA Library

For all aptamer selections, the process is started by designing a proper DNA library of about 10^{15} random sequences. Each library used for aptamer selection is designed to contain the sequence of the forward primer followed by 30-45 N's (the DNA synthesizer will chose random bases to place on each N, thus creating the random library) and ends with the complementary sequence of the reverse primer. The primer sequences are constant for all the random sequences contained on the pool and are used for PCR amplification of the pools during selection. The primary or forward primer is labeled with FITC at the 5' end to incorporate the label into the pool during PCR amplification. The secondary or reverse primer is labeled with biotin at the 5' end for the preparation of ssDNA after PCR amplification. Preparation of the ssDNA will be explained below.

The primer and library sequences used for this project were designed using the program Oligo Analyzer 3.0 available online through the Integrated DNA technologies'

webpage. When designing the DNA library, several details have to be considered. Because the library has to be denatured at 95^{o}C during PCR amplification, it cannot form a stable hairpin. To avoid having a library that is too stable, the selected sequence cannot have a melting temperature above 10 ^{o}C. Because the library contains a fluorescein isothiocyanide (FITC) label on the 5'-end, the design avoids having guanine as the last base at the 5'-end as it can quench the fluorophore. Each DNA sequence contains two primer sites between 18-20 bases long. When designing each primer sequence, care must be taken to not choose a sequence with forms self-dimers (binds to itself with three or more consecutive bonds and $|\Delta G^{o}|$ <5 kcal/mole). It is also important that the primers do not form heterodimers (primer 1 binds to primer 2 with three or more consecutive bonds and $|\Delta G^{o}|$ <5 kcal/mole). If the primers form dimers, the dimers will compete with the full sequence for PCR amplification. Furthermore, PCR prefers the amplification of shorter DNA sequences. The primers must anneal into the library at a temperature between 55-60 ^{o}C. To obtain such an annealing temperature, the primer must have a GC content of 50% or more. Since we can only choose one annealing temperature on the PCR machine, both primers must have the same annealing temperature ($\pm 1^{o}$ C). As with the library, the primers cannot form stable structures. Therefore, the selected sequences must form hairpins with a melting temperature lower than 10 ^{o}C. All these requirements were met when designing the library used for the selection.

Chemical Synthesis of the Random Library by 3400 DNA Synthesizer

Synthetic nucleic acids (DNA or RNA) are chemically synthesized by solid phase using phosphoramidite chemistry. In nature, DNA synthesis occurs when the DNA polymerase incorporates new nucleotides in the 5'-3' direction. The enzyme uses

energy stored on the tri-phosphate bond to catalyze the formation of a new phosphodiester bond between the bases. Chemical synthesis of synthetic nucleic acids does not involve the use of tri-phosphate nucleotides, but rather uses phosphoramidite chemistry to incorporate new bases in the 3'-5' direction. The oligo synthesis takes place on a solid support, know as controlled pore glass (CPG). This solid support is a non-swellable glass bead with high surface area and narrow pore size distribution. The first base or modification on the 3'-end is covalently bound to the solid support and remains attached until the synthesis is completed. The subsequent bases are then introduced as phosphoramidites. In order to avoid the incorporation of the base in the wrong position, all active groups on the phosphoramidite are blocked by protecting groups (Figure 2-1). As seen on figure 2-1, the oxygen on the 3' position is protected by a dimethoxytrityl (DMT) group. This group is also present in the solid support. On the other hand, the 5'- phosphate group on the phosphoramidite is protected with a di-isopropyl amine and 2-cyanoethyl group. Finally, the base is protected by the incorporation of a benzoyl group.

To initiate the DNA synthesis, the DMT protecting group on the solid support needs to be removed prior to the addition of the following base by introducing dichloroacetic acid or trichloroacetic acid. In order to incorporate the next base, the di-isopropyl amine group protecting the 5'-phosphate group is removed by simultaneously delivering the base and tetrazole (activator). The tetrazole replaces the di-isoprolyl amine, becoming a good leaving group. The 3'-OH in the previous base (attached to the CPG) can now do a nucleophilic attach to the phosphate group, displacing the di-isopropyl amine. Since no reaction is 100% efficient, some sequences will fail to

incorporate the base, leaving a free 3'-OH. In order to avoid building oligomers with different base composition and length, unreacted free 3'-OH groups are capped using acetic anhydride. These sequences are truncated during this step. Finally, an oxidation step is carried out to oxidize the phosphite linkage formed to a more stable phosphate linkage. This cycle is repeated until the desired oligomer is synthesized. Because the DMT group has an absorbance at 412 nm, the DNA synthesizer measures DMT absorbance during each base incorporation and uses this value to calculate the DNA synthesis efficiency for each base incorporation.

As mentioned on the previous chapter, the longer the library is, the more diversity it contains. Therefore, in theory, the library should be as long as possible. Unfortunately, the DNA synthesis yield decreases with each base incorporation. To have an idea of the overall synthesis yield, assuming every base incorporation has an average yield of 99%, the overall yield for an 80-base long oligomer would be $(99\%)^{79}$ (the first base is already present in the solid support) or 45%. Therefore, the length of the DNA library used during selection is limited by the DNA synthesis efficiency. To obtain a good synthesis yield, a length of 70-80 bases is preferred.

DNA Deprotection and Preparation for High Performance Liquid Chromatography (HPLC) Purification

After DNA synthesis is complete, the newly synthesized oligomers remain covalently attached to the CPG on the 5'-end. The free oxygen in the phosphate group is protected by a 2-cyanoethyl group, the bases remain protected with a benzoyl group and the 3-end is protected by the DMT group (Figure 2-2). Also, the synthesis product consists of a mixture of full-length oligomers and truncated sequences, thus requiring HPLC purification. Before the oligomer can be used, the oligomer needs to be cleaved

from the CPG and the protecting groups (except for DMT) need to be removed. This was accomplished by incubating the DNA synthesis product in an ammonium hydroxide:methylamine (1:1) solution at 65 ^{o}C for 30 min. The DMT group needs to be retained as it is required for HPLC purification.

To prepare the synthesis product for HPLC purification, deprotected DNA was precipitated by incubating in cold ethanol and 3.0 M sodium chloride (NaCl) for 1 hour at -20 ^{o}C. The precipitate was then collected by centrifugation at 4,000 rpm for 30 min at 4 ^{o}C. The supernatant was discarded and the DNA was resuspended in 0.10 M triethylamine acetate (TEAA). This solution was centrifuged one more time at 14,000 rpm for 1 min to remove any remaining CPG that may have been transferred during deprotection and precipitation. This step is critical as any CPG remaining in the solution can block the HPLC column.

HPLC

As mentioned above, the DNA synthesis product consists of a mixture of full-length oligo and truncated sequences. Therefore, all truncated sequences need to be removed and purified full-length oligomer collected. This was accomplished by using reverse-phase ion-pairing HPLC. A C_{18} column (Econosil, 5 µM, 250 x 4.6 mm) from Alltech (Deerfield, IL) was used as stationary phase along with acetonitrile (ACN) and 0.1 M triethylamine acetate (TEAA) in water as mobile phases on a ProStar HPLC station (Varian, CA). As the stationary phase is non-polar, polar compounds elute faster than non-polar compounds. Because DNA is ionic, it does not interact well with the mobile phase by itself. Therefore, the anions on the DNA molecule are paired with triethylene amine cations, making the DNA molecule neutral and more non-polar.

The DNA product was introduced into the column and allowed to interact with the stationary phase. As mentioned in the previous section, full-length DNA product contains a DMT group on its 3'-end. On the other hand, truncated sequences contain an acetate group, which is smaller and more polar than the DMT group. The presence of this group aids in the separation of DNA product from the truncated sequences, allowing the full-length DNA to interact longer with the stationary phase. Therefore, the truncated sequences eluted from the column first. The elution was achieved by using a gradient elution with acetonitrile and 0.10 M triethylamine acetate in water. The chromatography began at 100% ACN, which is non-polar. As the chromatography progressed, the percentage of TEAA was gradually increased until the sample was eluted. The gradient used is dependent on the length of the oligo being purified. For example, to purify an 80 base pair long library, a gradient of 10% TEAA to 60% TEAA in 30 min is typically used. For smaller sequences, a faster gradient is more suited (e.g. 10% TEAA to 85% TEAA in 30 min). The 80 base pair long library was purified using a gradient of 10% TEAA to 60% TEAA in 30 min.

Once the DNA oligo was purified, the sample was dried. Because the oligomer still contained the DMT group on the 5'-end, a final incubation with 80% acetic acid for 30 min was performed to remove the final protecting group. After removal of the DMT group, the acetic acid was evaporated and the DNA was resuspended in water. The DNA concentration in the stock solution was then calculated using the Beer-Lambert equation $A = \varepsilon bc$, where A is absorbance of the sample, ε is the extinction coefficient of the DNA oligo, b is the light path of the cuvette and c is the sample concentration.

Polymerase Chain Reaction (PCR) Optimization of the Library and Primer Set

Polymerase chain reaction (PCR) is a technique used to exponentially expand DNA. PCR is divided into three stages: denaturation stage, annealing stage and elongation stage. PCR uses *Taq* HS DNA Polymerase. This Polymerase contains a mixture of *Taq* Polymerase and a monoclonal antibody to *Taq* Polymerase, which binds to the polymerase until the temperature is elevated. The binding of this antibody prevents nonspecific amplification due to mispriming and/or formation of primer dimers during reaction assembly. The antibody is then denatured in the initial PCR DNA-denaturation step, releasing the polymerase and allowing DNA synthesis to proceed.

To perform PCR, a 10 µM stock solution on both primers (forward and reverse primers were mixed at a 10 µM concentration each) and a 10^{-12} M library stock solution (template) were prepared. Following this step, optimization of the number of cycles was performed to obtain the best amplification of the library pool without observing any nonspecific amplification. The PCR samples were prepared using 1x PCR buffer, 125 µM dNTP's, 5 U/µL Hot stat Taq polymerase, primers and library. Four samples were prepared as well as three corresponding control samples, which contain everything except the library.

Each sample and corresponding control was removed from the PCR machine after each desired number of cycles had completed. Once the PCR was completed, the PCR products were analyzed by agarose gel electrophoresis (3% agarose) using ethidium bromide as a dye to observe the DNA bands. The optimized number of cycles is the cycle that gives the brightest band and displays no nonspecific amplification.

Once the number of cycles was successfully optimized, the next step was to optimize the annealing temperature. The PCR machine is capable of providing with

eight (8) different temperatures for simultaneous PCR amplification. In order to optimize the annealing temperature, a temperature gradient was used with the lowest primer melting temperature (57 ^{o}C) ± 3 ^{o}C as the range. The PCR selected the eight temperatures depending on the temperature range.

Once the PCR was completed, the PCR products were analyzed by agarose gel electrophoresis using ethidium bromide as a dye to observe the DNA bands. The optimized annealing temperature is the temperature at which the brightest band is observed without any nonspecific amplification. The optimized annealing temperature was subsequently used for the amplification of the selected library pool.

Gel Electrophoresis

The PCR product was analyzed by resolving the amplified DNA products on a 3% agarose gel by electrophoresis. The DNA was visualized using 0.5 mg/ml ethidium bromide staining, which intercalates with DNA and fluoresces upon exposure to UV light. The 3% agarose gel was prepared by adding 1.2 g agarose to 40 ml of 1 X Tris/Borate/EDTA (TBE) buffer (Fisher Scientific Inc., Pittsburg, PA) and melted using a microwave for 1 minute. The solution was poured on a gel casting system using an 8 well comb and allowed to cool down prior to sample analysis. Eight microliters of the PCR product or control (contains PCR buffer, dNTPs and primes, but does not contain template) were mixed with 2 µL of loading buffer (bromophenol blue and glycerol) and loaded into the gel. A 25 bp DNA ladder was used to estimate the size of DNA as shown in Figure 2-3. The gel was run at a constant voltage (100 V) for 30 min to move the negatively charged DNA through the gel towards the positive electrode. The bands were visualized

Cell Culture

Adherent CAOV3 (human ovarian epithelial adenocarcinoma cells) and HeLa (Human cervical epithelial adenocarcinoma cells) were obtained from ATCC (American Type Culture Collection). CAOV3 cells were cultured in Medium 199:MCDB 105 mixed in a 1:1 ratio (Sigma Aldrich Co., St. Louis, MO) HeLa cells were cultured in RPMI-1640 (ATCC, Manassas, VA). Other cells tested for binding to the selected aptamers were cultured as described by ATCC. All media were supplemented with 10% Fetal Bovine Serum (FBS) (Heat Inactivated from GIBCO) and 100 IU/ml penicillin-streptomycin.

Cell-Based SELEX

Ovarian cancer cells are adherent cells. This means that they grow attached to each other and to the bottom of the flask. To perform SELEX, the cells need to be suspended in the media by breaking the adhesion interactions between them. This is achieved by incubating the cells with trypsin for 45 secs. Following trypsin treatment, the cells are placed in the incubator for two hours to regenerate the proteins that may have been digested by the enzyme. Once the cells are suspended in the media, the cell concentration is determined using the heamocytometer. The selection process is then initialized.

To perform SELEX, the ssDNA library pool (20 nmoles) is dissolved in binding buffer (4.5 g/L glucose, 5.0 mM $MgCl_2$, 0.1 mg/mL tRNA and 1.0 mg/mL BSA, all in Dulbecco's PBS with calcium chloride and magnesium chloride). After dissolving, the DNA is denatured by heating at 95 ^{o}C for 15 min and is rapidly cooled on ice for 10 min before incubation with the cells. This forces the random library sequences to fold into the most favorable structures. Target cell culture containing approximately 2-3 x 10^6 cells is centrifuged at 950 rpm for 5 min at 4 ^{o}C to pellet the cells. The pellet is washed

twice with washing buffer (5.0 mM $MgCl_2$, 4.5 g/L glucose, all in 1 X PBS). The cell pellet is then incubated with the DNA library by resuspending the cells in the ssDNA library pool. The incubation mixture is placed on ice in an orbital shaker for 30 min. The cells are then washed three times with washing buffer to remove unbound DNA sequences. The bound sequences are eluted in 500 µL binding buffer by heating at 95 ^{o}C for 15 min and centrifuged at 14,000 g for 1 min.

The supernatant containing the DNA sequences is then incubated with a negative cell line (5-fold excess of positive cell line) to perform a subtraction of the sequences that bind. These sequences are removed since they are not selective binders for the target cell line. The remaining sequences are amplified by PCR using FITC- and biotin labeled primers. The selected sense ssDNA is separated from the biotinylated antisense ssDNA by streptavidin-coated Sepharose beads (*63*).

For the first round selection, the counter selection was eliminated because of the possibly low amount of bound sequences. The entire selection process was then repeated, starting with the target positive cells. To acquire aptamers with high affinity and specificity, the washing strength was enhanced gradually by extending the wash time (2-5 min), increasing the volume of washing buffer (3-5 mL) and the number of washes (3-5 washes). The enrichment of specific sequences was assayed using flow cytometry as explained below. Once the library was enriched for the target, it was sequenced and subject to a sequence alignment using Clustal X. Potential aptamers were identified by selecting sequences from families showing high sequence homology. This is explained in the following chapter.

PCR Amplification of the First Selected Pool

During the first round of selection, the pool contains, in theory, only one copy of every sequence. Therefore, if only a portion of this pool is used for amplification and further selection rounds, only a fraction of the sequences present will be carried over to the next round. In order to avoid loosing potential binding sequences, the whole eluted pool on the first round was subject to an initial amplification. The PCR mix was prepared as described above in a final volume of 1,000 µL, and PCR amplified for 10 cycles. After the first PCR amplification, all the PCR products in each tube were pooled together and used as the template for the next PCR procedure.

Preparation of Single-Stranded DNA

After PCR amplification, the selected pool was turned into dsDNA, where the sense strand is FITC-labeled and the antisense strand is biotin-labeled. Since SELEX requires the use of an ssDNA pool, the PCR amplified pool needed to be converted back into ssDNA. For this purpose, streptavidin coated high performance Sepharose beads (GE Healthcare, NJ) were used to make a small affinity column. The dsDNA product was passed through the column five times, allowing the binding of biontiylated dsDNA to the streptavidin beads. The beads were then washed with 2.5 mL of PBS to remove any remaining forward primer. After washing, the dsDNA was de-hybridized with alkaline 0.2 M NaOH solution, releasing the fluorophore-labeled strand (sense strand). In order to remove the sodium salts, a size exclusion NAP-5™ column was used to desalt the pool. The ssDNA was loaded on the column, allowed to interact with it and eluted with water. The larger DNA molecules were eluted first leaving the salts in the column. The desalted ssDNA was quantified by a UV spectrophotometer and

vacuum dried. The PCR products were re-suspended in binding buffer just before use in next round of selection.

Flow Cytometry

Flow cytometry uses the principles of light scattering, light excitation, and emission of fluorochrome molecules to generate specific multi-parameter data from particles and cells in the size range of 0.5 µm to 40 µm diameter. Cells are hydro-dynamically focused in a sheath of PBS before intercepting an optimally focused light source (Figure 8). The sample is injected into the center of a sheath flow. The combined flow is reduced in diameter, forcing the cell into the center of the stream, one cell at a time. As the cells or particles of interest intercept the light source they scatter light and fluorochromes are excited to a higher energy state. This energy is released as a photon of light with specific spectral properties unique to different fluorochromes. Scattered and emitted light from cells and particles are converted to electrical pulses by optical detectors. Forward SCatter (FSC) gives information on relative Size and Side SCatter (SSC) give data on relative granularity or internal complexity. Flow cytometers can detect chromosomes, proteins, or molecules such as nucleic acids if attached to a particle such as a microsphere (*63*, *70*, *84*, *85*, *98*).

To monitor the enrichment of aptamer candidates after selection, the FITC labeled ssDNA pool was incubated with 1 x 10^6 positive or negative cells in 200 µL binding buffer and incubated on ice for 20 min. Cells were washed twice with binding buffer and resuspended in 250 µL buffer. The fluorescence was determined with a FACScan cytometer (BD Immunocytometry Systems) by counting 30,000 events. The FITC-labeled unselected ssDNA library was used as a negative control.

Results

Design and Optimization of the Selection Library

In order to initiate the selection process, a DNA library was designed using the parameters described in the Materials and Methods section. An 80 nt long ssDNA library with a randomized core of 42 nt flanked on both, the 3' and 5'ends by a 19 mer fixed primer binding sites was designed, synthesized and HPLC purified. FITC-labeled library was synthesized using an ABI 3400 DNA/RNA synthesizer (Applied Biosystems, Foster City, CA) at the 1 μM scale using solid-state phosphoramidite chemistry, as described above. The sequence of the library was as follows, 5-ACT CAA CGA ACG CTG TGG A N_{42} TGA GGA CCA GGA GAG CAG T.

The DNA was cleaved off the solid support CPG and ethanol precipitated. Reverse phase HPLC (RP-HPLC) was employed to purify the product with the protecting DMT group. An HPLC program with a 0.1 M TEAA gradient of 10%-65% and run time of 30 min was used to purify the library. The HPLC purified product was then deprotected in mild acidic conditions using acetic acid, vacuum dried and re-suspended in water. A Cary Bio-300 UV spectrometer (Varian, Walnut Creek, CA) was used to quantify the DNA. A square quartz cuvette with 1 cm path length was used for the absorption measurements. DNA was stored at -20 °C before use.

The primers were acquired from IDT technologies. The forward primer was ordered with a 5’- FITC label and the reverse primer was labeled with biotin. The primers were diluted in water to a final concentration of 500 μM. The forward primer was a 19 mer sequence 5’-FITC-ACT CAA CGA ACG CTG TGG A with a melting temperature of 56.8 °C and GC content of 52.6%, an extinction coefficient of 208560 L/mole.cm and a molecular weight of 6359.3 g/mole. The reverse primer was a 19 mer

sequence 5’-Biotin-ACT GCT CTC CTG GTC CTC A with a melting temperature 57.7 °C and GC content of 57.9% with a molecular weight of 6084.1 g/mole, an extinction coefficient of 163700 L/mole.cm.

PCR efficiency is critical in cell-based SELEX because eluted DNA sequences for each round of selection have to be amplified by PCR. In order to achieve a reproducible and efficient PCR, which yields adequate products, the reaction conditions must be optimized. The PCR was optimized for the annealing temperature, number of cycles as well as the concentrations of all reagents including primers and library. All PCR mixtures are prepared by combining 50 mM KCl, 10 mM Tris HCl (pH 8.3), 1.5 mM $MgCl_2$, dNTPs (each at 2.5 mM), 0.5 µM each primer, and Hot start *Taq* DNA polymerase (5 U/µL). Amplifications were carried out in a Biorad 1 Cycler at 95 °C for 30 sec (denaturation), 57 °C for 30 sec (annealing), and 72 °C for 30 sec (extension), followed by a final extension step for 3 min at 72 ^{o}C.

Once the DNA library and primer set was synthesized, the PCR conditions were optimized to determine the annealing temperature for the primer set. In order to determine the annealing temperature of the primer set, the number of cycles was optimized. Seven tubes were prepared, four samples and three controls. Tubes were picked after 14, 16, 18 and 20 cycles (Figure 2-3 A). After the PCR, a 3% agarose gel was run and stained with ethidium bromide. Sixteen cycles of amplification was selected because it allowed the amplification of the DNA sequences with enough product but without any nonspecific amplification, which usually appears as small bands slightly greater or smaller than the required sequences.

Once the number of cycles was optimized, the annealing temperature was optimized using the best number of cycles. To optimize the annealing temperature, a temperature gradient was performed. The temperature gradient was set from 55.3 ^{o}C to 60.0 ^{o}C. The machine selected the gradient to run as follows: 55.3 ^{o}C, 55.7 ^{o}C, 56.3 ^{o}C, 57.0 ^{o}C , 58.2 ^{o}C , 59.1 ^{o}C , 59.7 ^{o}C, and 60.0 ^{o}C. After the PCR, a 3% agarose gel was run and stained with ethidium bromide. The best band was observed at 55.3 ^{o}C (Figure 2-3 B). Since at low temperatures nonspecific amplification is promoted, a higher annealing temperature was used. The annealing temperature used during selection for the PCR amplification of the selected sequences was 57 ^{o}C. Due to an increase of non-specific amplification during the selection process, the annealing temperature was increased to 60 ^{o}C to reduce the non-specific bands and improve the PCR yield.

Monitoring of the Selection Progress

In order to yield aptamers that bind and recognize ovarian cancer cells, the CAOV3 cell line was used as positive cell line and HeLa cells were used as a negative cell line. As we desire to select aptamers selective for ovarian cancer and not normal ovarian cells, the best negative cell line would be a one derived from normal epithelial human ovarian cells. Unfortunately, normal ovarian cell lines are not commercially available. We, therefore, chose HeLa cells as negative control.

Selection was started by dissolving 20 nmol of library into 500 µL of binding buffer (4.5 g/L glucose, 5.0 mM $MgCl_2$, 0.1 mg/mL tRNA and 1 mg/mL BSA). Before incubation with approximately 4 x 10^6 CAOV3 cells, the DNA pool was denatured at 95 ^{o}C for 15 min and quickly cooled on ice. During the first selection round, the unselected pool was incubated with the CAOV3 cells for 60 min at 4 ^{o}C with constant shaking. After washing 3 times with 3 mL of washing buffer, the selected pool was eluted in water by heating at

95^{o}C and PCR amplified. For the first round of selection, the whole pool was PCR amplified using 10 cycles to ensure multiple copies of each sequence are present. This is a critical step, as only part of the pool is PCR amplified and used for the following selection round. After the initial amplification, the number of PCR cycles was optimized and the pool was amplified for an additional 5 cycles of PCR. The amplified pool was used for the following round.

This process was repeated for the following rounds, except the initial amplification of the pool is omitted (it is unnecessary as the pool contains multiple copies of each sequence at this point). The washing strength was increase with subsequent rounds. Also, the incubation time of the pool with the target cell line, as well as the number of target cells used was reduced during subsequent rounds. Negative selection was incorporated during the 15th round of selection. Negative selection was performed for 1 hour at 4 ^{o}C prior to positive selection. The selection process is summarized on Table 2-1.

The enrichment of the library through successive selection rounds was monitored by flow cytometry. As the selection progresses, the number of sequences binding to the target cell line increases. Therefore, the enriched pool shows an increase in mean fluorescence intensity. Once the pool shows no increase in fluorescence intensity, the pool has been fully enriched and the selection has been completed. The selection showed enrichment after 9 rounds of SELEX. (Figure 2-4 A). The pool also showed binding to the negative cell line (Figure 2-4 B). This enrichment was removed by negative selection. After 19 rounds of selection, the pool showed no further increase in fluorescence intensity (Figure 2-4 A). As the selection reached its end, the pool was

sent for sequencing. The sequencing, alignment and aptamer characterization are discussed in the following chapter.

Concluding Remarks

An 80-base long library was designed using the IDT Oligoanalyzer 3.1 software. The library was synthesized and purified in our laboratory, while the primers were ordered from IDT. The PCR conditions for the amplification of the library were optimized. After optimization, the library was used for selection. Cell-SELEX was successfully applied for the enrichment of a random library for binding to the CAOV3 cell line. Enrichment was observed after 9 rounds of SELEX, with binding to the negative cell line (HeLa). After incorporation of negative selection, the enrichment for HeLa cells was reduced. The selection reached its end after 19 rounds of SELEX.

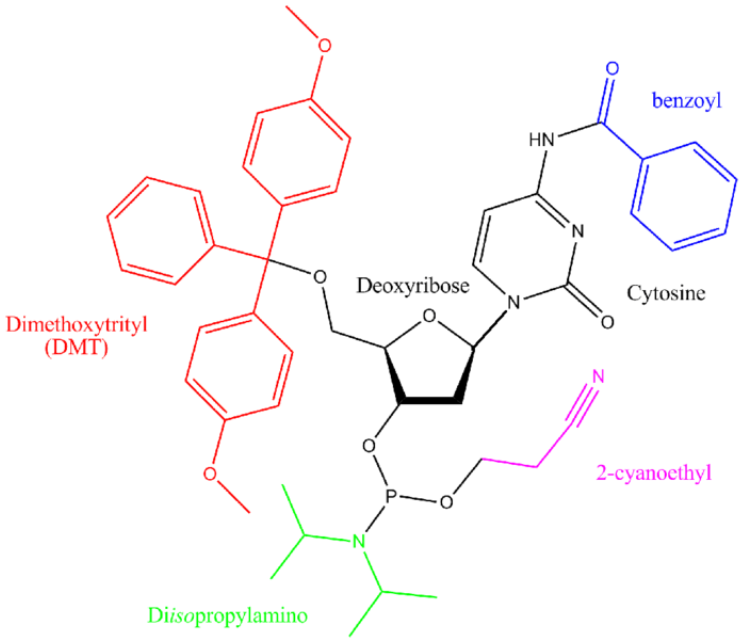

Figure 2-1: Representative structure of a phosphoramidite: cytosine

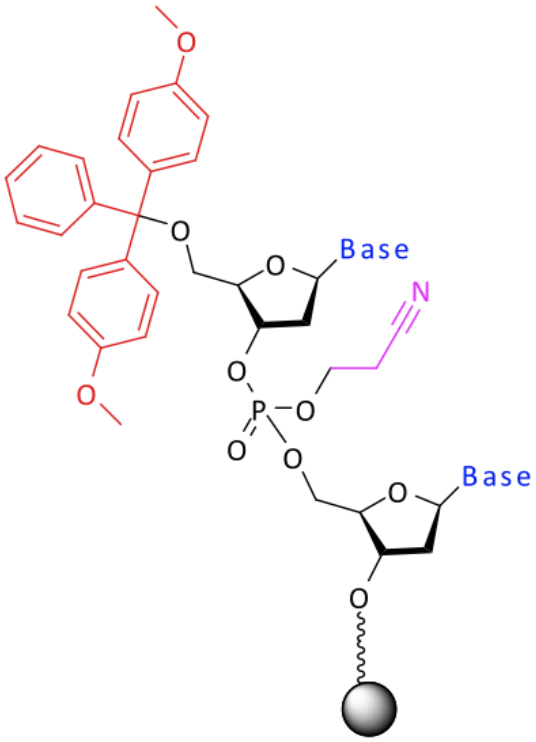

Figure 2-2: Representative structure of a newly synthesized oligomer

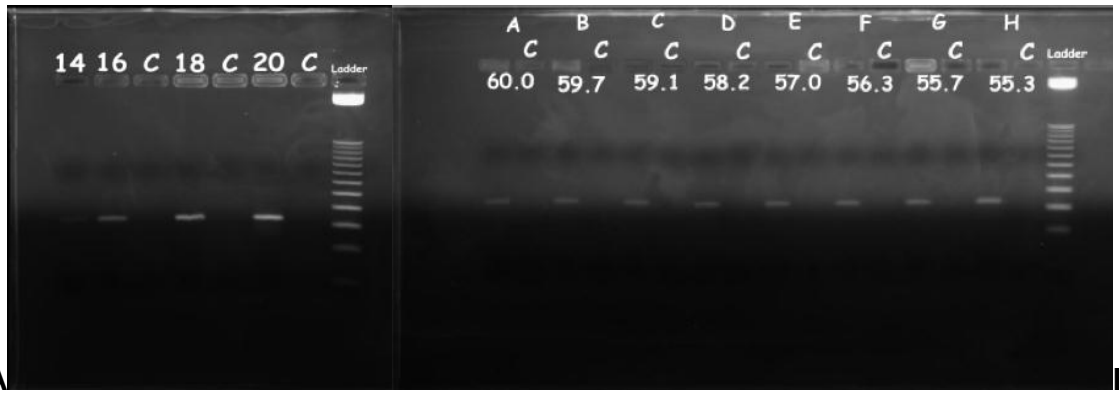

A B

Figure 2-3: Gel electrophoresis images (A) showing PCR cycles used to determine the best amplification cycle and (B) showing PCR cycles used to determine the best annealing temperature. C = control.

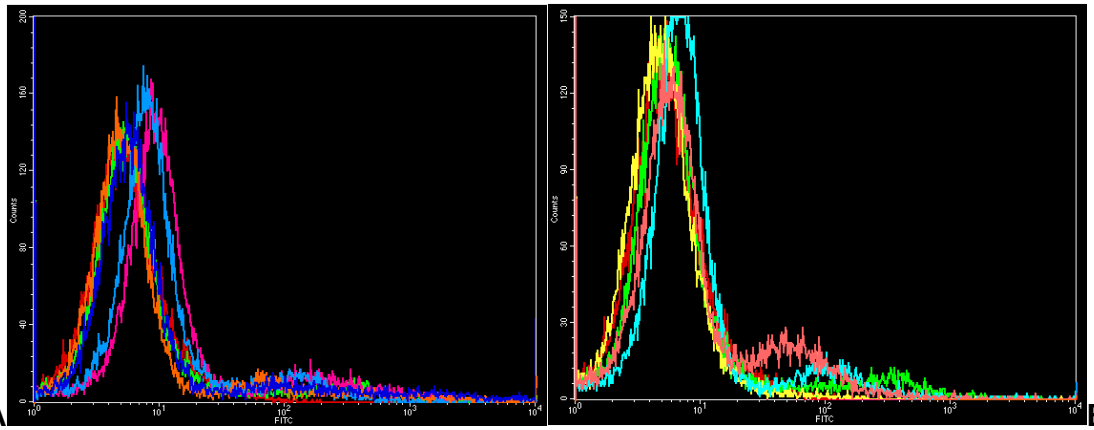

A B

Figure 2-4: Monitoring of the selection progress. (A) Binding of the enriched pools to CAOV3 cells. The red histogram corresponds to cells only. The green histogram corresponds to unselected library. Dark blue corresponds to the 9th round. Pink corresponds to the 15th rounds and light blue corresponds to the 19th rounds. (B) Binding of the enriched pools to HeLa cells. The red histogram corresponds to cells only. The green histogram corresponds to unselected library. The light blue histogram corresponds to the 9th round. The pink histogram corresponds to the 15th round. The Yellow histogram corresponds to the 19th round

Table 2-1: Summary of the selection progress.

Round	CAOV3 cells	Incubation time	PCR cycles	DNA eluted	Wash	HeLa
1	8	60	10 + 5	381.5	3 mL 3x	N/A
2	7	55	14	150.3	3 mL 3x	N/A
3	6	50	18	934	3 mL 3x	N/A
4	5	45	18	265	3 mL 3x	N/A
5	5	40	18	252.2	3 mL 3x	N/A
6	4	35	10	161.2	3.5 mL 3x	N/A
7	3	35	14	266.9	3.5 mL 3x	N/A
8	3	35	14	137.8	3.5 mL 3x	N/A
9	4	35	16	117.9	3.5 mL 3x	N/A
10	3	35	14	503	3.5 mL 3x	N/A
11	3	35	16	346.3	3.5 mL 3x	N/A
12	3	35	16	153.2	4 mL 3x	N/A
13	3	35	18	369.2	4 mL 3x	N/A
14	3	35	18	81.7	4 mL 3x	N/A
15	3	35	18	213.8	4 mL 3x	10
16	3	35	18	145.3	4 mL 3x	10
17	3	35	18	152.2	4 mL 3x	10
18	3	35	18	134	4 mL 3x	10
19	2	35	20	597	4 mL 3x	10

CHAPTER 3
BIOCHEMICAL CHARACTERIZATION OF THE SELECTED ATPAMERS

Introductory Remarks

During the selection process, the pool is enriched for sequences that have an affinity for the target cell. Nonetheless, some non-binder sequences remain in the pool. It is, therefore, necessary to screen the pool for potential aptamer sequences. Those aptamer candidates are selected based on sequence homology; one or two sequence members of the same homologous family are selected, synthesized and tested for binding to the target and control cell line. Once the aptamer sequences have been identified, each aptamer is further characterized to determine binding affinity and selectivity. In this chapter, the biochemical characterization of the aptamers selected against CAOV3 cells is described.

Materials and Methods

454 Sequencing

454 sequencing is a next generation sequencing based on sequencing by synthesis. During 454 sequencing, each sequence on the pool is immobilized into a 454 bead. Each bead-bound library is then emulsified with amplification reagents in a water-in-oil mixture. Each unique library sequence is PCR amplified within the bead, resulting in several million copies of each library sequence per bead. Each bead is then removed from the emulsion and loaded onto a Pico Titer Plate device for sequencing. Each bead is then incubated with sequencing enzymes. The sequencing system flows each individual nucleotide in a set order. For every nucleotide complementary to the template added, a chemiluminescent signal is emitted and recorded by the CCD camera. The

signal strength is proportional to the number of nucleotides incorporated in a single nucleotide flow. Each signal is then converted into the sequence for each bead (*99*).

Preparation of the DNA library

Once the selection was completed and full pool enrichment was achieved, the selected pools were sequenced to identify the potential aptamer candidates. To sequence the pools, a primer containing the 454 primers, a barcode sequence (MID) and the library's primer sequence was synthesized (Figure 3-1). The barcode is used to identify different pools, which are sequenced together. These primers were used to PCR amplify the selected pool using FastStart High Fidelity PCR System (Roche). To PCR amplify the selected pool using 454 primers, a PCR mix containing 1X FastStart High Fidelity Reaction buffer, 200 µM dNTP solution, 0.4 µM primer solution, 100 pg-10 ng selected pool and 2.5 U of FastStart High Fidelity Enzyme in a final volume of 50 µL was prepared. The mix was then PCR amplified as described on the previous chapter.

Purification of the PCR product

The PCR product was purified using the QIAquick PCR purification kit. The PCR purification kit has a maximum binding capacity of 10 ug. The maximum elution volume is 30 µL. After PCR amplification, the enriched pool (now double-stranded DNA) was diluted in 5 volumes of buffer PB (supplied by the purification kit) to 1 volume of the PCR sample. The QiAquick spin column was placed in the provided 2 mL collection tube and the sample was added and centrifuged at 13,000 rpm for 30-60 sec. The flow-through was discarded and the column was centrifuged at 13,000 rpm for 30-60 sec. After centrifugation, the column was washed with 750 µL Buffer PE and centrifuged at 13,000 rpm for 30-60 s. The flow-through is discarded and the column is centrifuged for an additional 1 min. The QIAquick column was then transferred to a clean 1.5 mL

centrifuge tube and the DNA was eluted by adding 50 µL Buffer EB (10 mM Tris CL, pH 8.5) or water (pH 7.0-8.5) to the center of the QIAquick membrane and centrifuged the column for 1 min.

Verification of the DNA product

After purification, the DNA pool was analyzed on a 3% agarose gel to ensure the PCR product was the right length and purified. To analyze the PCR product, 10 µL of the PCR product were mixed with 2 µL of loading dye, loaded on a 3% agarose gel and separated using a constant voltage of 100 V. The DNA concentration was quantified by measuring absorbance at 260 nm using the following equation: ug/mL = A_{260} X 50 ug/mL. Once quantified, the PCR product was diluted with tris buffer to a final concentration of 5 ug/mL and submitted for sequencing to the ICBR sequencing core.

Sequence Alignment and Selection of Aptamer Candidates

After sequencing, the primer regions of each sequence were removed and the random portions of the library aligned using Clustal X to group the sequences into families with sequence homology (Figure 3-2). Sequence candidates were selected from each homologous family, synthesized with a biotin label and HPLC purified. Other sequences from smaller families were selected as well for screening. Each aptamer candidate was screened for binding to the target cells as described in the following section.

Screening of the Aptamer Candidates

To determine if the aptamer candidates are indeed binding to the target cell line, 1 x 10^6 target cells were incubated with biotin-labeled aptamer or biotin-labeled library in 200µl binding buffer and incubated at 4 ^oC for 20 min. After washing twice with washing buffer, cells are incubated with streptavidin-PE-Cy5.5 for 20min on ice. After the

incubation, cells were washed twice with binding buffer and resuspended in 250µl buffer. The fluorescence was determined with a FACScan cytometer (BD Immunocytometry Systems) by counting 30,000 events.

Confocal Microscopy

The aptamer's binding was also verified by confocal microscopy. To do so, the aptamers and random library were synthesized and labeled with 5'-TMR. The cells were seeded in a glass-bottom petri dish and allowed to grow to confluency. After washing twice with 2 mL of washing buffer, cells were incubated with 250 nM aptamer or library solution at 4 ^{o}C for 20 min. After washing three times with washing buffer, cells were imaged by confocal microscopy using an Olympus FV500-IX81 confocal microscope (Olympus America Inc., Melville, NY). A 5 mW 543 nM He-Ne laser is the excitation source for TAMRA throughout the experiments. The objective used for imaging is a PLAPO60XO3PH 60x oil immersion objective with a numerical aperture of 1.40 from Olympus (Melville, NY).

Determining Aptamer Affinity (binding constant, apparent Kd)

The binding affinity of the aptamers was determined by flow cytometer as explained above. The biotin-labeled unselected library was used as a negative control to determine nonspecific binding. All binding assays were performed in triplicates. The mean fluorescence intensity of the unselected library was subtracted from that of the aptamer with the target cells to determine the specific binding of the labeled aptamer. The equilibrium dissociation constant (Kd) of the aptamer-cell interaction was obtained by fitting the dependence of intensity of specific binding on the concentration of the aptamers to the equation Y = B max X/(Kd + X), using Sigma Plot (Jandel, San Rafael, CA).

Determining Aptamer Specificity

The selected aptamers were screened against different cell lines to verify selectivity. For this purpose, the selected aptamers were incubated with 1 x 10^6 cells of each cancer cell lines (Table 3-2). The unselected library was used as the negative control. After washing, the binding pattern for each aptamer was determined by flow cytometry as described above.

Effect of Temperature on the Aptamer Binding

Since the selection is performed at 4 ^oC, it is important to verify if the aptamer retains its binding to the target cell line at 37 ^oC. Those aptamers able to bind to the target cell at 37 ^oC can be used to further develop in vivo studies. Binding assays were performed as described above. To determine binding at 37 ^oC, 1 x 10^6 target cells were incubated with biotin-labeled aptamer or biotin-labeled library in 200 µl binding buffer and incubated at 4 ^oC or 37 ^oC for 20 min. After washing twice with washing buffer, cells are incubated with streptavidin-PE-Cy5.5 for 20 min on ice. After the incubation, cells were washed twice with binding buffer and resuspended in 250 µL buffer. The fluorescence was determined with a FACScan cytometer (BD Immunocytometry Systems) by counting 30,000 events.

Competition Assay

As some of the sequences posses some sequence homology, competition studies were performed to the determine if the aptamers bind to the same target. For this purpose, 1 x 10^6 target cells were incubated with 3 µM (1000X excess) FITC-labeled aptamer in 200 µL binding buffer at 4 ^oC for 20 min. Biotin-labeled aptamer was then directly added to the solution to a final concentration of 250 nM. After washing twice with washing buffer, cells are incubated with streptavidin-PE-Cy5.5 for 20 min on ice.

After the incubation, cells were washed twice with binding buffer and resuspended in 250 µl buffer. The fluorescence was determined with a FACScan cytometer (BD Immunocytometry Systems) by counting 30,000 events.

Internalization Studies

There are several examples exists on the literature showing the internalization of aptamers (*99*). Therefore, the selected aptamers were tested for cell internalization. In order to determine if the aptamers selected against CAOV3 cells can be internalized, about 2 x 10^6 target cells were washed twice with washing buffer and incubated with 250 nM biotin-labeled aptamer or library solution at 37 ^oC or 4 ^oC for one hour. After washing, the cells were incubated with streptavidin-PE-Cy5.5. After washing, the cells were analyzed by flow as described above.

The internalization was further confirmed using a Zeiss confocal microscopy. Cells were seeded on a glass-bottom petri dish (MatTek Corporation, Ashland, MA) to confluence. Cells were incubated with 250 nM aptamer-PE-Cy5.5 or library-PE-Cy5.5 for 2 hours at 37 ^oC. Half an hour prior to the end of the incubation, Hoechst 33342 (MP, Solon, OH) was added to a final concentration of 1 µM. After washing, cells were imaged by confocal microscopy.

Results

Analysis of the Sequencing Data

In order to align the sequences, the constant primer regions were removed. This is important because the alignment software will align the primer regions rather than the random stretch. Because the 454 sequencing yields a large number of sequences (about 3,000 per pool), a program written in perl (program was written by Dimitri Van

Simaeys) was used. Once the primer sequences were removed, the constant regions were aligned using Clustal X.

Three large homologous families and three smaller families were identified. A representative sequence from each family was chosen, synthesized *in house* with a biotin group on the 5'-end and screened for binding to the target and control cell line. From the 15 different aptamer candidates tested for binding, seven sequences showed binding to the target cell line (Figure 3-3 and Table 3-2). Although the enriched pools showed minimum binding to HeLa cells, all the selected sequences showed binding to these cells. Since DOV-3, DOV-4 and DOV-6a showed the highest mean fluorescence intensity, their binding was verified by confocal microscopy as described above. As shown on Figure 3-4, both DOV-3 and DOV-4 showed higher fluorescence intensity than the library. On the other hand, the fluorescence signal obtained with DOV-6a was the same as that observed for DOV-6a. Therefore, both DOV-3 and DOV-4 have the potential of being used as probes for tissue imaging.

Binding Affinity

We determined the apparent dissociation constant for three of the selected aptamers, and all were in the nanomolar range (Table 3-1). These aptamers were selected because they showed the highest fluorescence intensity. As mentioned on the introduction, aptamers have been shown to have high affinities for their target, ranging from μM to pM. Therefore, the affinities observed for the aptamers selected are comparable to other aptamers selected against whole cells and are comparable to antibody affinity.

Selectivity Assay

Once the aptamer candidates are screened for binding and characterized for binding affinity towards the target, the aptamers need to be screened for selectivity. Theoretically, these aptamers should be selective to only the target cell. However, it has been reported that one aptamer from a group of aptamers selected with the counter selection strategy could still bind to the negative cell line (*100*). This shows that the counter selection may not be efficiently enough to eliminate all nonspecific sequences.

In order to determine if the aptamers selected are indeed selective for CAOV3 cells, all the selected aptamers were tested for binding to other cancer cell lines. As shown on Table 3-2, all the aptamers showed binding to several of the cancer cell lines tested. Interestingly, none of the aptamers bind to leukemia cell (CEM and Ramos) or the liver cancer cell line LH-60. Furthermore, all the aptamers, except DOV-2, bind to the counter-selection cell line, HeLa. These findings suggest that the aptamers bind to a common marker for epithelial cancer.

Competition Studies

Although the aptamers selected are members of different families, we wished to determine if they bound to the same target. To do so, competition studies were performed between DOV-2a, DOV-3, DOV-4 and DOV-6. The binding of the competitor aptamer present in excess was verified by observing the fluorescence intensity of the FITC label on channel one as a means of demonstrating its presence in the cell membrane. Meanwhile, the aptamer binding was monitored on channel three (monitoring the signal from PE-Cy5.5). None of the aptamers seem to compete with each other. Figure 3-5, shows the results obtained for DOV-2a. The signal from excess FITC-labeled DOV-2a (pink histograms on the top) remains the same for all the

samples. Meanwhile, when incubating excess FITC-labeled DOV-2a with PE-Cy5.5 labeled DOV-2a, a reduction in the PE-Cy5.5 is observed. This is expected, as DOV-2a should compete with itself. On the other hand, the signal from PE-Cy5.5 labeled DOV-3 and DOV-4 are not affected by the presence of excess DOV-2a. The same procedure was repeated using FITC-labeled DOV-3 and DOV-4 (data not shown); similar results were obtained for all the aptamers. Therefore, each aptamer seems to be binding to different targets on the cell membrane.

Temperature Effect in Aptamer Binding

The stability of aptamer binding to target cells was also assayed at different temperatures. As aptamers were selected at 4 ^{o}C, a study was done to verify the suitability of using these aptamers at physiological temperature. For this purpose, the aptamers were incubated with the target cells at 4 ^{o}C and 37 ^{o}C. As shown in Figure 3-6, there was no significant change in fluorescence intensities among the two temperatures tested for DOV-3, DOV-4 or DOV-6a. However, DOV-2a showed a significant decrease in binding intensity when incubated with the target cell line at 37 ^{o}C. Nonetheless, all the aptamers retain binding to CAOV3 cells at physiological temperature. This observation is important as it is an indication that all the aptamers can be successfully used *in vivo* studies.

Internalization Studies

Aptamer internalization was assayed by flow cytometry using biotin-labeled aptamers. Cells were incubated with biotin-labeled aptamers at either 4 ^{o}C or 37 ^{o}C. After washing, the cells were further incubated with streptavidin-PE-Cy5.5 to labeled the biotin moiety on the aptamer. If the aptamer is internalized, the streptavidin PE-Cy5.5 wont be able to bind to the biotin group on the aptamer. If the aptamer is not

internalized, the biotin will remain available for binding to the streptavidin PE-Cy5.5. The aptamer incubated at 4 ^{o}C serves as the positive control, as internalization is inhibited at this temperature. As shown in Figure 3-7, the aptamers incubated at 37 ^{o}C showed a reduced fluorescence signal as compared to the same aptamer incubated at 4 ^{o}C. Therefore, the aptamers seem to be internalized.

Aptamer internalization was further verified by confocal microscopy. As shown in Figure 3-8, cells incubated with DOV-3 showed higher signal intensity than the library, thus indicating that the aptamer is binding to the cells. The fluorescence signal from the aptamer was observed at the same plane as the signal coming from Hoesch, the nuclear dye. Furthermore, most of the aptamer fluorescence signal was observed from within the cells inside what seems to be endosomes. Therefore, the DOV-3 is internalized after binding to its target on the cell membrane.

Concluding Remarks

Seven aptamer sequences have been successfully selected against the CAOV3 cell line. Three of this aptamers were characterized for their binding affinity showing apparent Kd's in the nanomolar range. The Kd's observed are in the range of affinities observed for other aptamers selected against whole cells. The aptamers were also tested for binding to other cancer cell lines. All the aptamers showed binding to some of the cancer cell lines tested. Although having an aptamer that is selective for ovarian cancer only is ideal, the fact that the aptamers bind to other cancer cells does not mean the aptamers are not useful for disease detection. Indeed, the aptamers have the potential of being used as general probes for the detection of cancer. More importantly, since the aptamers show a different binding pattern for each cell line, this pattern, along with the binding patter of other aptamers previously selected for other cancer cell lines,

can be used for the profiling of cancer. Furthermore, since the aptamers were shown to be internalized by flow cytometry and confocal imaging, they can be used for drug delivery studies.

Forward primer (Primer A-Key):

5'-CGTATCGCCTCCCTCGCGCCATCAG-*{MID}*-*{Forward primer sequence}*-3'

Reverse primer (Primer B-Key):

5'-CTATGCGCCTTGCCAGCCCGCTCAG-*{MID}*-*{Reverse primer sequence}*-3'

Figure 3-1: Representation of the 454 primers

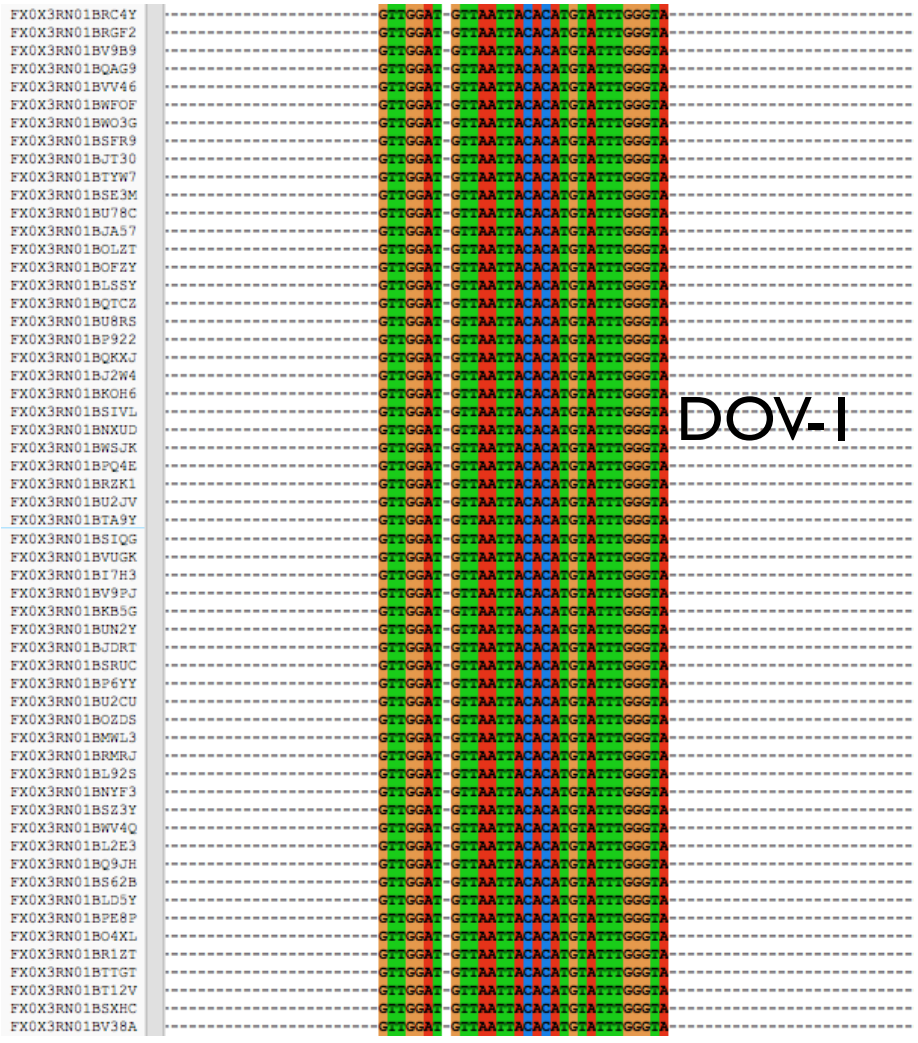

Figure 3-2: Representative sample of sequence alignment: DOV-1

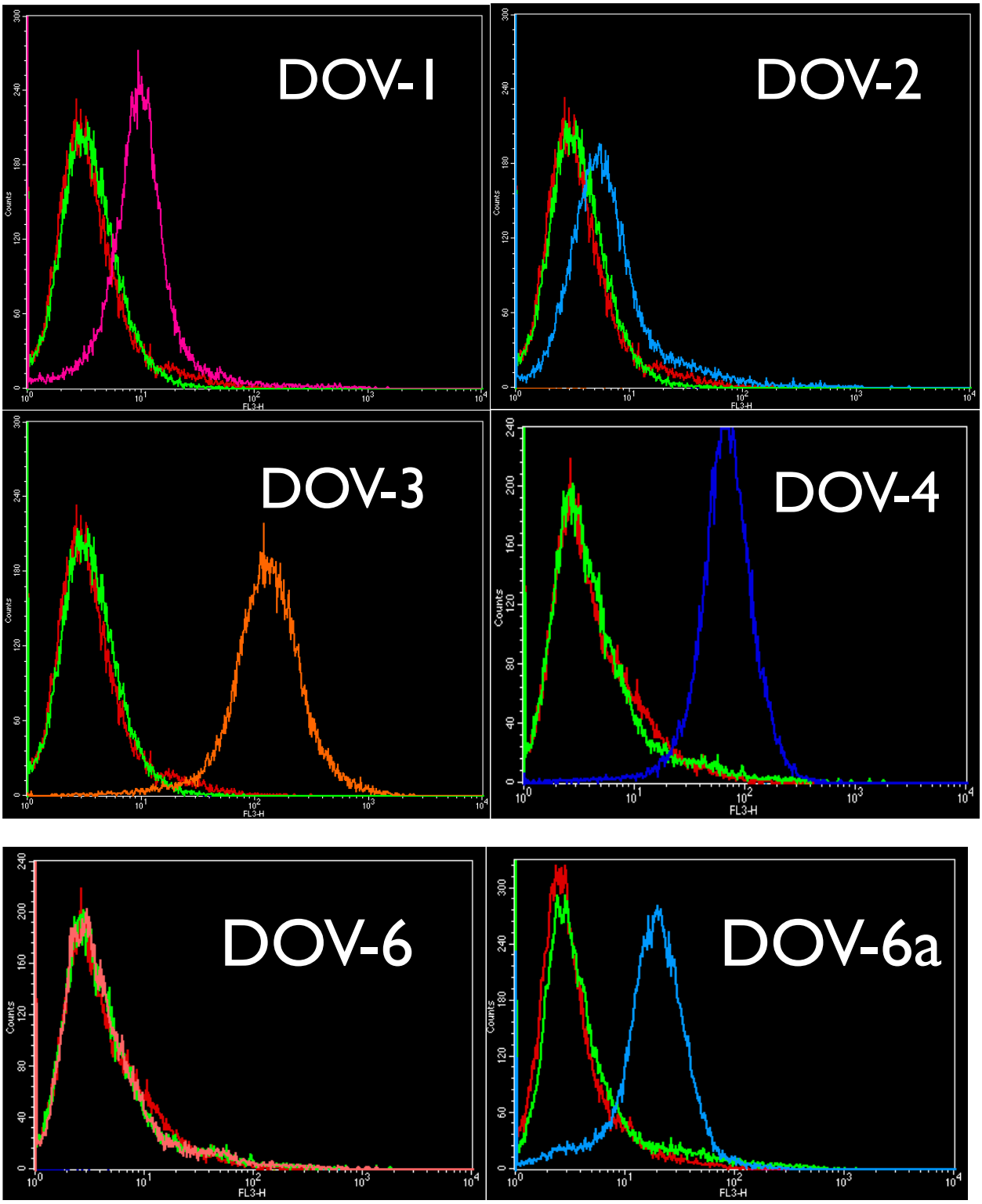

Figure 3-3: Representation of aptamer candidate binding to CAOV3 cells.

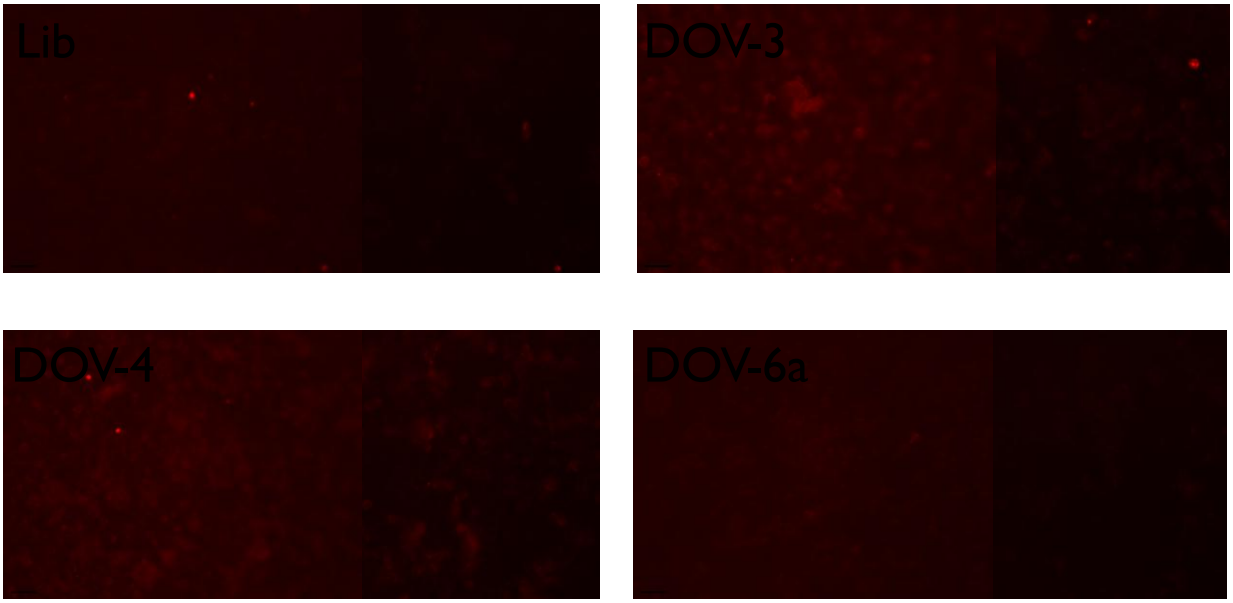

Figure 3-4: Confocal microscopy of CAOV3 cells with TMR-labeled DOV-3, DOV-4 and DOV-6a

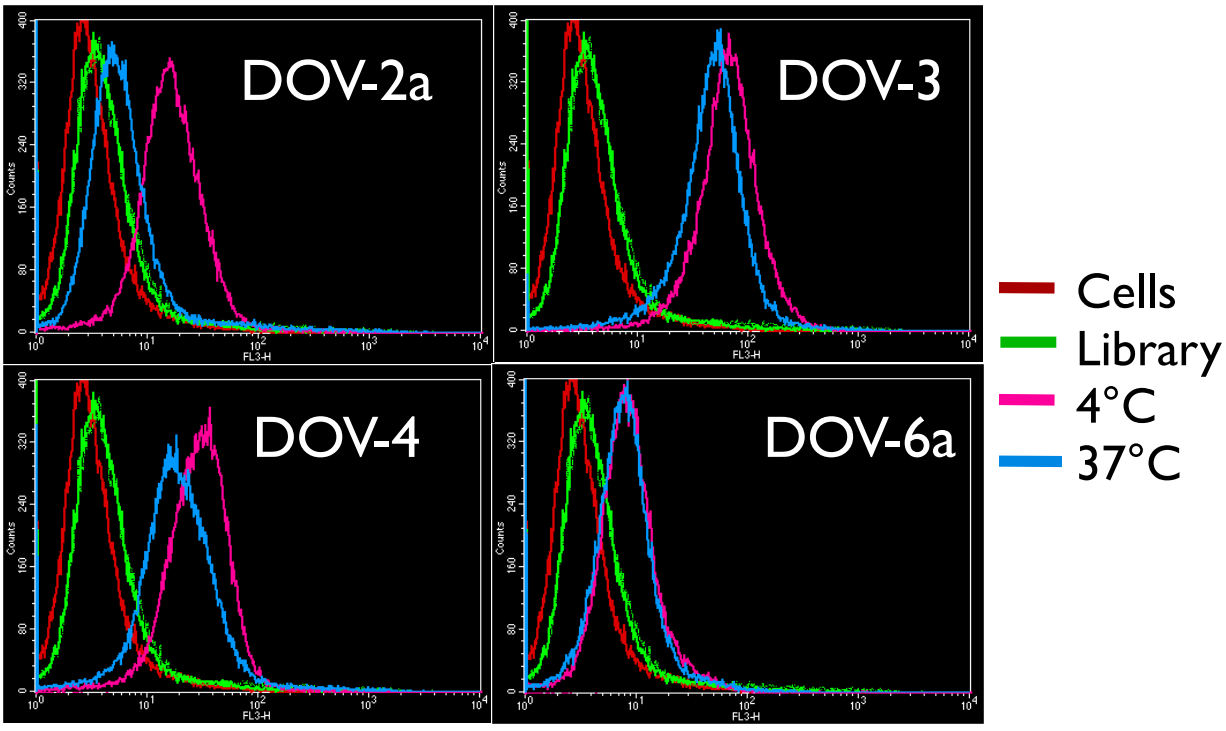

Figure 3-5: Aptamer binding to the target cell line at 4^{o}C and 37^{o}C.

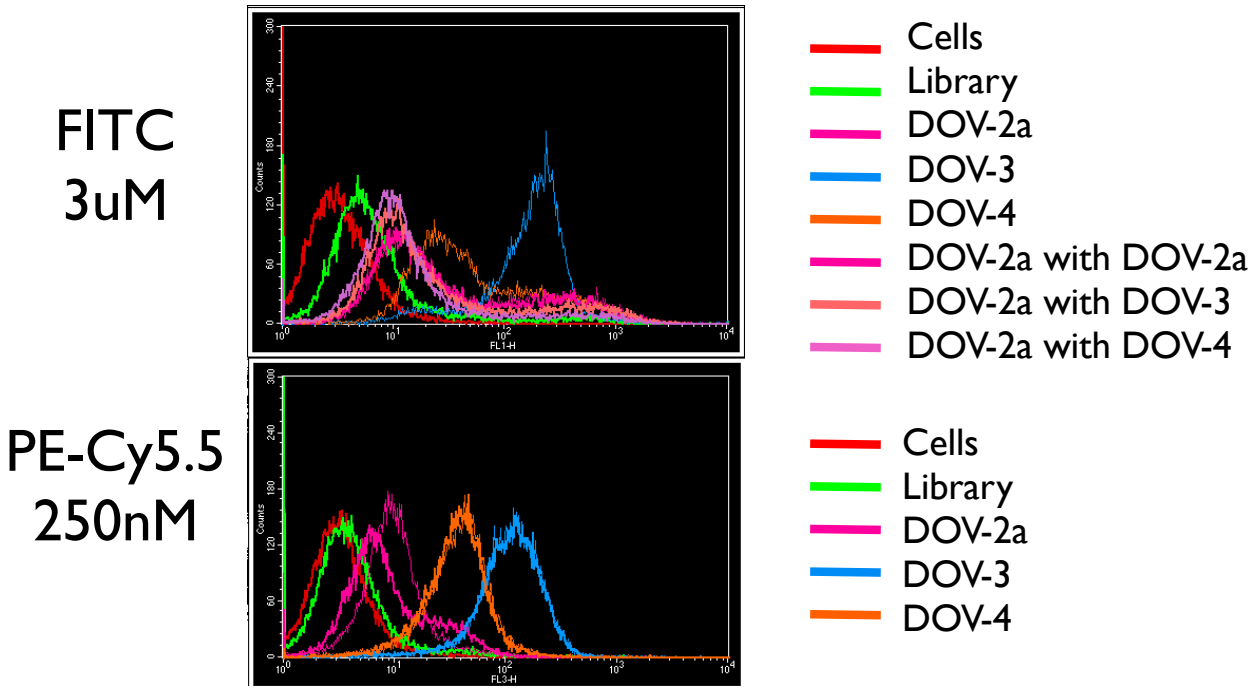

Figure 3-6: Competition studies using excess FITC-labeled DOV-2a competing against PE-Cy5.5 labeled DOV-2a, DOV-3 and DOV-4.

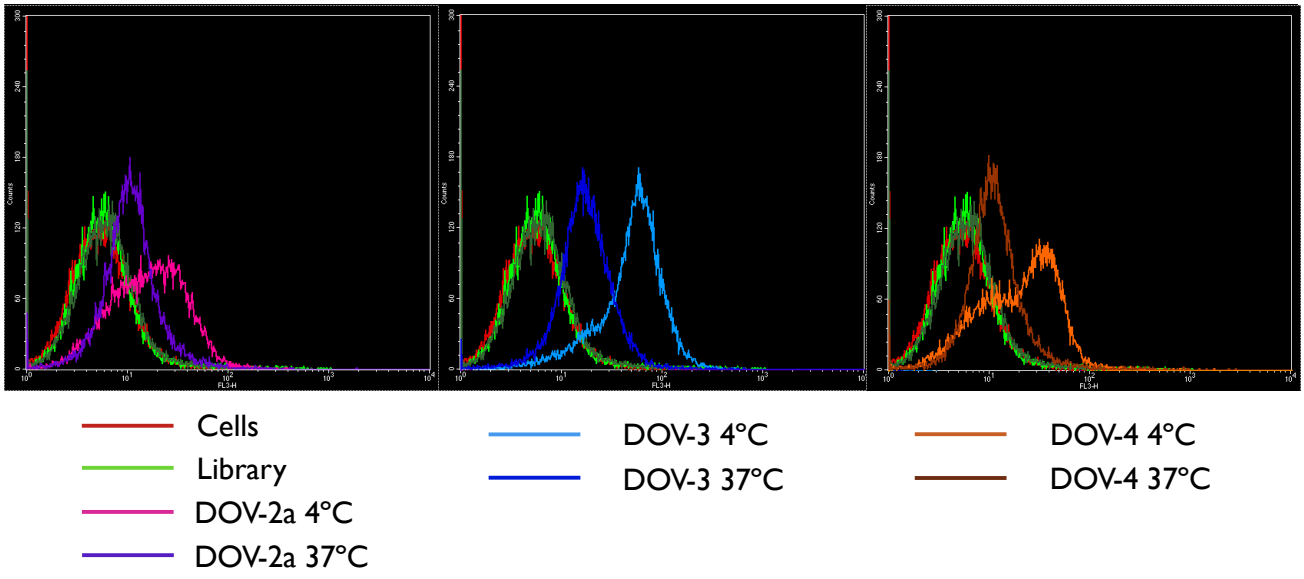

Figure 3- 7: Internalization studies by flow cytometry

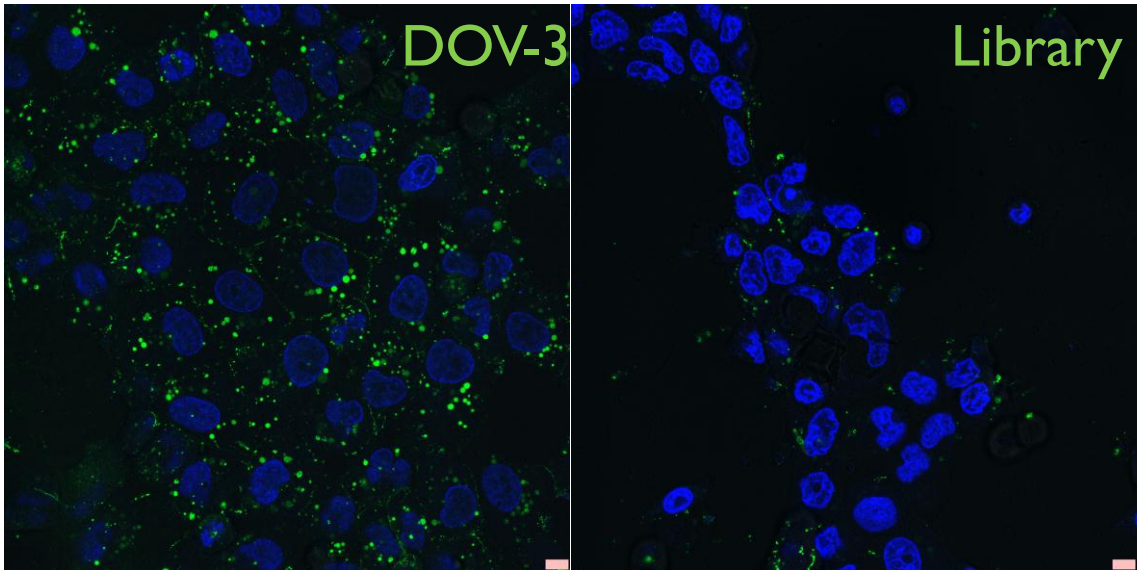

Figure 3-8: Internalization studies of DOV-3 on CAOV3 cells by confocal microscopy.

Table 3-1: List of aptamers selected and their affinity

Aptamer	Sequence	Kd (nM)
DOV-1	ACT CAA CGA ACG CTG TGG ACG TTG GAT GTT AAT TAC ACA TGT ATT TGG GTA TGG TGA GGA CCA GGA GAG CA	ND
DOV-2	ACT CAA CGA ACG CTG TGG ATA GCG GAC GAA CTT TTA GCA GAA CAC AGC CTC GGC TGA GGA CCA GGA GAG CA	ND
DOV-2a	ACT CAA CGA ACG CTG TGG ATG TGA AAG AAG GAG GAT CTT TAG GCT TGG ACT GTA TGA GGA CCA GGA GAG CA	ND
DOV-3	ACT CAA CGA ACG CTG TGG ATG CAG AGG CTA GGA TCT ATA GGT TCG GAC GTC GAT GAG GAC CAG GAG AGC A	130±30
DOV-4	ACT CAA CGA ACG CTG TGG AGG GCA TCA GAT TAG GAT CTA TAG GTT CGG ACA TCG TGA GGA CCA GGA GAG CA	40±20
DOV-5	ACT CAA CGA ACG CTG TGG ATT GGT GTG GAC GGT AGT TGT ACA GGG GGT AAC CAA TGA GGA CCA GGA GAG CA	ND
DOV-6a	ACT CAA CGA ACG CTG TGG AAT GTT GGG GTA GGT AGA AGG TGA AGG GGT TTC AGT TGA GGA CCA GGA GAG CA	40±20

Table 3-2: Summary of the aptamer selectivity assay.

Aptamer	CAOV3	TOV	H-23	LH-60	HCT-116	HeLa	Ramos	CEM	DLD-1	A172	HT29
DOV-1	+	++	-	-	++	+	-	-	++	+	-
DOV-2	+	+	-	-	+	-	-	-	++	++	-
DOV-3	++++	++++	++++	-	++++	+++	-	-	++++	++++	+++
DOV-4	++++	++++	++++	-	++++	+++	-	-	++++	++++	+++
DOV-5	++	++	+	-	+	+	-	-	-	+	-
DOV-6a	-	++	-	-	+	+	-	-	++	+	-

Note: A threshold based on the fluorescence intensity of the PE-Cy5.5-labeled library was chosen so that 99% of the cells have fluorescence intensities below it. When PE-cy5.5 labeled aptamer was incubated with the cells, the percentage of cells with fluorescence intensity above the set threshold was used to evaluate the binding.1 <10%, + 10-30%, ++ 30-60%, +++ 60-80%, and ++++ >80%.

CHAPTER 4
APTAMER-BASED DETECTION OF OVARIAN CANCER CELLS IN BLOOD

Introductory Remarks

There is currently no recommended blood screening for ovarian cancer in the general population, due to the lack of an effective blood test. The only clinically available blood tests for ovarian cancer are used in the context of suspected ovarian cancer at the time of clinical presentation - CA125 and the recently marketed Ova1 test are both used as adjunct tests to aid in diagnosis of ovarian cancer (*67*, *68*). Unfortunately, neither of these tests is sufficiently accurate for clinical decision-making. For example, CA125 is elevated in only approximately 50% of patients with early stage disease (*32*) and is elevated in many benign conditions. As a result, there currently is no effective way to reliably diagnose ovarian cancer short of surgery and more than 50,000 women annually undergo surgery for suspected ovarian cancer when they actually have benign conditions that could be managed much less invasively. Although CA125 blood testing is recommended for cancer screening in women with major predisposition to ovarian cancer due to inheritance of germline susceptibility mutations (i.e., BRCA 1 or 2 mutations, etc.), this recommendation comes with a clear warning that there is no known effective strategy for early detection (*67*, *68*). Development of a blood-based strategy that could reliably diagnose ovarian cancer would be a major improvement in management of this disease. Additionally, it could serve as a foundation for additional investigation of its utility in screening and early detection.

A promising strategy for development of such a test might focus on a marker that is found across malignant phenotypes of ovarian cancer, but not in normal or benign conditions - such a marker has been elusive. Recent findings regarding exfoliated

tumor cells present in the circulation, and specifically those demonstrating features of stem cells, suggests that these cells might represent a fruitful target. Such Circulating tumor cells (CTCs) have been demonstrated across all malignant cancer types, including ovarian cancer (*101*, *102*). The fact that CTCs can be found in patients *before* the primary tumor is detected and are not present in the blood of healthy individuals or individuals with nonmalignant disease makes them a very promising target for our efforts to develop an effective blood test for accurate diagnosis and early detection.

Materials and Methods

Binding in Complex Media

Since the aptamer selection is performed in binding buffer (PBS), it is imperative to determine if their binding will be retained when used in complex media. To assess if the aptamer binding is retained in more complex media, aptamer binding studies where performed in cell culture media, 100% FBS and human plasma as described in the previous chapter. In short, about 2 x 10^6 cells were resuspended in cell culture media, FBS or human plasma containing biotin-labeled aptamer or biotin-labeled library to a final concentration of 250 nM, and incubated for 20 min at 4 ^oC. After washing twice with washing buffer, cells were incubated with streptavidin Pe-Cy5.5 for 20 min at 4 ^oC. After washing, cells were analyzed by flow cytometry.

Detection of spiked ovarian cancer in whole blood

Since DOV-4 shows the best signal intensity by flow cytometry, this aptamer was chosen for further applications. In order to determine if the aptamer DOV-4 can be used for the detection of CAOV3 cells spiked in whole blood, different CAOV3 cell concentrations were spiked in 1 mL of whole blood ranging from 1million to 10,000 cells.

Further treatment of the blood was applied as a means of improving the limit of detection.

Direct incubation in blood

In order to determine the limit of detection, 1 mL of whole blood was spiked with different CAOV3 concentrations ranging from 1 million to 10,000. After spiking the blood, biotin-labeled DOV-4 or library was added to a final concentration of 250 nM and incubated for 20 min at 4 ^{o}C without any pretreatment. After washing, the samples were incubated with streptavidin PE-Cy5.5 for 20 min at 4 ^{o}C. After washing, the samples were analyzed by flow cytometry. A total of 10 million events were counted per sample.

Detection of spiked cells after ficoll

In order to further improve the detection limit, spiked blood was submitted to a Ficoll gradient to remove red blood cells. For Ficoll gradient, blood was layered on top of the Ficoll layer avoiding mixing of both layers. The samples were then submitted to centrifugation at 800 rpm for 30 min with the centrifuge break off. Because the red blood cells contain iron, they are heavier than the rest of the blood cells and, therefore, pellet at the bottom of the tube. Once the centrifugation was completed, the sample contained three layers. The top layer consisted of blood plasma, the bottom layer contained the Ficoll along with red blood cells and the interface contained the rest of the blood cells along with the spiked CAOV3 cells. In order to recover the blood cells on the interface, the plasma was collected and discarded without removing any of the cells in the interface. The interface was then collected and further washed by centrifugation. The bottom layer, containing the Ficoll and red blood cells, was discarded.

After washing to remove any remaining Ficoll, the blood cells were incubated with 250 nM biotin-labeled aptamer or library for 20 min at 4 ^{o}C. After washing, the samples

were incubated with streptavidin PE-Cy5.5 as described above. After washing, the samples were analyzed by flow cytometry. A total of 5 million cells were counted for every sample

Dual detection

As the detection of CAOV3 cells with the DOV-4 aptamer had a high detection limit, we explored the use of a dual labeling to further lower the assays sensitivity. Since the CAOV3 cells are EPCAM positive, a dual detection method was developed using EPCAM-FITC and DOV-4 PE-Cy5.5. For this purpose different CAOV3 cell concentrations, ranging from 5,000 to 500 cells, were spiked in 1 mL of whole blood, pretreated for the removal of red blood cells by Ficoll gradient and incubated with EPCAM-FITC and 250 nM DOV-4 PE-Cy5.5 or Isotype-FITC and 250 nM Library. After washing, the samples were incubated with streptavidin PE-Cy5.5 as described above. The samples were washed twice and analyzed by flow. A total of 5 million cells were counted for every sample.

Results

Aptamer Binding in Complex Media

Since the aptamer selection is performed in an artificial buffer, the aptamer binding has to be confirmed when used in more complex and biologically relevant media. Therefore, the aptamer binding was confirmed for the incubation with the cells in full cell culture media, 100% FBS and human plasma. As observed on Figure 4-1, the aptamers tested retain their binding in the tested medium. Therefore, these aptamers have the potential of being used for the development of a cancer detection method from biological fluids. This potential aptamer use was explored in the following sections.

Detection of Spiked Ovarian Cancer Cells in Whole Blood

The aptamer DOV-4 was selected to used for the development of a FACS-based detection method for ovarian cancer circulating tumor cells. In order to assess the detection limit of the method, several COAV3 cell concentrations were spiked in 1 mL of whole blood and assayed with DOV-4 for the detection by flow cytometry. The dot plot was used to analyze the data. In order to determine the amount of detected cells, a threshold was set using the library-treated blood sample such that 99% of the cells were within this threshold. The number of cells counted plotted against the number of cells spiked showed a linear relationship with an R^2 of 0.97 (Figure 4-2). As shown in Figures 4-2 and 4-3, as few as 10,000 CAOV3 cells spiked in 1 mL of whole blood could be detected by Flow without any pretreatment. By using the linear regression obtained by excel, the theoretical limit of detection (LOD) was calculated by dividing the standard deviation of the line (also known as standard error of the predicted y-value for each x in the regression) by the slope and multiplying by three. The theoretical LOD was determined to be 380 cells per 1 mL of blood. Yet, this LOD cannot be achieved with the method as described above as the control resembles the sample. Indeed, the sample and control are identical when less than 10,000 cells are spiked in 1 mL of whole blood.

In order to further improve the detection limit, the samples were subject to a Ficoll gradient to remove red blood cells. As red blood cells are the major group of cells present in blood, their removal reduces the sample background. Therefore, a lower detection limit was expected after pretreatment of the samples. Unfortunately, the detection limit was not significantly improved (data not shown). This limitation was mainly due to the fact that target cells were not fully separated from the other blood cells in the dot plot. Therefore, a dual labeling using EPCAM-FITC and DOV-4 PE-Cy5.5 was

used to further separate the target cells from the blood cells. As shown on Figure 4-4, the dual labeled CAOV3 cells can be fully separated from the blood cells. By using this method, as few as 500 cells was achieved (Figure 4-5). The number of cells counted plotted against the number of cells spiked showed a linear relationship with an R^2 of 0.99 (Figure 4-5). The theoretical LOD for this method was calculated as described above and was determined to be 91 cells. Nonetheless, the limit of detection could not be further improved because of limitations of flow cytometry. As can be see on Figure 4-5, the analysis of samples spiked with 500 cells yielded the detection of less than 100 cells. The detection of less than 100 cells by flow cytometry is unreliable as the samples resemble the control.

Concluding Remarks

We have shown the potential use of DOV-4 in tandem with EPCAM labeling for the detection of circulating ovarian cancer cells in whole blood. The method developed is easy to perform and requires minimum sample preparation. Nonetheless, the limit of detection is limited to 500 cells per 1 mL of whole blood. In order to consider a circulating tumor cell detection method clinically relevant, a limit of detection of 1-5 tumor cells per 1 mL of whole blood must be achieved. Unfortunately, this limit of detection cannot be achieved using flow cytometry, as the cell background is too high and the method cannot differentiate between controls and samples.

The circulating tumor cells are far outnumbered by normal cells in the blood (1 CTC per 10^6-10^7 normal blood cells), especially during the early development of the disease (*103*). Therefore, a successful molecular platform must be able to enrich them in addition to detecting them. To accomplish this, we propose utilizing the aptamer selected and conjugated them to magnetic nanoparticles for the specific recognition of

CTCs/CSCs in ovarian cancer. The work presented here serves as a proof of the feasibility of using the selected aptamers for the detection of ovarian cancer. Therefore, we plan to utilize these ovarian cancer-specific molecular probes and improve the methodology for enrichment of CTCs/CSCs and depletion of other blood cells, for the capture and detection of ovarian cancer cells in blood.

To date, the number of CTC's present on each stage of ovarian cancer is not known. Therefore, the development of a new method showing high capture efficiency will be useful in the determination of how many CTC's are present on each stage, and, therefore, to develop a blood-based detection method for ovarian cancer.

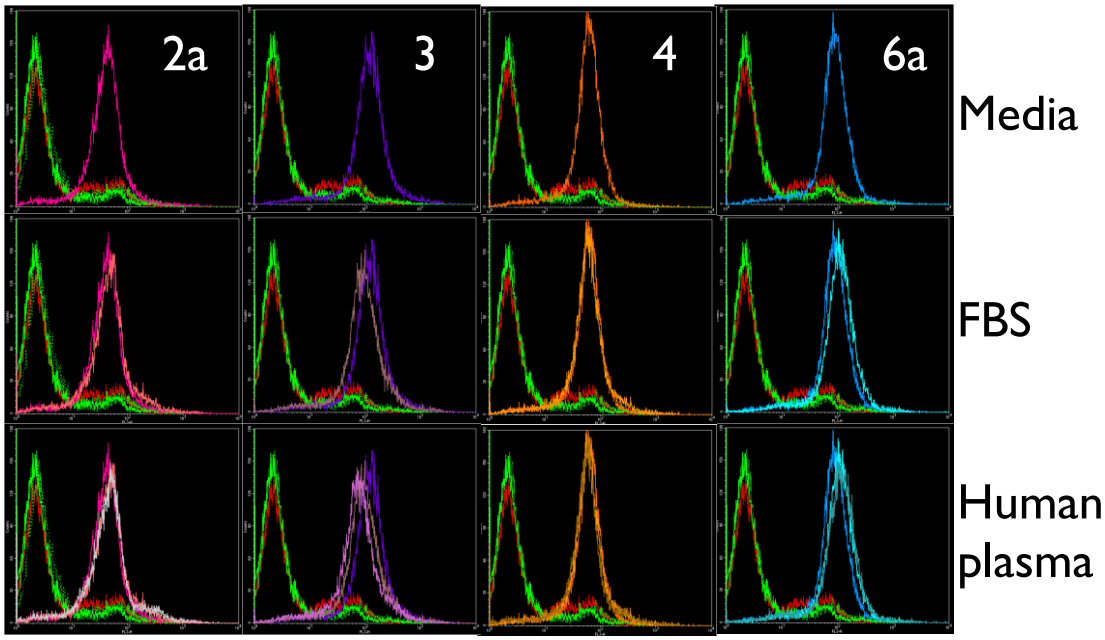

Figure 4-1: Aptamer binding to CAOV3 cells in complex media.

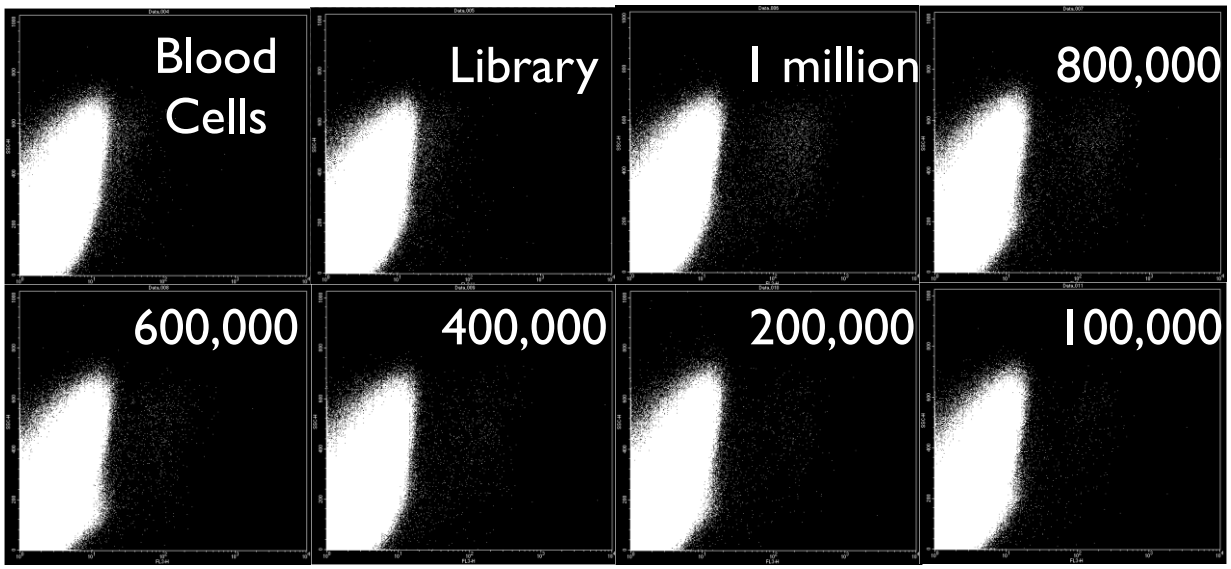

Figure 4-2: Direct incubation of the aptamer DOV-4 for the detection of CAOV3 cells spiked on whole blood

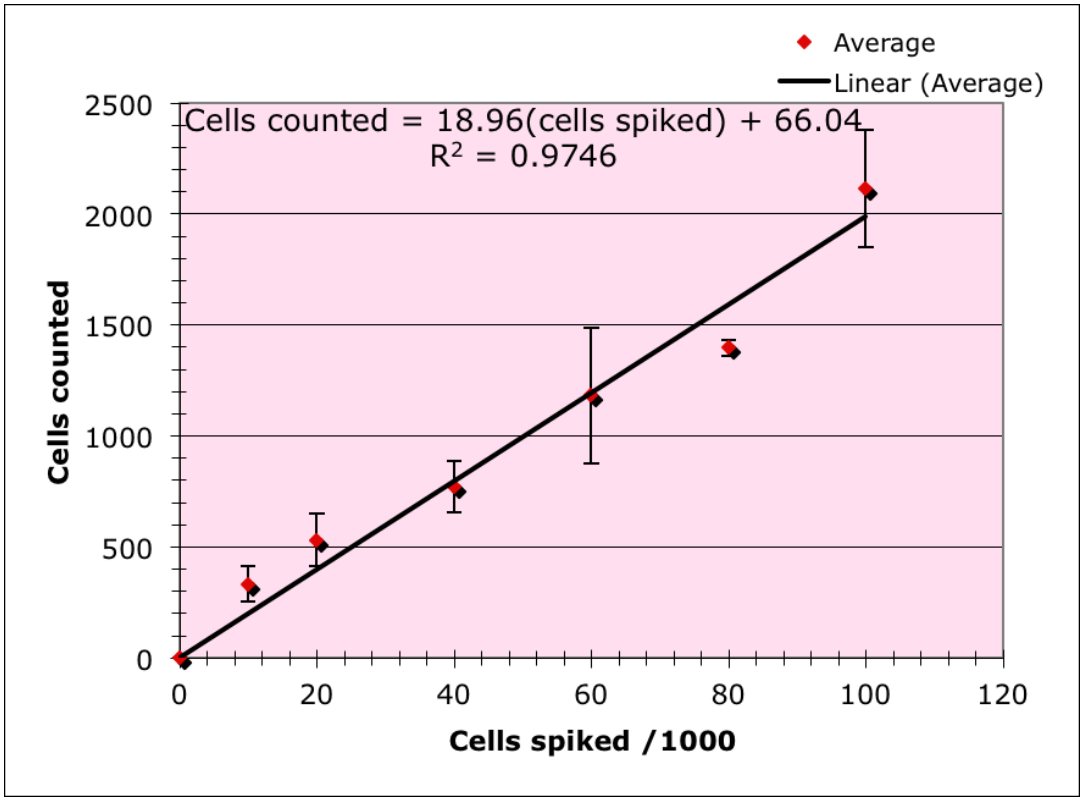

Figure 4-3: Detection of CAOV3 cells spiked in whole blood by FACS.

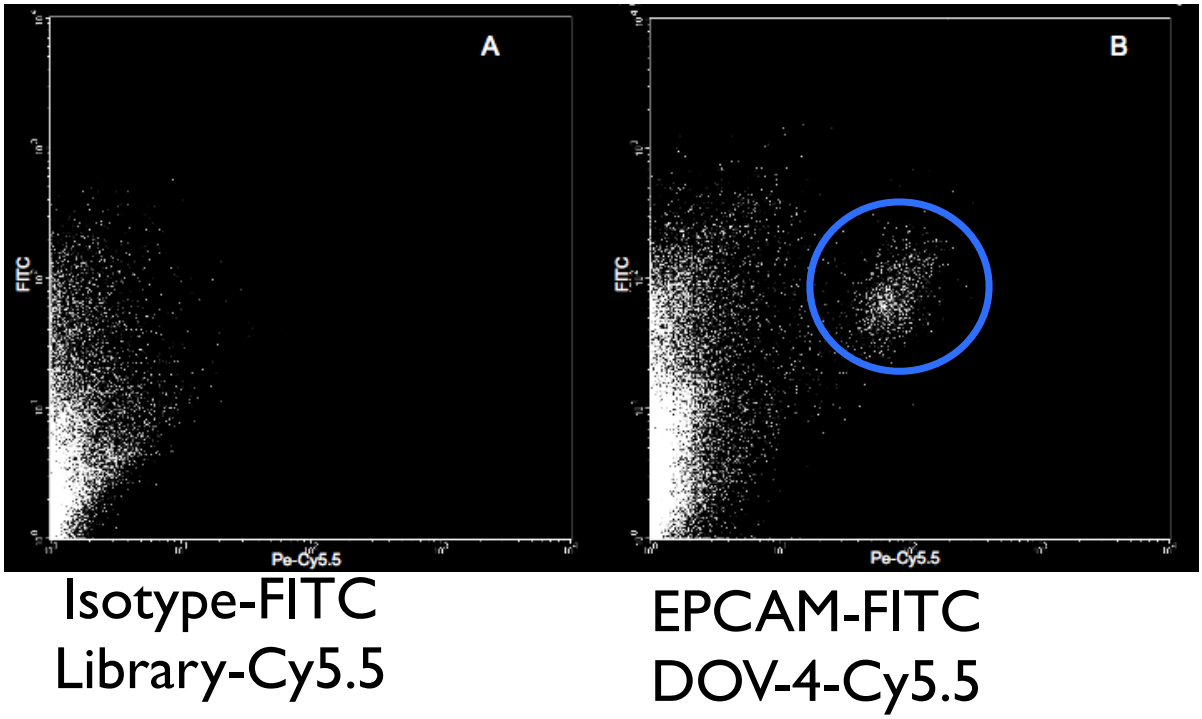

Figure 4-4: Dual labeling of CAOV3 cells using EPCAM FITC and DOV-4 PE-Cy5.5

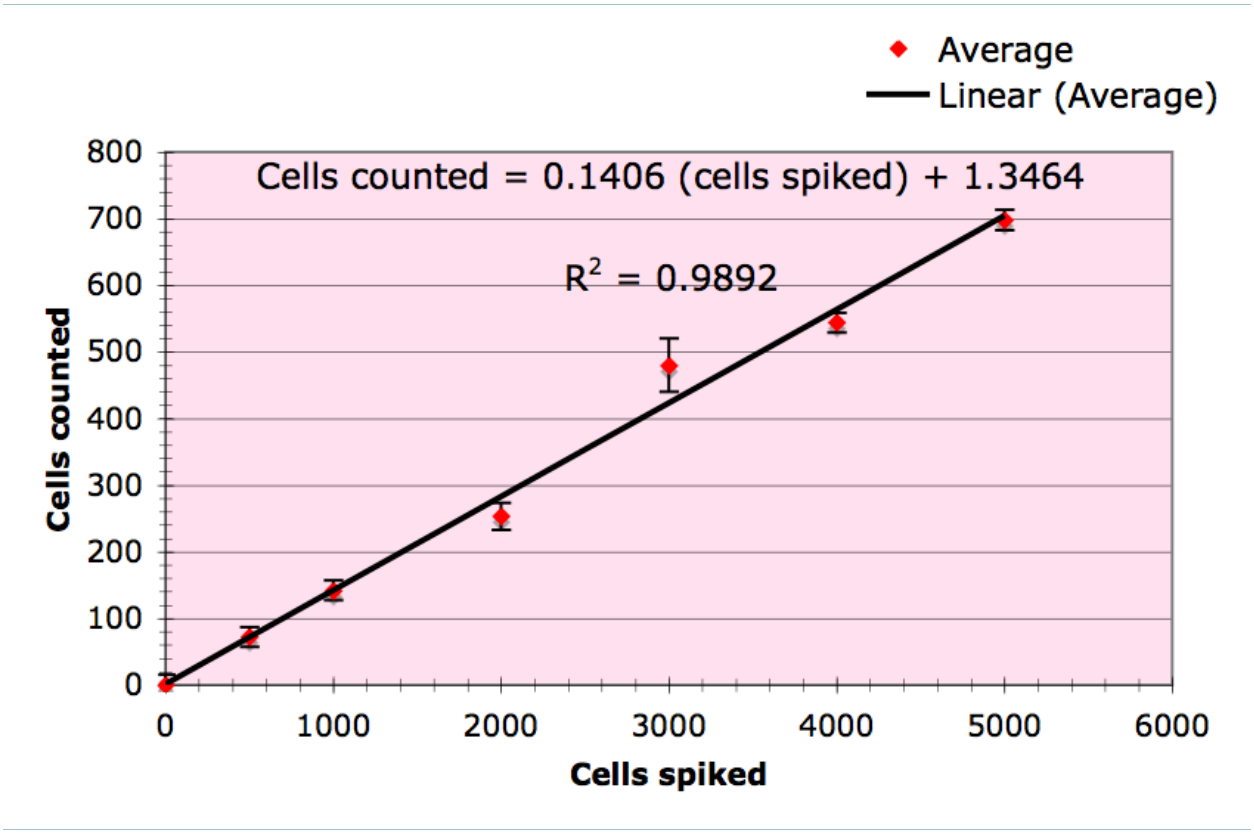

Figure 4-5: Dual detection of CAOV3 cells spiked in whole blood by FACS

CHAPTER 5
ELUCIDATION OF THE APTAMER TARGET ON THE CELL MEMBRANE

Introductory Remarks

Since cell-based SELEX is performed without prior knowledge of the identity of the target on the cell membrane, it is important to find out what type of molecule the aptamer binds to. The most obvious possibility is that the aptamer binds to a protein. This can be confirmed by protease digestion. If the target molecule is a protein, protease digestion often destroys the ability of the aptamer to bind the cells. Using this approach, the targets of several aptamer selected in the Tan group have been identified as membrane proteins (Sgc8 aptamer selected against CCRF-CEM cells binds to PTK-7; TD05 aptamer selected against Ramos cells binds to surface membrane protein IgM) (*37*, *86*). These pieces of evidence suggest surface membrane proteins are common candidates for aptamer targets. On the other hand, other biomolecules can be targeted during the selection process. For example, carbohydrate moieties on the cell membrane, as well as lipids can also serve as targets during the selection process. Thereof, these biomolecules should also be considered during the process of aptamer target identification.

Materials and Methods

Protease Treatment

As observed by other cell-SELEX, the principal aptamer targets are membrane proteins. In order to determine if the aptamers selected bind to membrane proteins, the cells were treated with proteinase K and trypsin prior to performing aptamer binding assays. Trypsin is a serine protease with substrate selectivity for the carboxyl side of lysine and arginine. Meanwhile, proteinase K is a broad-spectrum serine protease.

Trypsin

For trypsin digestion, approximately 5 x 10^6 CAOV3 cells were dissociated with non-enzymatic buffer, washed with PBS and then incubated with 1 mL of 0.05% trypsin/0.53 mM EDTA in HBSS for 0, 5, 15 and 20 min at 37 ^oC. After incubation, the activity of the proteinases was quenched with FBS. After washing with binding buffer, the treated cells were used for aptamer-binding assay using flow cytometer as described above.

Proteinase K

For proteinase K, approximately 5 x 10^6 positive cells were dissociated with 1 mL of 0.05% trypsin/ 0.53 mM EDTA in HBSS, washed with PBS containing 10% FBS and then incubated with 1 mL 0.1 mg/mL or 0.5 mg/mL proteinase K in PBS at 37 ^oC for 0, 5, 15 and 20 min. The activity of the proteinases was quenched with FBS. After washing with binding buffer, the treated cells were used for aptamer-binding assay using flow cytometer as described above.

Inhibitors of Protein Glycosylation

In order to determine if the aptamer target is a glycoprotein, the cells were treated with four different inhibitors of glycosylation. Two inhibitors of O-linked glycosylation and two inhibitors of N-linked glycosylation were incubated with CAOV3 cells for 24 hours. After incubation, the cells were assayed for aptamer binding as described above. If the target is a glycoprotein, a reduction in the aptamer's mean fluorescence intensity will be observed.

Monensin

Monensin transports ions, such as Li^+, Na^+, K^+, Rb^+ and Tl^+, across the cell membrane, blocking protein transport. CAOV3 cells were seeded on a petri dish and

incubated with 1 μM, 2 μM and 5 μM monensin for 24 hours. After the incubation, the cells were tested for binding to the aptamer as described above. Untreated cells were used as positive control. If the aptamer binds to a glycoprotein, a reduction in the mean fluorescence intensity should be observed.

Tunicamycin

Tunicamycin inhibits GlcNac phosphotransferase (GPT), blocking all N-linked glycosylation and inhibiting the synthesis of all N-linked glycoproteins. CAOV3 cells were seeded on a petri dish and incubated with 1 μM tunicamycin for 24 hours. After the incubation, the cells were tested for binding to the aptamer as described above. Untreated cells were used as positive control. If the aptamer binds to a N-linked carbohydrate moiety from a glycoprotein, a reduction in the mean fluorescence intensity of the aptamer, as compared to untreated cells, will be observed.

Swainsonine

Swainsonine is a known inhibitor of N-linked glycosylation. It inhibits glycoside hydrolases and disrupts Golgi alpha manosidase II. This inhibitor has been previously used in the literature to determine if the target of interest is a N-linked glycoprotein (104, 105). CAOV3 cells were seeded on a petri dish and incubated with 5 μM and 10 μM swainsonine for 24 hours. After the incubation, the cells were tested for binding to the aptamer as described above. Untreated cells were used as positive control. If the aptamer binds to a N-linked carbohydrate moiety from a glycoprotein, a reduction in the mean fluorescence intensity of the aptamer, as compared to untreated cells, will be observed.

Benzyl-2-acetamido-2-deoxy- α-D-galactopyranoside

Benzyl 2-acetamido-2-deoxy-α-D-galactopyranoside is a know inhibitor of O-linked glycosylation. Also inhibits 2,3(O)-sialyltransferase and disrupts glycoprotein targeting (104). CAOV3 cells were seeded on a petri dish and incubated with 1mg/mL benzyl 2-acetamido-2-deoxy-α-D-galactopyranoside for 24 hours. After the incubation, the cells were tested for binding to the aptamer as described above. Untreated cells were used as positive control. If the aptamer binds to an O-linked carbohydrate moiety from a glycoprotein, a reduction in the mean fluorescence intensity of the aptamer, as compared to untreated cells, will be observed.

Glycosidase Treatment

Carbohydrate moieties on the surface of membrane proteins (glycoproteins), as well as lipids (glycolipids) present possible candidates for the aptamer target. To address if the aptamer recognizes a carbohydrate moiety on the surface of the protein, a series of glycosidases (Sigma Aldrich Co., St. Louis, Mo) were used to digest all carbohydrate moieties on the cell membrane.

PNGase F

PNGase F is a glycosidase capable of removing most N-linked carbohydrate moieties. This enzyme removes the full length N-linked carbohydrate. For the PNGase F digestion, approximately 2×10^6 positive cells were resuspended with non-enzymatic buffer, washed with PBS and then incubated with 5,000 to 50,000 U of PNGase F in reaction buffer (provided with the kit) at 37 ^{o}C for 1, 2 and 3 hours. The concentration of the glycosidases and the incubation time were optimized to obtain maximum carbohydrate digestion without affecting the cell viability. After washing with binding

buffer, the treated cells were used for aptamer-binding assay using flow cytometry as described above.

Neuraminidase

Neuraminidase is an O-linked glycosidase. Although PNGase F is capable of removing the full-length N-linked sugars, no such O-linked glycosidase exists. Since most O-linked carbohydrates contain a sialic acid moiety at the end of the chain, cells were treated with Neuraminidase. Neuraminidase is a glycosidase that cleaves the glycosidic linkage of neuraminic acids (or sialic acid). For the Neuraminidase digestion, approximately 2 x 10^6 positive cells were resuspended with non-enzymatic buffer, washed with PBS and then incubated with 50 and 150 U of Neuraminidase in reaction buffer (provided with the kit) at 37 ^oC for 1, 2 and 3 hours. The concentration of the glycosidases and the incubation time were optimized to obtain maximum carbohydrate digestion without affecting the cell viability. After washing with binding buffer, the treated cells were used for aptamer-binding assay using flow cytometry as described above.

α-Fucosidase

Alpha-1,2 Fucosidase is a glycosidase which releases alpha-1,2-fucose from the non-reducing end of complex carbohydrates. For the Fucosidase digestion, approximately 2 x 10^6 positive cells were resuspended with non-enzymatic buffer, washed with PBS and then incubated with Fucosidase in reaction buffer (provided with the kit) at 37 ^oC for 1 hour. After washing with binding buffer, the treated cells were used for aptamer-binding assay using flow cytometry as described above.

Treatment of Cells with Azide-Labeled Sugars

Click chemistry by azide-alkyne recognition is a very selective reaction. The metabolic incorporation of azide-labeled sugars (Figure 5-12A) into the cell membrane's

carbohydrates has been previously explored (*106*, *107*). Their incorporation into the cell does not affect cellular functions, thus allowing the use of these artificial sugars *in vitro* as well as *in vivo* (*106*). Many alkyne reagents exist that can be chemical conjugated to these azide sugars, such as alkyne-biotin (Figure 5-12B), thus allowing the modification of these sugars for multiple applications.

To determine if the aptamer target is an oligosaccharide moiety, the cell's carbohydrates were labeled with biotin groups via click chemistry and further conjugated to neutravidin (Figure 5-13). If the target of the aptamer is indeed a carbohydrate, the neutravidin molecule will block access to the target, and a reduction in the mean fluorescence intensity will be observed. The cell labeling was accomplished by metabolically labeling all the carbohydrates on the cell with azide-labeled glucose, galactose and mannose (Fisher, Rockford, Il). In order to incorporate the azide label to the cells, the cells were incubated with 40 μM azide labeled sugars (Figure 5-12A) for 7 passages to allow complete incorporation of the non-natural sugars into all the cell's carbohydrate moieties. After incubation, the aptamer binding was verified by incubating 5×10^5 cells with 250 nM biotin-labeled aptamer or library solution for 20 min at 4 ºC. After washing, the cells were incubated with streptavidin-PE-Cy5.5 for 20 min at 4 ºC. After washing, the cells were analyzed by flow cytometry as described above. A total of 20,000 events were counted.

Once the cells were labeled with the azide sugars, all sugars were labeled with a biotin group using click chemistry by incubating 3×10^6 cells with 50 μM, 100 μM or 250 μM biotin-alkyne reagent (Fisher, Rockford, Il, Figure 5-12B) for 2 hour or 3 hours at room temperature. After washing, the biotin-labeled sugars were blocked by incubating

with 5 mg/mL neutravidin solution dissolved in BB. In order to monitor the incorporation of the azide sugars into the cell, streptavidin-Alexa 488 was added to the neutravidin solution to a concentration of 1 µg/mL. After washing, streptavidin was blocked with 1 mM biotin solution prior to aptamer incubation. After washing, the cells were incubated with 250 nM biotin-labeled aptamer or library solution for 20 min at 4 ºC. After washing, the cells were incubated with streptavidin-PE-Cy5.5 for 20 min at 4 ºC. After washing, the cells were analyzed by flow cytometry as described above. A total of 20,000 events were counted.

To further determine if the decrease in aptamer binding was due to the introduction of neutravidin into the cell's carbohydrate moieties or if the effect is merely due to steric interference, the cells were treated with 0.1 mg/mL proteinase K for 20 min at 37 ºC to remove the cell membrane's extracellular proteins prior to treatment of the cells with the alkyne-biotin reagent and introduction of the neutravidin group as described above.

Results

Protease Treatment

Trypsin and Proteinase K have previously been used to determine if the aptamer target on the cell membrane is a protein (*37*, *86*). In order to determine if the aptamers selected for CAOV3 bind to a membrane protein, cells were incubated with trypsin or proteinase K and tested for binding to DOV-2a, DOV-3, DOV-4 and DOV-6a. As can be seen on Figure 5-1, the aptamer binding is conserved after treatment with both proteases. Furthermore, the mean fluorescence intensity increases after proteinase K treatment. In order to determine if the protease concentration used was insufficient, cells were also treated with a higher proteinase K concentration (0.5 mg/mL). As shown

in Figures 5-2 and 5-3, the aptamer binding for DOV-3 and DOV-4 (respectively) is retained and no difference is observed between the treatment with 0.1 mg/mL or 0.5 mg/mL. These results suggest that the aptamer target is either not a cell membrane protein, or the protein is not accessible to proteases.

Inhibitors of Glycosylation

Since protease cleavage might be hindered by heavy glycosylation, the cells were further treated with inhibitors of glycosylation. The inhibitors were selected to have different effects on the protein glycosylation and transport. Monensin was selected as an inhibitor of protein transport. Tunicamycin and swainsonine were selected as both inhibit N-linked glycosylation. Finally, Benzyl-2-acetamido-2-deoxy- α-D-galactopyranoside was selected as an inhibitor of O-linked glycosylation. After treatment with four inhibitors of glycosylation, the aptamer binding is maintained (Figure 5-4). Because the inhibitors used reduce protein glycosylation and export to the cell membrane, these results suggest the aptamer target is unlikely to be a glycoprotein.

Glycosidase Treatment

Since the aptamer target seems unlikely to be a protein or glycoprotein, carbohydrate moieties on the cell membrane were explored as potential aptamer targets. To do so, cells were treated with different glycosidases: PNGase F, Neuraminidase and Fucosidase. PNGase F is a known N-linked glycosidase and was chosen to determine if the aptamer target is a N-linked carbohydrate moiety. Three different PNGase F concentrations were tested, 5,000, 20,000 and 50,000 U. As shown on Figure 5-5, no changes in the aptamer binding were observed. In order to determine if the glycosidase incubation time was insufficient, the enzyme was incubated with the cells for 1, 2 and 3 hours. As can be observed in Figure 5-6, no change was observed.

As a final assessment of the effect of PNGase F on the aptamer binding, cells were treated with 0.1 mg/mL Proteinase K for 20 min at 37 ºC prior to treatment of the cells with 50,000 U PNGase F for 3 hours. After treating the cells with both, the protease and glycosidase, the aptamer binding was not affected by the glycosidase treatment (Figure 5-7).

As the aptamer binding is retained after treatment with a N-linked glycosidase, the possibility of having an O-linked glycosidase as target was explored. Since there is no known O-linked glycosidase capable of removing the full-length sugar, cells were treated with Neuraminidase. Two glycosidase concentrations were tested, 50 and 150 U. As shown on Figure 5-8, the aptamer binding improves with the treatment of the cells with Neuraminidase. The cells were further treated with 150 U Neuraminidase for 1, 2 and 3 hours, but no change in the aptamer binding was observed (Figure 5-9). The cells were also treated with 0.1 mg/mL proteinase K for 20 min at 37 ºC followed by treatment with 150 U of Neuraminidase for 3 hours. As observed in Figure 5-10, the mean fluorescence intensity further increases after the sequential treatment of the cells with proteinase K and Neuraminidase. Treatment with Fucosidase yielded similar results (Figure 5-11). These results suggest the aptamer target is not a N-linked carbohydrate moiety, yet the possibility of having the aptamer binding to the core of an O-linked protein remains.

Treatment of Cells with Azide- Labeled Sugars

In order to verify if the incorporation of the azide group on the sugar moieties affects the aptamer's capability of recognizing its target, aptamer binding was verified after metabolically labeling CAOV3 cells with azide-labeled glucose, mannose or galactose, as well as cells labeled all three sugars. As shown on Figure 5-13, the

incorporation of these non-natural sugars doesn't affect the aptamer's capability of recognizing its target on the cell membrane. The incorporation of the azide group into the cell was corroborated by incubating the cells with streptavidin- Alexa 488 (data not shown). In order to ensure full labeling of the azide sugars with the alkyne-biotin moiety, the alkyne-biotin concentration was optimized to 250 nM. Furthermore, the alkyne incubation time was optimized to 3 hours (Figure 5-14). As shown on Figure 5-14, treatment of the azide-labeled cells with 250 nM alkyne solution for 3 hours, followed by incubation with 5 mg/mL neutravidin solution resulted in a decrease in the aptamer binding to the target cells.

To further determine if the decrease in aptamer binding was due to the introduction of neutravidin into the cell's carbohydrate moieties or if the effect is merely due to steric interference, the cells were treated with 0.1 mg/mL proteinase K for 20 min at 37 ºC to remove the cell membrane's extracellular proteins prior to treatment of the cells with the alkyne-biotin reagent and introduction of the neutravidin group. As shown on Figure 5-15, treatment of the cells with proteinase K prior to the introduction of the neutravidin group results in lower mean fluorescence intensity, thus a reduction in the aptamer binding is observed. Since previous experiments showed that treatment of the cells with proteinase K result in an increase in the aptamer binding, this reduction in aptamer binding must be due to the blocking of the aptamer target by the neutravidin group.

Concluding Remarks

Initial efforts to identify the aptamer target have been explored. Cell treatment with proteases showed no effect in the aptamer target, suggesting the aptamer target is unlikely to be a membrane protein. Furthermore, treatment with inhibitors of

glycosylation further disproved glycoproteins as potential aptamer targets. Although the cells were treated with glycosidases to determine if the aptamer target is a carbohydrate, the results are inconclusive. Treatment of the cells with PNGase F showed no change in the aptamer binding. This can be due to the fact that PNGase F is not as efficient when used in native proteins. Therefore, other N-linked glycosidases capable of cleaving N-linked sugars from native proteins need to be explored. Furthermore, treatment with Neuraminidase further improves the aptamer binding to the cells. These results may suggest the aptamer might be binding to the core of an O-linked carbohydrate. On the other hand, since sialic acid has a negative charge and DNA is a poly anion, the removal of sialic acid residues with Neuraminidase may be improving the aptamer binding by reducing the repulsion between equal charges. The results obtained by blocking the carbohydrate moieties with neutravidin suggest the aptamer target may be oligosaccharide. Yet, further treatment with other glycosidases and the use of a cocktail of glycosidases, such as N-DEGLY and E-DEGLY (Sigma Aldrich Co., St. Louis, Mo), will be explored to further prove or disprove carbohydrates as the aptamer target.

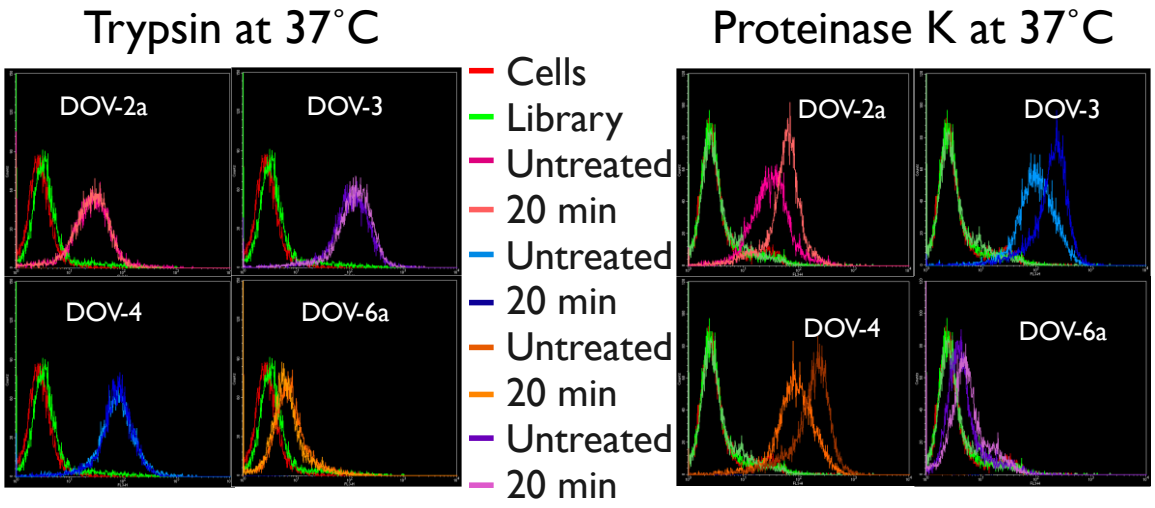

A B

Figure 5-1: Effect of protease treatment on the aptamer binding. (A) Treatment of CAOV3 cells with trypsin for 20 min at 37 ^{o}C (B) Treatment of CAOV3 cells with Proteinase K for 20 min at 37 ^{o}C

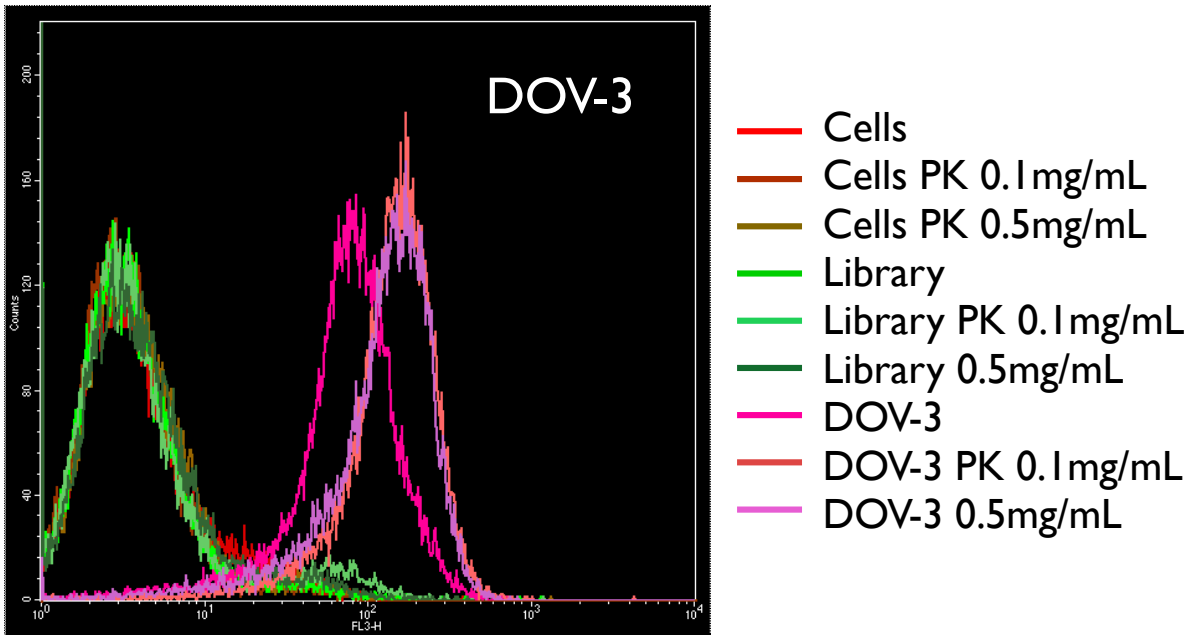

Figure 5-2: DOV-3 binding after treatment of CAOV3 cells with 0.1 mg/mL and 0.5 mg/mL proteinase K.

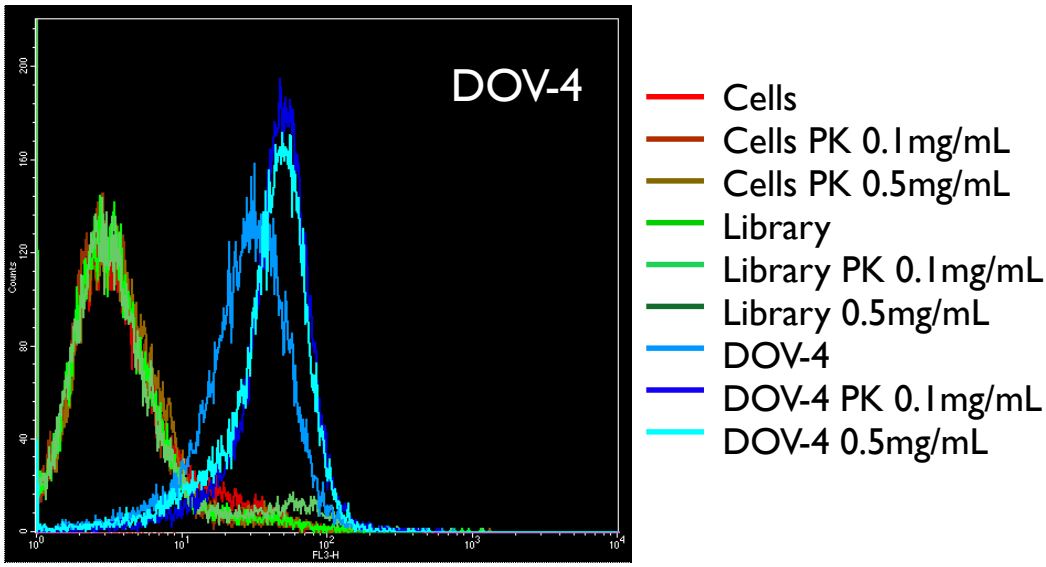

Figure 5-3: DOV-4 binding after treatment of CAOV3 cells with 0.1 mg/mL and 0.5 mg/mL proteinase K.

A

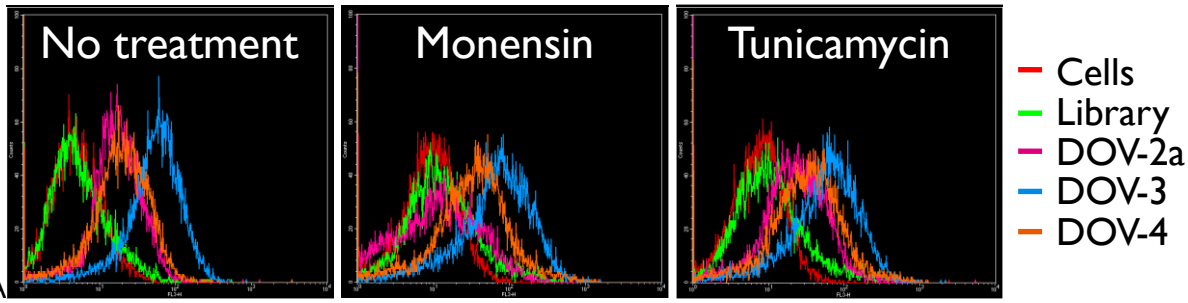

B

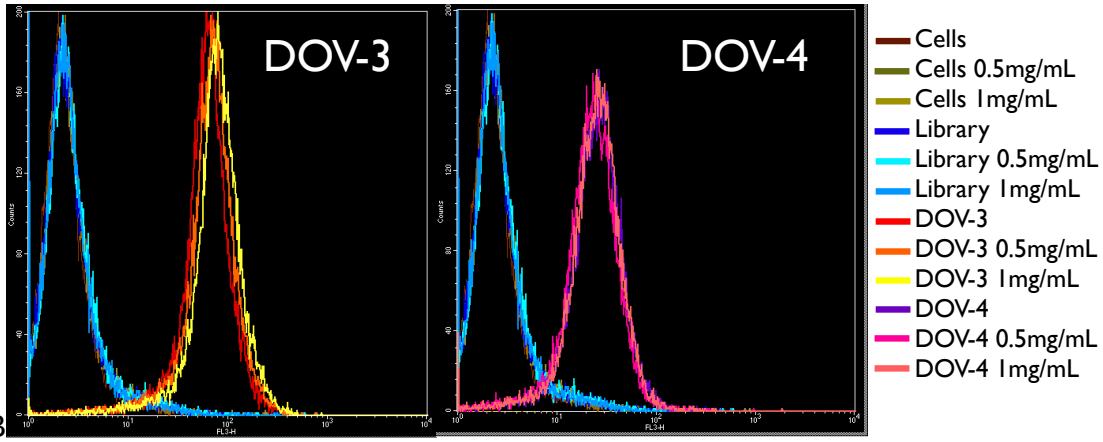

Figure 5-4: Effect of the treatment with inhibitors of glycosylation on the aptamer binding (A) Treatment with 1 μM monensin and tunicamycin. (B) Treatment with 1 mg/mL Benzyl-2-acetamido-2-deoxy- α-D-galactopyranoside (C) treatment with Swainsonine

C 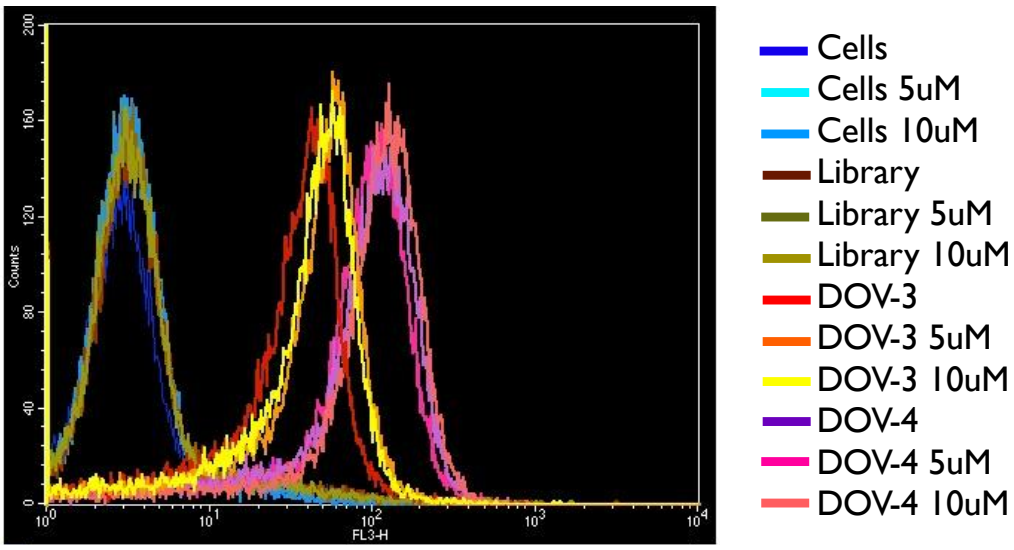

Figure 5-4: Continued

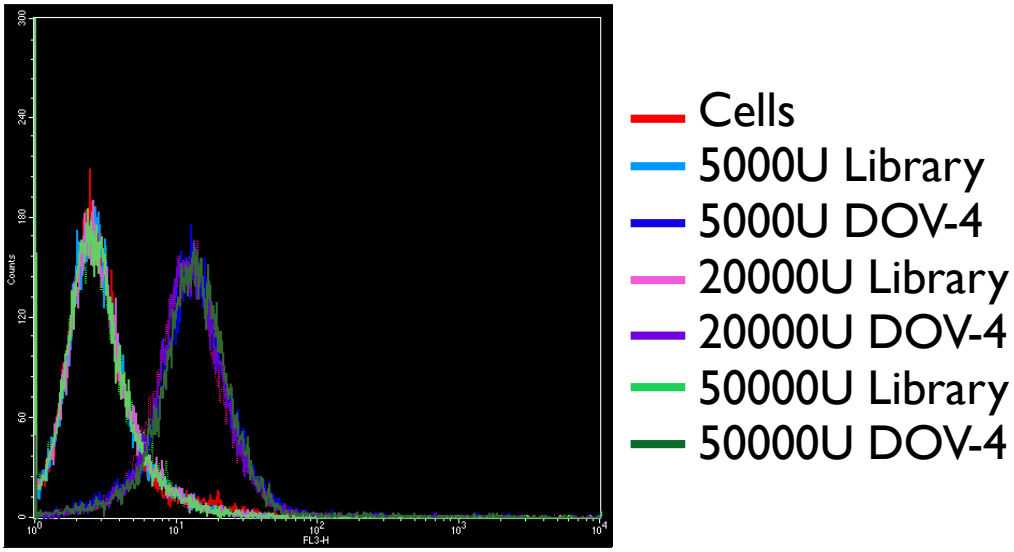

Figure 5-5: PNGase F treatment: Optimization of enzyme concentration

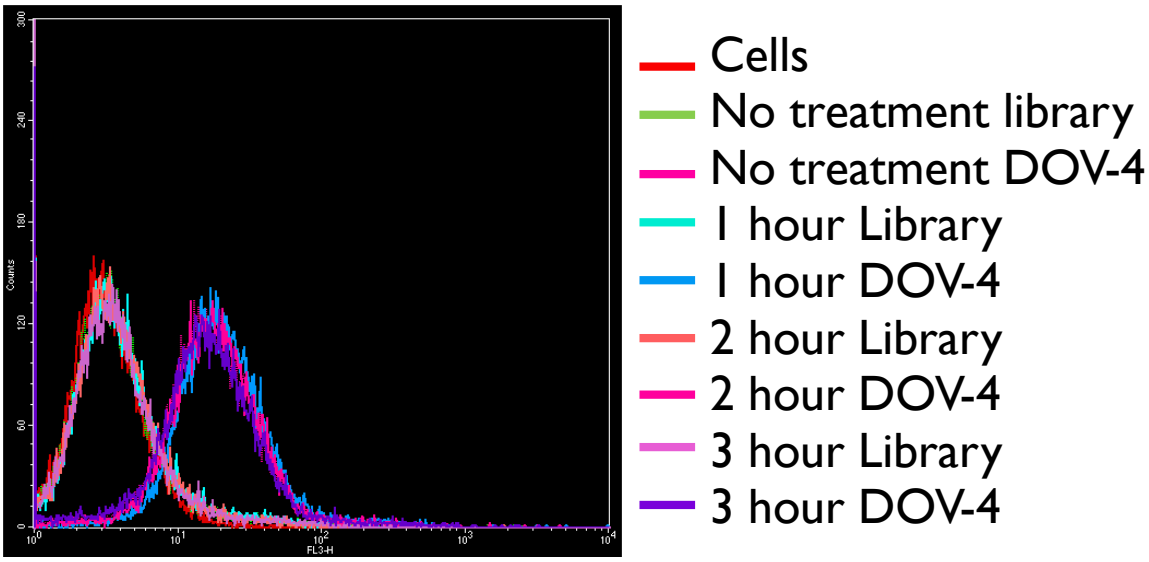

Figure 5-6: PNGase F Treatment: Optimization of incubation time

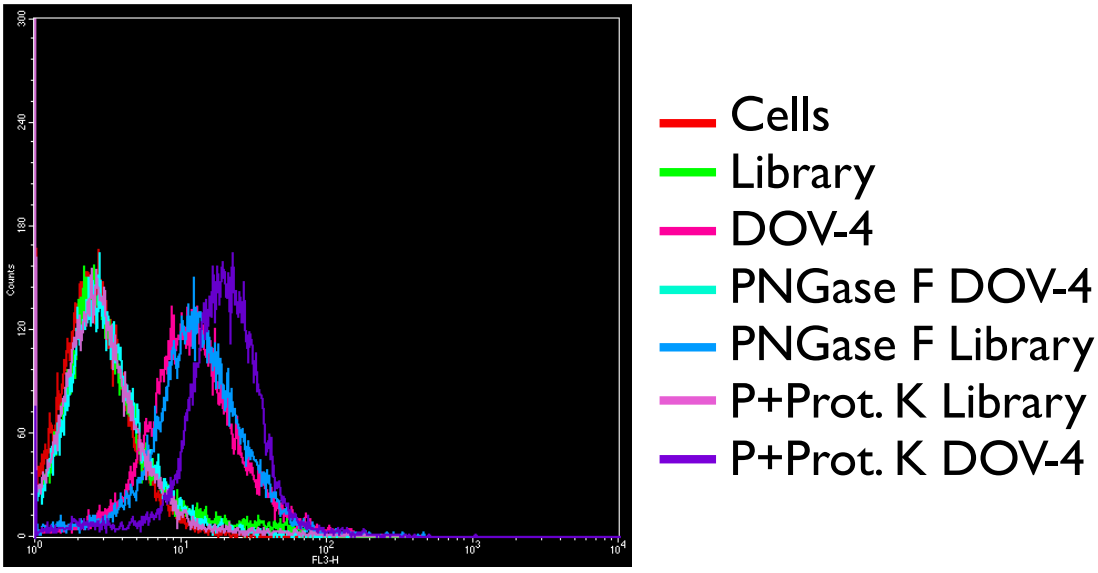

Figure 5-7: PNGase F treatment, followed by treatment with proteinase K for 20 min.

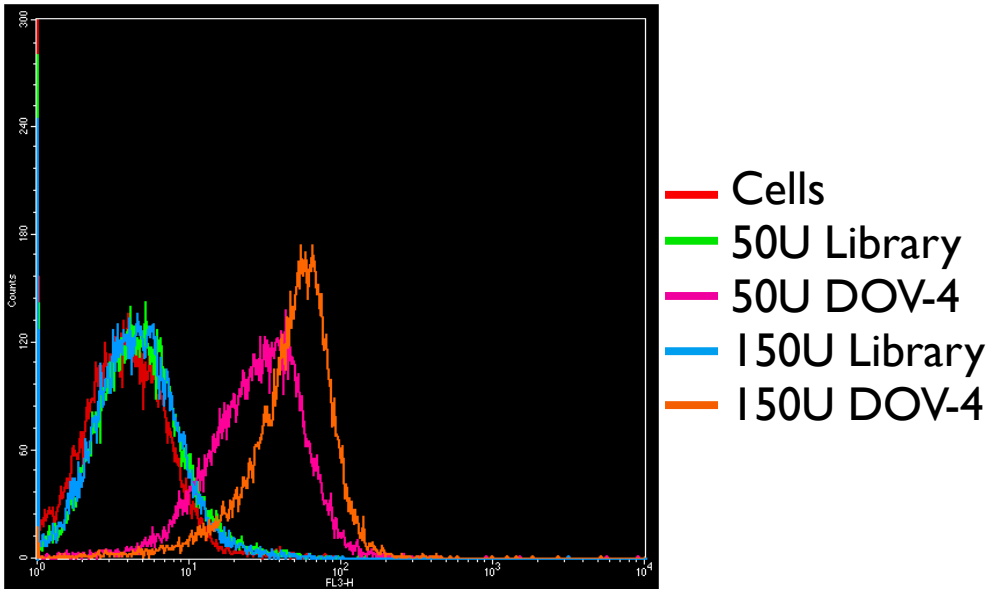

Figure 5-8: Neuraminidase treatment: optimization of enzyme concentration

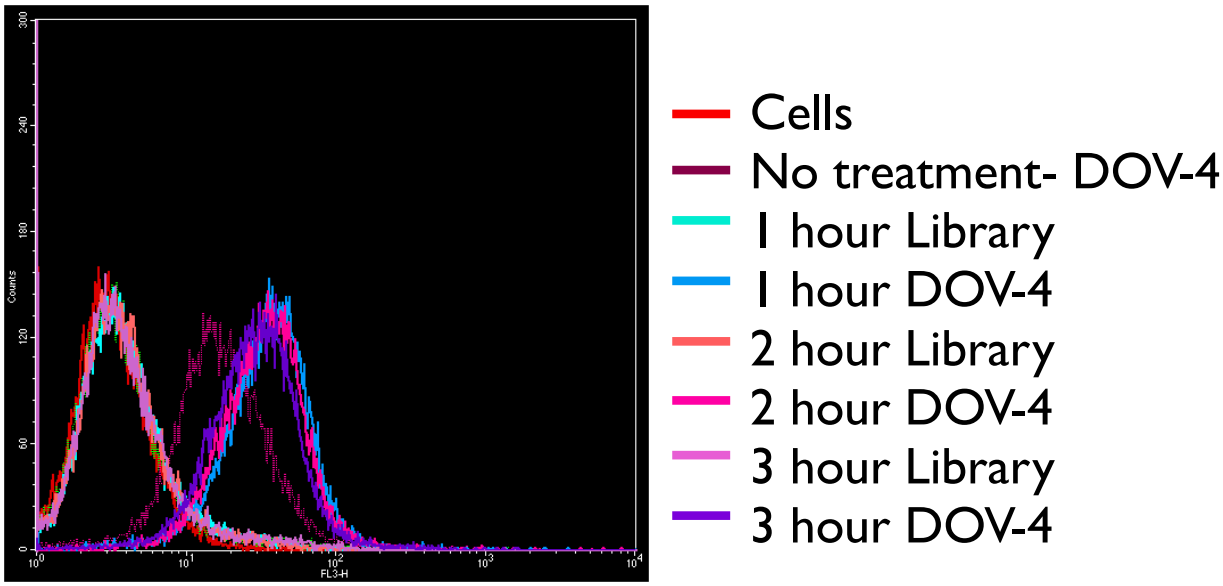

Figure 5-9: Neuraminidase treatment: Optimization of the incubation time

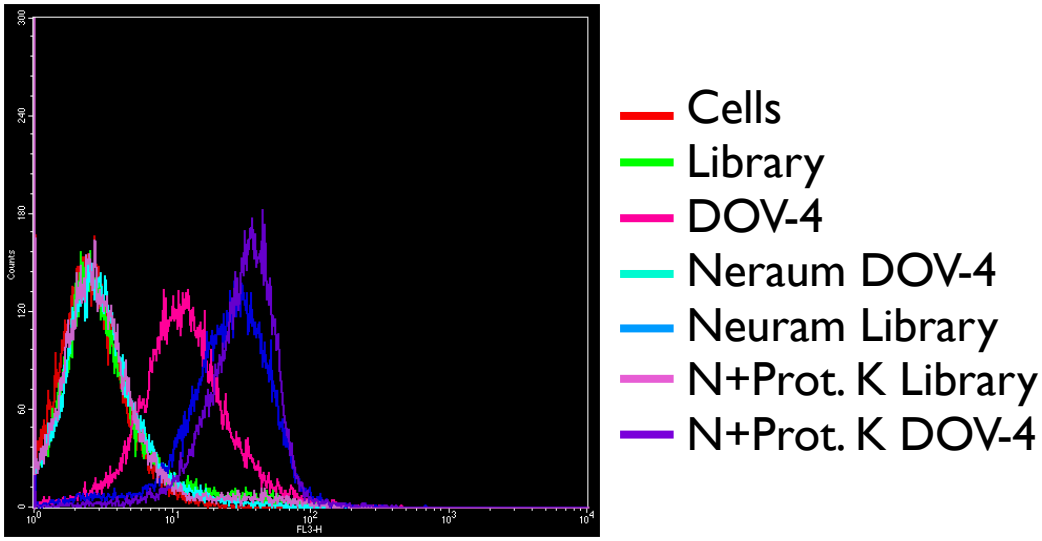

Figure 5-10: Neuraminidase treatment, followed by treatment with proteinase K for 20 min

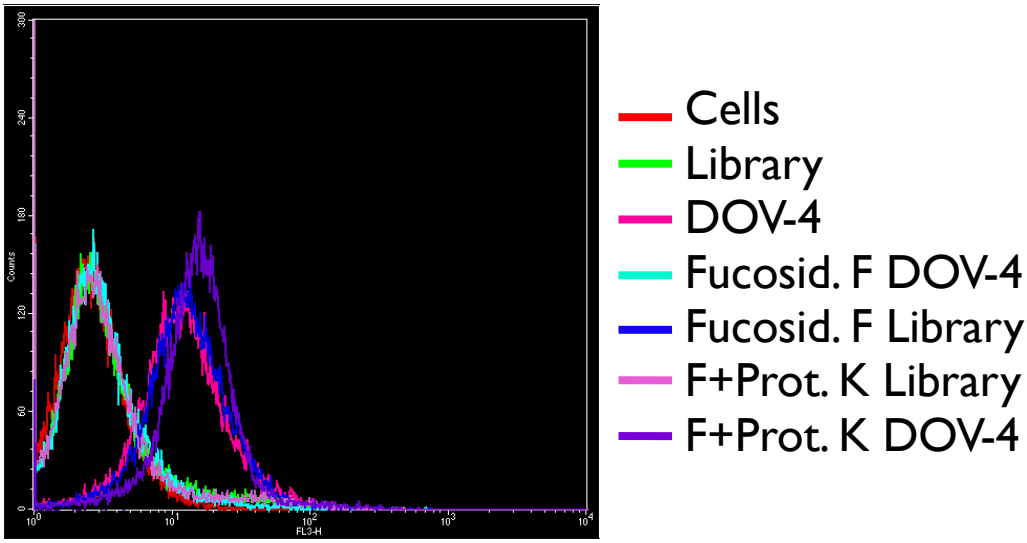

Figure 5-11: Fucosidase treatment, followed by treatment with proteinase K for 20 min.

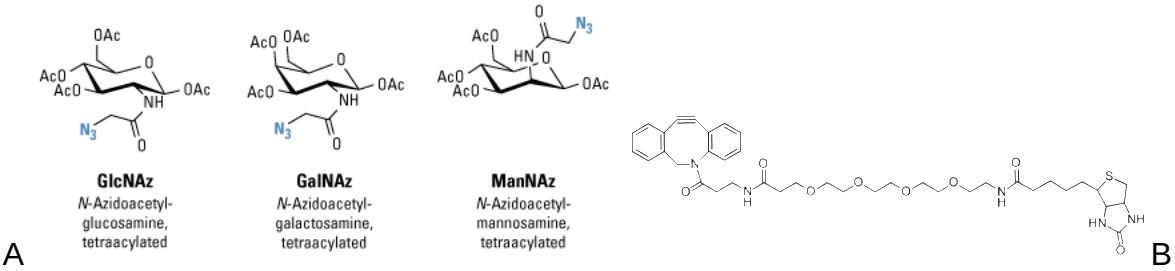

A B

Figure 5-12: Structures of azide sugars and biotin-alkyne: (A) Azide sugars used. (B) biotin-alkyne reagent used.

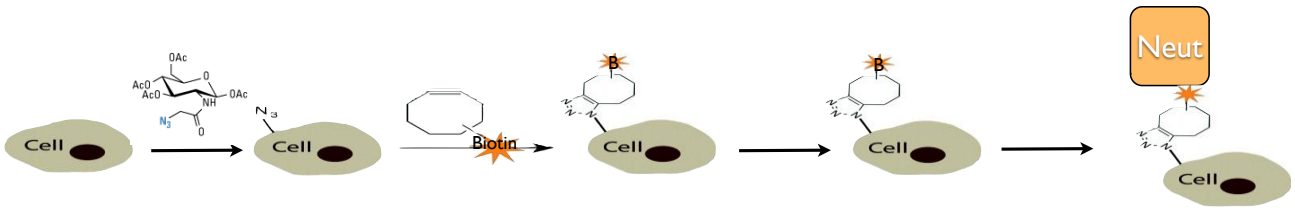

Figure 5-13: Schematic representation of the labeling of carbohydrates with neutravidin via azide-alkyne chemistry and biotin-neutravidin interaction.

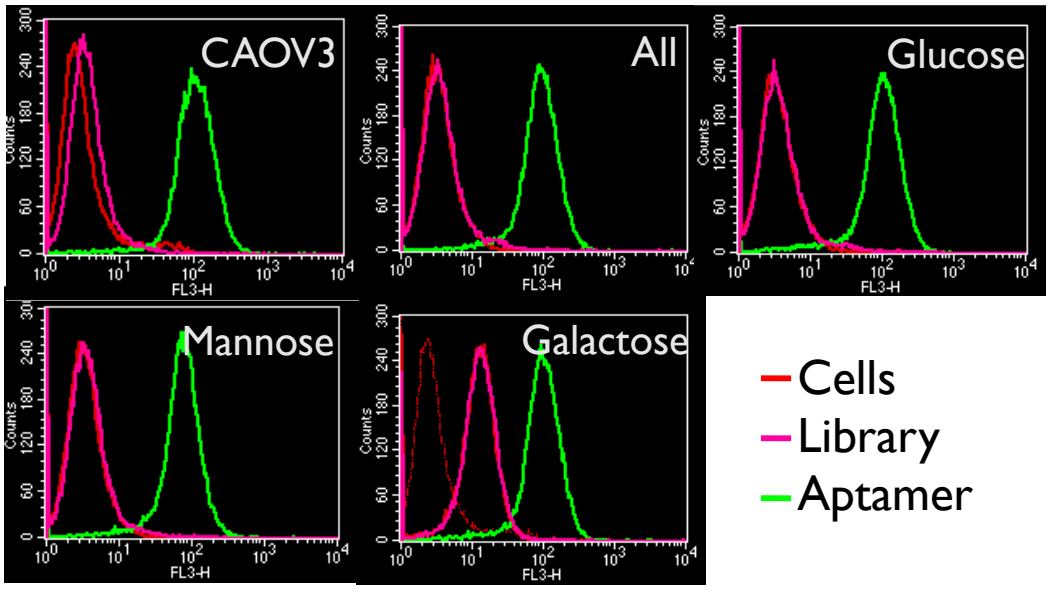

Figure 5-14: Aptamer binding after the metabolic incorporation of azide-labeled sugars. Aptamer binding was confirmed for untreated cells, cells labeled with all three sugars, azide-glucose, azide-mannose or azide-galactose.

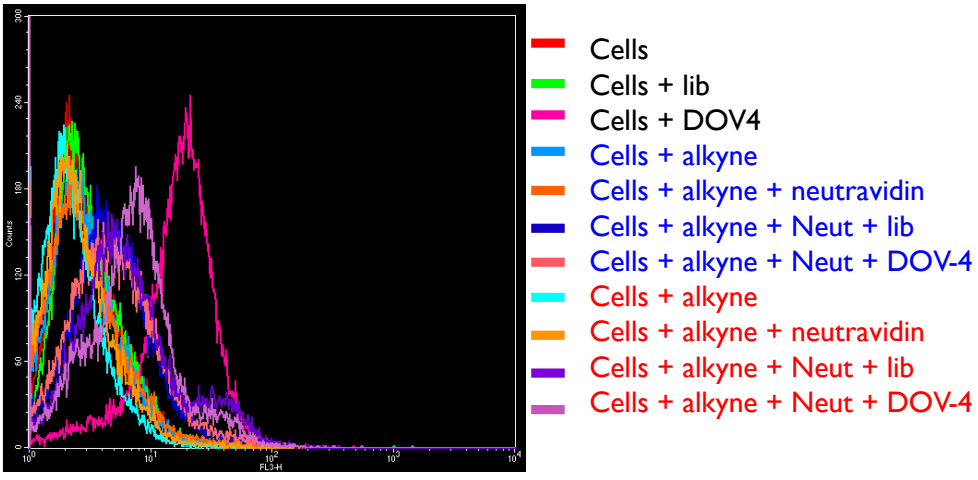

Figure 5-15: Optimization of the alkyne incubation time. Black: untreated cells. Blue: cells treated with alkyne solution for 3 hours. Red: cells treated with alkyne solution for 2 hours.

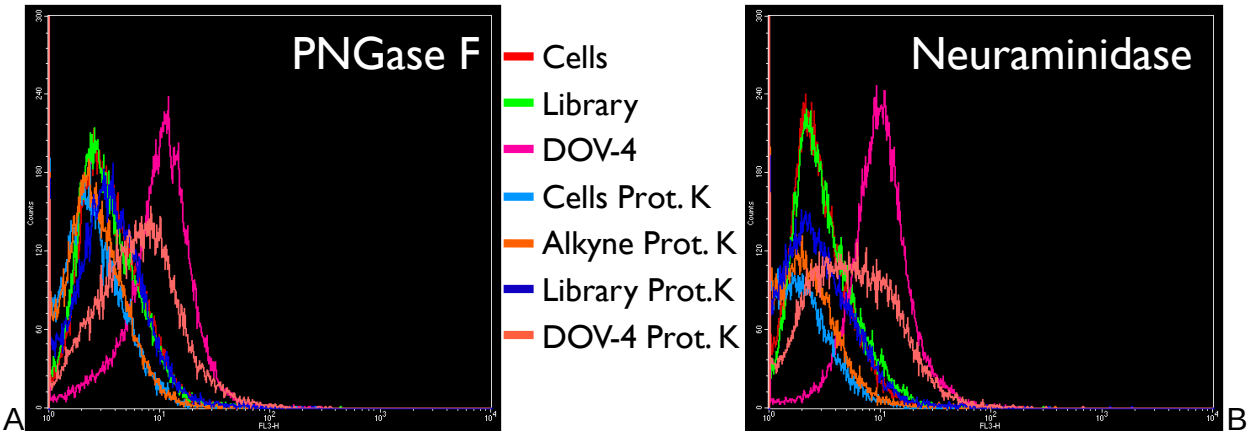

Figure 5-16: Effect of proteinase K treatment on the aptamer binding. (A) Treatment with proteinase K followed by treatment with PNGase F. (B) Treatment with proteinase K followed by treatment with Neuraminidase.

CHAPTER 6
CONCLUSION

Summary of Dissertation

A panel of six aptamers binding to CAOV3 cells was selected by cell-SELEX. Each aptamer was characterized to determine binding affinity and selectivity. The aptamer affinities lie between 40 and 130 nM. The aptamers showed cross-reactivity to other cancer cell lines, including the negative cell line (HeLa). Although the aptamers bind to other cell line, they show no binding to normal blood cells. Furthermore, one of the selected aptamers showed no binding to a ovarian benign cyst cell line, while a second aptamer showed no binding to normal epithelial lung cancer. Therefore, their use as probes for the enrichment and detection of circulating tumor cells in blood remains a potential application for disease detection. This application was explored and a proof-of concept method for the detection of ovarian cancer cells spiked in whole blood was developed using flow cytometry. After testing the aptamer DOV-4 and EPCAM as dual labeling for the detection of circulating tumor cells by Flow cytometry, a limit of detection of 500 cells per milliliter of whole blood was observed. Thereof, this aptamer shows great potential for the detection of circulating tumor cells. Nonetheless, their utility needs to be validated using real samples. On the other hand, the aptamer target on the cell membrane needs to be identified. Our initial efforts of identifying the aptamer target have shown that the target is unlikely to be a membrane protein, as the aptamer binding is retained after treatment with trypsin and proteinase K. Treatment of the cells with inhibitors of glycosylation, as well as treatment with several glycosidases showed no effect in the aptamer binding. Nonetheless, further testing of the cells with different glycosidases needs to be performed.

Future Work

As the aptamer target remains elusive, further efforts will be done to identify it. Other glycosidases will be used for the cleavage of carbohydrate moieties on the cell membrane. Furthermore, the glycosidases will be used as a cocktail to ensure full removal of the carbohydrate moieties. If the aptamer binding remains after further glycosidase treatment, the target is more likely to be a lipid. As an attempt to identify the target lipid, purified commercially available lipids will be used to form micelles. The micelles will be tested for binding to the aptamers.

Further aptamer applications will also be explored. A mice protocol was written and approved by the IACUC (protocol # 200801491). Here, we propose to grow CAOV3 solid tumors in nude mice. The tumors will then be imaged *in vivo* using DOV-4 conjugated to a NIR dye or a NIR dye-labeled magnetic nanoparticle. The use of aptamers in conjunction with ultrasound contrast agents will also be explored. Furthermore, the aptamer will be immobilized into a nanoparticle containing cisplatin for the targeted therapy of CAOV3 solid tumors.

The aptamers selected will be further used for the profiling of ovarian cancer. Before the aptamers can be used for profiling, they have to be validated for the binding and detection of ovarian cancer patient samples. In order to accomplish this goal, patient samples provided by the H. Lee Moffitt Cancer Center and Research Institute will be assayed with the aptamers. Those aptamers that are capable of recognizing the ovarian cancer patient samples will be used to create a profile for ovarian cancer staging. Each aptamer will be assayed for binding to patient samples from all four stages to determine which aptamers bind to each stage. The binding pattern of each aptamer will be analyzed and correlated to the different stages of ovarian cancer.

In order to accomplish this goal, 50 patient samples will be evaluated. Also, 20 samples from normal epithelial cells will be used as negative controls. To perform the analysis, the tissue samples will be suspended in solution using non-enzymatic cell dissociation solution (Cellgro) and filtered with 40 μM Cell Strainer (BD Falcon). Once the cells are put into solution, 10^{5}-10^{6} cells from each patient sample and negative control will be washed three times with washing buffer and incubated with 250 nM FITC-labeled aptamer in binding buffer on ice for 20 min. After washing the samples three times with washing buffer, the aptamer binding will be determined using flow cytometry as explained above. The binding pattern for each aptamer will be evaluated and correlated with the stage of ovarian cancer represented by each patient sample. Once this task is successfully completed, the aptamer panel can be used, not only to diagnose, but to stage ovarian cancer. This is important as the treatment of ovarian cancer depends on the cancer stage and classification. Also, the development of multiple aptamers capable of recognizing ovarian cancer will provide with the selectivity and sensitivity needed for the development of an assay for early detection of ovarian cancer. Using this panel of aptamers for early detection will provide with lower false negative and false positive results.

APPENDIX A
SELECTION OF MYCOPLASMA POSITIVE CELLS

Introduction

Mycoplasma is a genus of bacteria frequently present in cell cultures around the world, and present a serious problem in cell-based research (*108*). These bacteria contain no cell wall, making them resistant to most antibiotics, such as penicillin. Because of their small size (around 0.3-0.8um), mycoplasma cannot be observed by phase contrast microscopy. Furthermore, unlike other bacterial contamination, mycoplasma species grow very slowly and, therefore, do not cause visible changes to the cell culture media nor destroy the cell culture. Because of the lack of visible signs of mycoplasma contamination, it is estimated that 15% of all cultures in the United States are affected (*109*, *110*).

Although no visible changes are present, mycoplasma contamination affects nearly every cellular function and parameter, including growth, metabolism, morphology, cell attachment, membrane characteristics and chromosomal changes. Therefore, publications and data gathered using mycoplasma-contaminated cells are suspect and subject to scrutiny (*108*, *111*, *112*). Moreover, many mycoplasma detection methods are commercially available and should be used for routine mycoplasma contamination testing on all mammalian cell cultures (*110*, *111*, *113*-*115*).

Cell-SELEX or cell-based Systematic Evolution of Ligands by EXponential enrichment is a technique used to select aptamer probes capable of binding to cell surface markers. Aptamers are short (around 100nt) single-stranded nucleic acids, DNA or RNA, which adopt a well-defined three dimensional structure, allowing them to recognize and bind to the target with high affinity and specificity (*37*, *63*, *82*, *116*).

Because this recognition capability depends on the presence of membrane surface markers, the success of cell-SELEX can be jeopardized by mycoplasma contamination.

In this work, we demonstrate the importance of mycoplasma contamination in Cell-SELEX, which was employed to select a pool enriched for mycoplasma-positive ovarian cancer cells. The selected aptamers were tested with to mycoplasma-negative cells, but no binding was observed. It is, therefore, likely that the aptamer target of the tested sequences was induced by the mycoplasma contamination.

Materials and Methods

Instrumentation and reagents

All oligonucleotides were synthesized by standard phosphoramidite chemistry using a 3400 DNA synthesizer (Applied Biosystems) using a 1 μM scale, and were purified by reversed-phase HPLC (Varian Prostar) using a C18 column and 0.1 M TEAA in water and acetonitrile as mobile phases. All PCR mixtures contained 50 mM KCl, 10 mM Tris-HCl (pH 8.3), 2.0 mM $MgCl_2$, dNTPs (each at 2.5 mM), 0.5 μM of each primer, and Hot start Taq DNA polymerase (5 units/μL). PCR was performed on a Biorad Thermocycler and all reagents were purchased from Takara. Monitoring of pool enrichment, characterization of the selected aptamers, and identification of the target protein assays were performed by flow cytometric analysis using a FACScan cytometer (BD Immunocytometry Systems). Trypsin and Proteinase K were purchased from Fisher Biotech. The TOPO T/A cloning kit and *E. coli* were purchased from Fisher. Cells were tested for mycoplasma contamination using the PCR based mycoplasma detection kit from Takara (CAT# 6601). The DNA sequences were determined by the Genome Sequencing Services Laboratory at the University of Florida.

Cell culture and buffers

The CAOV-3 and HeLa cell lines where obtained from the American Type Cell Culture (ATCC). The CAOV-3 ovarian cancer cell line was maintained in culture with MCBD 105:Medium 199 (1:1); the HeLa cell line was cultured in RPMI-1640. All media where supplemented with 10% FBS and 100 U/mL Penicillin-Streptomycin. All cell lines where incubated at 37 °C in a 5% CO_2 atmosphere.

During the selection, cells were washed before and after incubation with wash buffer (WB), containing 4.5 g/L glucose and 5 mM $MgCl_2$ in Dulbecco's phosphate buffered saline with calcium chloride and magnesium chloride (Sigma). Binding buffer (BB) used for selection was prepared by adding yeast tRNA (0.1 mg/mL) (Sigma) and BSA (1 mg/mL) (Fisher) to the wash buffer to reduce background binding.

SELEX library and primers

The HPLC-purified library contained a randomized sequence of 40 nucleotides (nt) flanked by two 20-nt primer hybridization sites:

(5'- ACT ACC AAC GAG CGA CCA CT $(N)_{40}$ AGA GTT CAG GAG AGG CAG GT-3'). The forward primers were labeled with 5'-FITC, and the reverse primers were labeled with 5'-biotin.

In Vitro cell-SELEX

In this study, mycoplasma-positive CAOV3 was used as the target cell line and mycoplasma-positive HeLa was used for counter-selection. For the first round, the cells were incubated with 20 pmol of naïve ssDNA library dissolved in BB. For later rounds, 75 pmol of enriched pool dissolved in BB to a final concentration of 250 nM was used for incubation. Before incubation, the ssDNA pool was denatured by heating at 95 °C for

5 min and was cooled rapidly on ice for 5 min, allowing each sequence to form the most stable tertiary structure.

The cells were washed twice with 3mL of WB and incubated with the DNA pool on ice in an orbital shaker for 30 min. The bound sequences were eluted in 500 µL BB by heating at 95 °C for 15 min, cooled on ice for 5 min and centrifuged at 14,000 rpm for 2 min. The supernatant containing the DNA sequences was then incubated with a negative cell line (HeLa) for 60 min on ice in an orbital shaker remove sequences binding to general surface markers. The unbound sequences were collected and amplified by PCR using the FITC- and biotin-labeled primers. Amplifications were carried out at 95 °C for 30 sec, 60 °C for 30 sec, and 72 °C for 30 sec, followed by final extension for 3 min at 72 °C. The selected sense ssDNA was separated from the biotinylated antisense ssDNA by streptavidin-coated sepharose beads (Amersham Bioscience). The ssDNA was eluted from the sepharose beads by melting in a 0.2 M NaOH solution. As the selection progressed, the cells were washed with increased stringency to remove weakly binding sequences (increased WB volume and number of washes).

The enrichment of specific sequences was assayed using flow cytometry as explained below. When the level of enrichment reached a plateau, pools of interest were cloned and submitted for sequencing.

Cloning using TOPO T/A

The T/A cloning strategy was selected for cloning mainly on the basis of its ease of use pertaining to the cloning of PCR products. T/A cloning takes advantage of the terminal transferase activity of *Taq* polymerase, which adds a single 3'-A overhang to each end of the PCR product. In order to prepare the PCR product for T/A cloning, the

enriched selected ssDNA pool was subjected to PCR amplification using non-labeled primers, as described above. The PCR was performed with a 15 min final extension stage to ensure efficient adenylation of the PCR product.

Once the PCR product was fully adenylated, it was then ligated into the TOPO T/A vector by incubating 2 µL of fresh PCR product with 1 µL of the TOPO vector in ligation buffer in a final volume of 10 µL for 20 min at room temperature. Then, the plasmid was transfected into *E. coli* by incubating 2 µL of the TOPO cloning reaction mixture with one shot of chemically competent *E. coli* provided by the cloning kit at 37 ^{o}C for 30 min in an orbital shaker. The transformed *E. coli* was grown in petri dishes containing Luria Bertani (LB) medium supplemented with 15 g/L of agar, 50 µg/mL of ampicillin and 40 µL of 40 mg/mL X-gal.

Since the plasmid contains a gene that provides resistance to the antibiotic used in the medium, only the bacteria that contain the plasmid will grow on the medium. As the PCR product is inserted inside the β-galactosidase gene in the plasmid, those bacteria containing a PCR product successfully ligated into the plasmid will form white colonies, while those bacteria containing empty plasmid will form blue colonies. The colonies containing PCR product were collected and submitted for sequencing by the University of Florida's sequencing core.

Aptamer binding studies by flow cytometry

To determine the binding of the aptamers, the target cells (5×10^5) were incubated with 250 nM of 5'-FITC labeled aptamers on ice for 20 min in 100 µL of BB. Cells were then washed twice with 500 µL of WB, and were suspended in 200 µL of BB for flow cytometric analysis, using a 5'-FITC labeled random sequence as the negative control. All the experiments for binding assays were repeated at least 2 times.

Results

In order to prove that mycoplasma contamination can affect the results obtained during Cell-SELEX, two cancer cell lines were chosen to perform a full selection. The ovarian cancer cell line CAOV3 was chosen for the selection of ovarian cancer aptamers. In order to identify aptamers that specifically bind to ovarian cancer cells, the cervical cancer cell line HeLa was used for counter-selection. Both cell lines were mycoplasma-positive during the selection process. The SELEX procedure is described briefly below. A detailed description is provided in the experimental section.

To start the selection process, 20 pmol of naive library was incubated with mycoplasma-positive CAOV3 cells to yield an enriched pool. Sequences showing non-specific binding to general cell surface markers were removed by incubating the enriched pool with HeLa cells (rounds 6 to 13). The eluted pool for each round of SELEX was amplified through PCR, after which the ssDNA pools of interest were recovered and monitored for enrichment toward CAOV3 by flow cytometry. As the selected pools were enriched with sequences that recognize and bind to the target cell line, an increase in fluorescence signal was observed (Figure 1a). The enriched pools showed minimum enrichment for HeLa-binding sequences (Figure 1b). After 13 rounds of SELEX, an enriched pool that specifically bound to the CAOV3 cell line, but marginally to HeLa cells, was obtained (Figure 1). Thus, the pool was successfully enriched for sequences binding surface markers expressed by CAOV3 cell line, but not by cervical cancer cells. To demonstrate that the selection was compromised by the presence of mycoplasma in the cell culture, the pools were also tested for binding to mycoplasma-negative cells, and little enrichment was observed (Figure 2).

Following completion of the selection process, two pools were chosen and submitted for cloning and sequencing: the final pool (round 13) and the previous pool (round 12). The sequences were aligned into families according to homology, and aptamer candidates were chosen from each family. Six sequences showing the best homology throughout the pools were selected as aptamer candidates, synthesized and tested for binding to mycoplasma-negative CAOV3 cells, and no binding was observed (Figure 3).

Concluding remarks

In conclusion, we have selected a pool that is capable of recognizing mycoplasma-positive CAOV3 cells but not mycoplasma-negative cells. These results are significant, as the effect of mycoplasma contamination was not expected to change the cell profile to the extent of selecting aptamers unable to cross-react with mycoplasma-negative CAOV3 cells. Therefore, this selection shows the importance of performing mycoplasma testing throughout the entire cell-SELEX process (at least weekly). Otherwise, the researcher runs the risk of selecting for a cell target that is an artifact produced by the mycoplasma infection. Furthermore, publications involving the selection of aptamers against whole cells should be required to show negative results for mycoplasma testing of the target cells to ensure that the data are reliable.

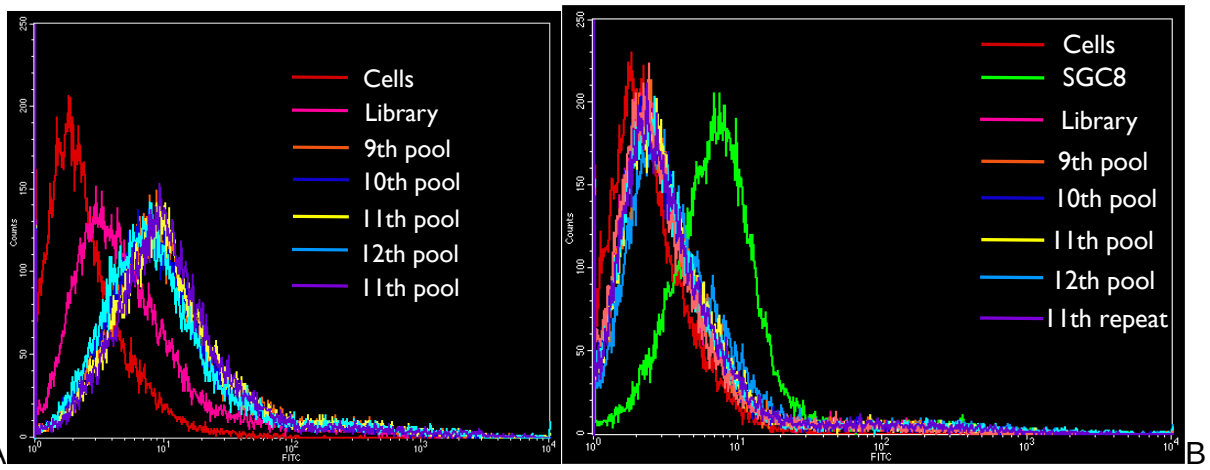

A B

Figure A-1: Monitoring of the selection progress: (A) Binding of the enriched pools to CAOV3 cells. The red histogram corresponds to cells only. The pink histogram corresponds to unselected library. Dark blue corresponds to the 10th round. Yellow corresponds to the 11th rounds. Light blue corresponds to the 12th rounds. Purple corresponds to 11th pool repeat. (B) Binding of the enriched pools to HeLa cells. The red histogram corresponds to cells only. The pink histogram corresponds to unselected library. Dark blue corresponds to the 10th round. Yellow corresponds to the 11th rounds. Light blue corresponds to the 12th rounds. Purple corresponds to 11th pool repeat. The green histogram corresponds to the binding of Sgc8 to HeLa cells.

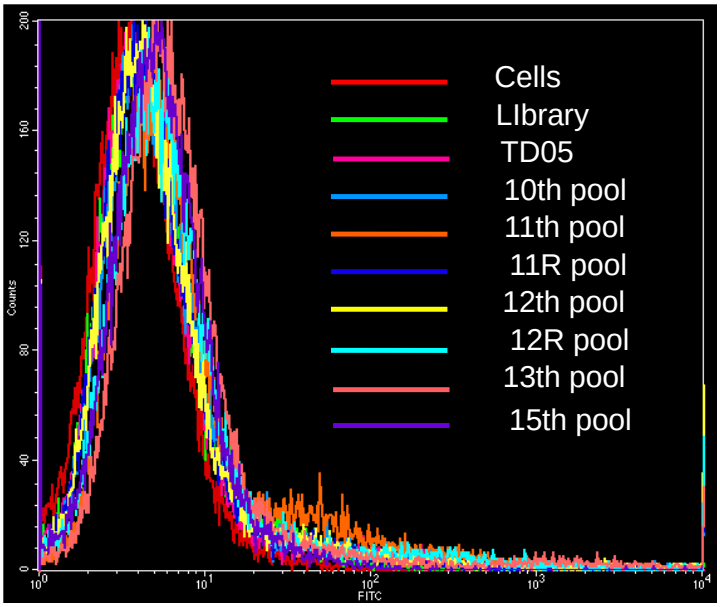

Figure A-2: Aptamer binding to mycoplasma negative CAOV3 cells.

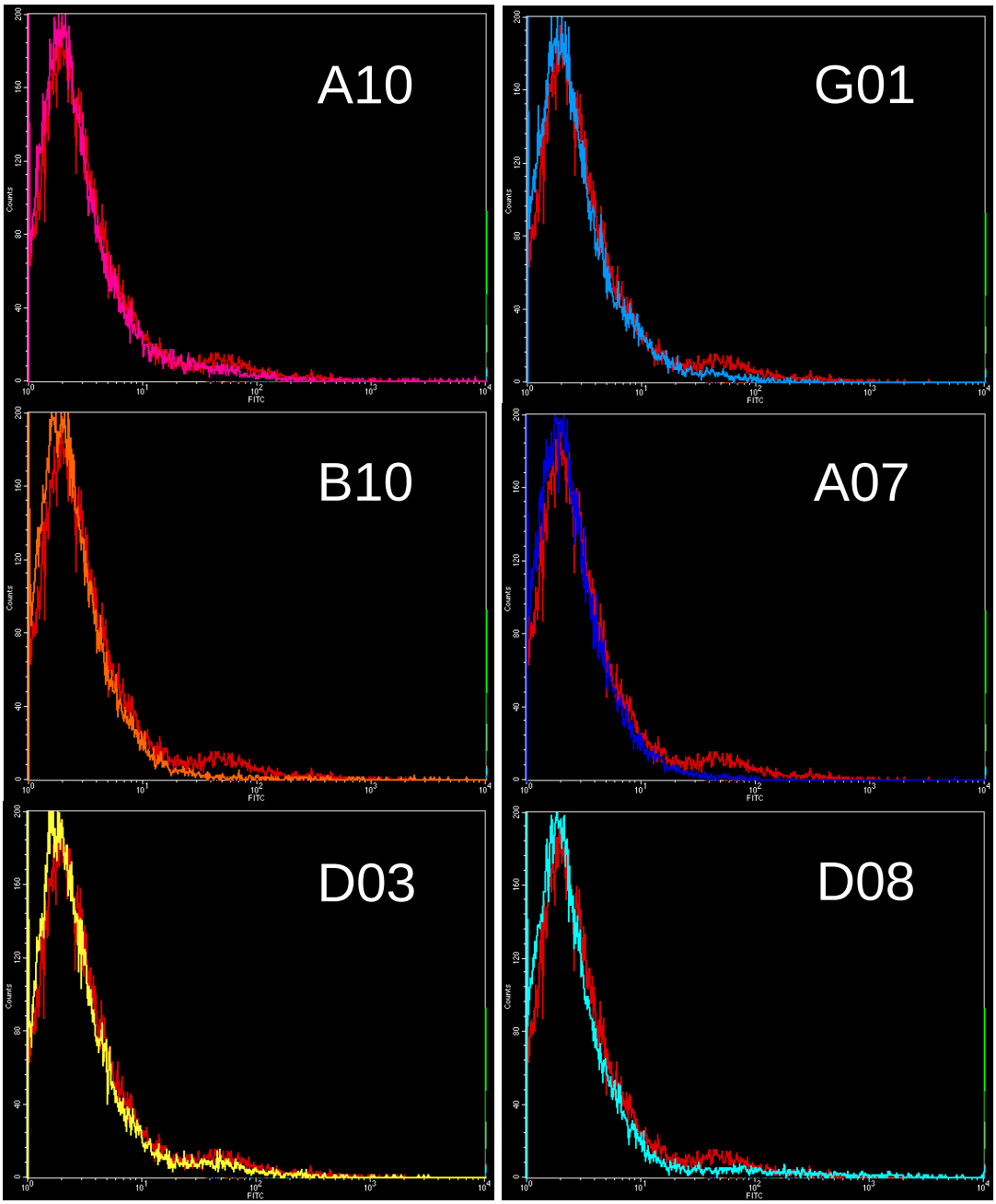

Figure A-3: Candidate aptamer binding to mycoplasma negative CAOV3 cells

APPENDIX B
CHEMICAL APTAMER CONJUGATION TO THE AAV CAPSID

Introduction

Gene delivery is one of the most promising therapeutic approaches available nowadays for the treatment of several diseases (*117*, *118*). This method is based on the introduction of genetic material into cells for the production of therapeutic proteins or blocking the expression of harmful proteins. Gene therapy can be done in vivo by directly implanting or injecting the therapeutic DNA. It can also be done ex vivo by harvesting the patient's cells, expand them and transfect them prior to implantation or injection of the cells into the patient (*119*).

An ideal gene transfer vector should be: safe, it must not induce cellular toxicity or provoke an immune reaction, economic, convenient, it must be capable of being delivered by injection, efficiently injecting target cells, and expressing the transgene product at a therapeutic level and under tight regulation for the required amount of time.

Viral and non-viral vectors systems have been developed for gene therapy. Non-viral vectors include liposomes, cell-penetrating peptides, polymers, and naked DNA. They involve physical or chemical transfer of genetic material, and are dependent on cellular transport mechanisms for uptake and expression in the host cell. Non-viral vectors are easy to make, accept different sizes of inserted DNA and display fewer immunological and safety problems. The principal drawback is the poor transduction efficiency, transient transgene expression and non-selective cell targeting (*117*, *120*).

Viral vectors are considered appealing delivery vehicles. Several virus families (adeno-, retro-, herpes- and AAV- viruses) have been used as gene transfer vectors for gene therapy. Viral vectors are very efficient, as their transfection efficiency approaches

100%, and can achieve prolonged expression. But, they have several limitations. There are safety concerns about the use of viral vectors, as random integration into host genome might give rise to insertion mutagenesis and they may elicit an immune response. Furthermore, the virus effect is governed by its viral tropism (target specificity), their ability to elicit strong and stable transgene expression is limited and is not possible to produce the vector at high titers (*121*, *122*).

AAV type 2 has shown a great promise for gene therapy as it posses several advantages: Non-pathogenic to humans, does not induce a strong immune response, can transduce both dividing and quiescent cells, viral particle is stable, can be produced at high titers, and has potential for long term expression. Still, there are several limitations that need to be addressed, such as size limitation of AAV capsid, control of the tropism of the vector and neutralization by antibodies (*123*).

AAV is a small, non-enveloped, single-stranded linear DNA parvovirus. The virion is icosahedral in shape and measures 20-25nm in diameter. The capsid contains three proteins, VP1, VP2 and VP3, in a 1:1:10 ratio with a total of 60 proteins per capsid. VP1, VP2 and VP3 differ from each other at their N terminus and have apparent molecular masses of 87, 72 and 62 kDa, respectively (*124*, *125*).

The genome of AAV contains two large open reading frames: the 5’ ORF (rep) encodes the non-structural Rep proteins for viral replication and the 3’ ORF encodes the structural capsid proteins. The Rep proteins are required in all phases of the viral life cycle, including transcription, replication, encapsidation, integration and rescue form the latent state. The capsid proteins are crucial for rescue, replication, packaging, and integration of AAV.

Eleven serotypes have been identified, each having different intrinsic properties. The greatest divergence between them lies in the capsid proteins leading to differences in both tropism and serological neutralization. AAV2 is the most widely used serotype and is the best characterized. AAV2 uses heparin sulfate proteoglycan (HSPG) as a primary receptor for cell attachment and it also utilizes co-receptors to assist its internalization.

The construction of recombinant AAV vectors is based on transient triple transfection protocols of target/producer cells, which requires: a plasmid with the sequence of the rAAV genome (cap and rep genes are deleted and replaced with the desired gene), a plasmid with sequences encoding the two AAV ORFs of rep and cap and a plasmid with the required helper functions encoded by the natural auxiliary virus. All 3 plasmids are co-transfected into permissive cells, and then packaged into rAAV2 virions containing only the therapeutic vector genomes

In the absence of helper virus, AAV infected cells cannot produce any progeny virus and enters a latent state. The AAV genome is integrated into a specific site, referred to as AAVS1, found on the chromosome 19. In rAAV viruses, the viral genes of rep are deleted, so the virus cannot integrate in the AAVS1 locus, which ensures that the treatment is innocuous and there is no risk of insertional mutations. When a latently infected cell encounters superinfection by any of the helper viruses, the integrated AAV genome undergoes productive lytic cycle.

The tropism of the vector can be altered by genetic modification of AAV capsid. It has been shown that several sites within the AAV2 capsid protein are amenable to the insertion of small peptides. But, the genetic insertion of foreign sequences reduces

vector titer or DNA packing efficiency or has other effects on vector biology. Also, some peptide epitopes are inefficiently or inappropriately displayed when engineered into AAV capsid. Therefore, the AAV's viral capsid proteins were chemically and metabolically labeled with biotin and further conjugated to biotin-labeled aptamers via biotin-streptavidin interaction to control the viral tropism.

Materials and Methods

Chemical Conjugation of the Aptamer Capsid

For the generation of chemically biotinylated AAV2-EGFP, 10^{10} particles AAV-EGFP were mock treated or incubated with 5 mg/mL sulfo-NHS-biotin in 50 µL PBS buffer (pH7.4) for 1 hr at room temperature, purified by ultrafiltration and analyzed by Western Blot with AAV antibody B1 (Figure B-1, A) and streptavidin-HRP (Figure B-1, B). After purification, the AAV was incubated with 1/10000 excess streptavidin in 100 µL PBS at room temperature. Excess streptavidin was removed by ultrafiltration using 150 KDa molecular weight cut-off filters. About 10^{12} streptavidin-labeled AAV virions were further conjugated with 1/100 excess biotin-aptamer (Sgc8) in 100 µL PBS for 15 min at room temperature. The final AAV-aptamer complex was purified by ultrafiltration. The aptamer-conjugated AAV was tested for transfection of non-permissive cells as explained below.

Construction of AAV-BAP for biotinylation of AAV in cells

The AAV virus was genetically modified to insert a biotin-acceptor peptide (BAP) sequence in the three capsid proteins. The BAP was biotinylated in cells expressing biotin ligase (encoded by BirA gene from bacteria). The metabolically biotinylated virus was purified by ultrafiltration and analyzed by Western Blot. AAV was further modified with streptavidin and biotin-labeled aptamer as explained above.

Aptamer-Mediated AAV Infection of CEM Cells

Aptamer-AAV2 mediated expression of EGFP in CCRF-CEM suspension cells. About 105 CCRF-CEM cells were transduced with biotinylated AAV2 or aptamer-biotin-streptavidin-biotin-AAV complex at 104 particles/cell. The cells were analyzed for the detection of GFP using fluorescence microscopy. Cells were also labeled with DAPI.

Results

Chemical Conjugation of the Aptamer Capsid

In order to control the viral tropism, the aptamer Sgc8 was conjugated to the AAV viral capsid. The AAV viral capsid proteins were chemically labeled with sulfo-NHS-biotin. The conjugation was confirmed by Western Blot (Figure B-1). The presence of the three AAV capsid proteins was confirmed by Western Blot using the antibody B-1 (Figure B-1 A), while the presence of biotin on the viral capsid was confirmed using streptavidin-HRP (Figure B-1 B). After biotinylation, the AAV was further labeled with streptavidin and biotin-labeled Sgc8.

Construction of AAV-BAP for Biotinylation of AAV in Cells

In order to produce metabolically biotinylated AAV, a biotin-acceptor peptide sequence (BAP) was introduced into the AAV plasmid inside the CAP gene (Figure B-2) and the virus was produced in cells expressing biotin ligase. The biotinylation of the virus was confirmed by Western Blot (Figure B-3).

Aptamer-Mediated AAV Infection of CEM Cells

In order to verify if the viral tropism can be controlled by the conjugation of an aptamer to the AAV capsid proteins, AAV2 was chemically conjugated to the aptamer Sgc8. The AAV contains a GFP-coding gene. Therefore, AAV-transfected cells will express GFP, while non-transfected cells remain GFP negative. The conjugation of the

Sgc8 to the AAV was achieved by chemically biotinylating the AAV capsid using Sulfo-NHS-biotin and further conjugating the AAV to biotin-labeled Sgc8 via streptavidin-biotin interaction. The aptamer-modified aptamer was then tested for the transfection of CEM cells, which express the Sgc8 target, PTK7. Sgc8-modified AAV and unmodified virus were incubated with CEM cells. The unmodified AAV was unable to transfect CEM cells (Figure B-4, Top). On the other hand, aptamer-modified AAV was able to transfect CEM cells (Figure B-4, bottom).

Conjugation of the AAV virus via metabolically introduced biotin was also explored. Metabolically-biotinylated AAV was conjugated to Sgc8 via streptavidin-biotin interaction as explained above. The aptamer-modified aptamer was then tested for the transfection of CEM cells. Sgc8-modified AAV and unmodified virus were incubated with CEM cells. The unmodified AAV was unable to transfect CEM cells (Figure B-5, Top). On the other hand, aptamer-modified AAV was able to transfect CEM cells (Figure B-5, bottom).

Concluding Remarks

AAV tropism could be achieved by the conjugation of the capsid proteins to an aptamer. AAV vectors can be conjugated with cell-specific aptamers through biotin-streptavidin interaction. Biotinylated AAV can be generated in a test tube using chemical reagents, or in culture cells using genetically modified AAV vectors. Once conjugated, the cell-specific aptamers can guide the AAV into target cells for expression of transgenes. This approach offers a proof of principle for development of novel cancer gene therapies. The incorporation of a suicide gene, such as saporin, into the AAV plasmid can lead to the development of a targeted cancer gene therapy. Furthermore, as new aptamers are selected showing selective binding to other disease cells, this approach can be applied for the delivery of therapeutic genes specific for the disease.

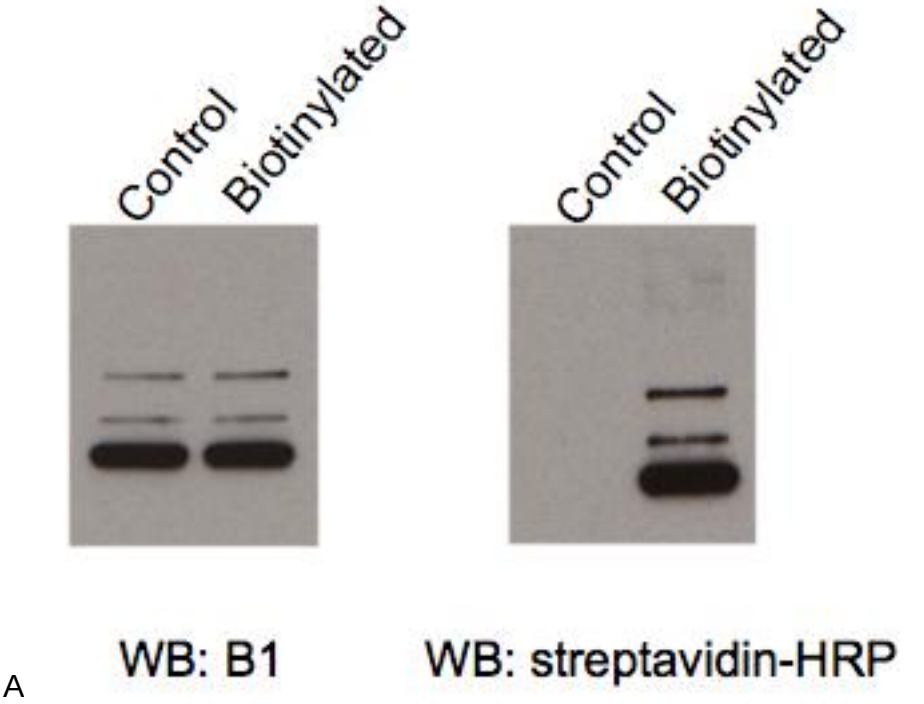

Figure B-1: Chemical biotinylation of the AAV capsid. The chemical reagent sulfo-N-hydroxysuccinimide (NHS)-Biotin (Thermo Fisher Scientific) was used to label AAV serotype 2 with biotin, and confirm biotinylation of AAV particle by Western blot analysis. (A) B1 antibody recognizing all the three capsid proteins of AAV; Control: no sulfo-NHS-Biotin in reaction. (B) Streptavidin-HRP detects the biotinylated AAV capsid.

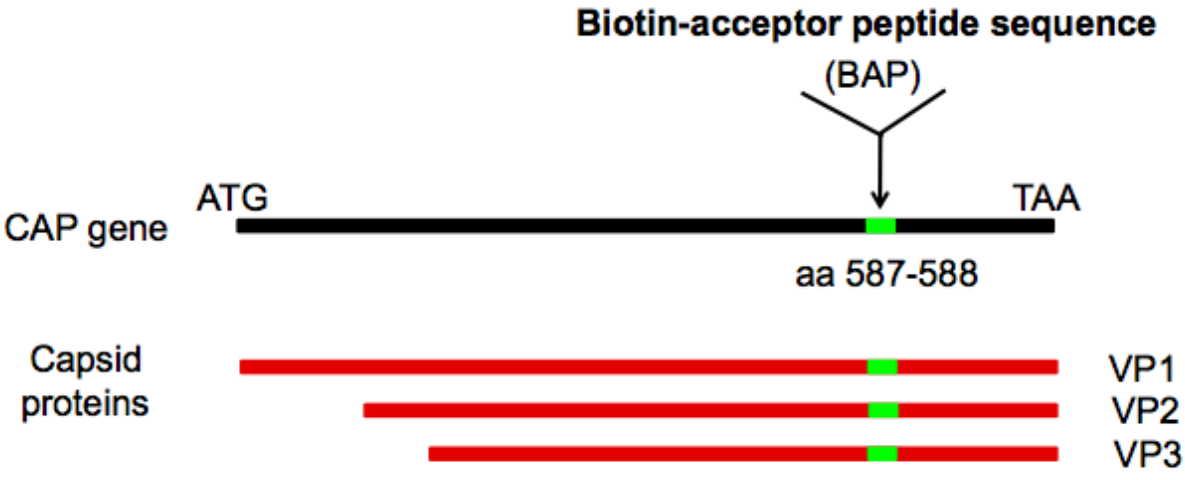

Figure B-2: Construction of AAV-BAP for biotinylation of AAV in cells

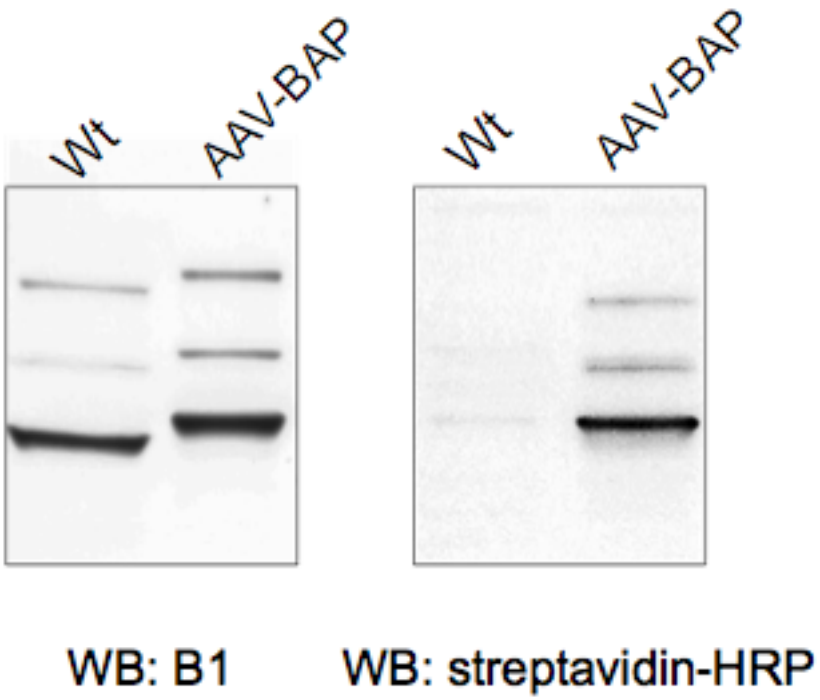

Figure B-3: Metabolic biotinylation of the AAV capsid. Biotinylation of AAV particle was confirmed by Western blot analysis. (A) B1 antibody recognizing all the three capsid proteins of AAV; Control: wild type virus. (B) Streptavidin-HRP detects the biotinylated AAV capsid.

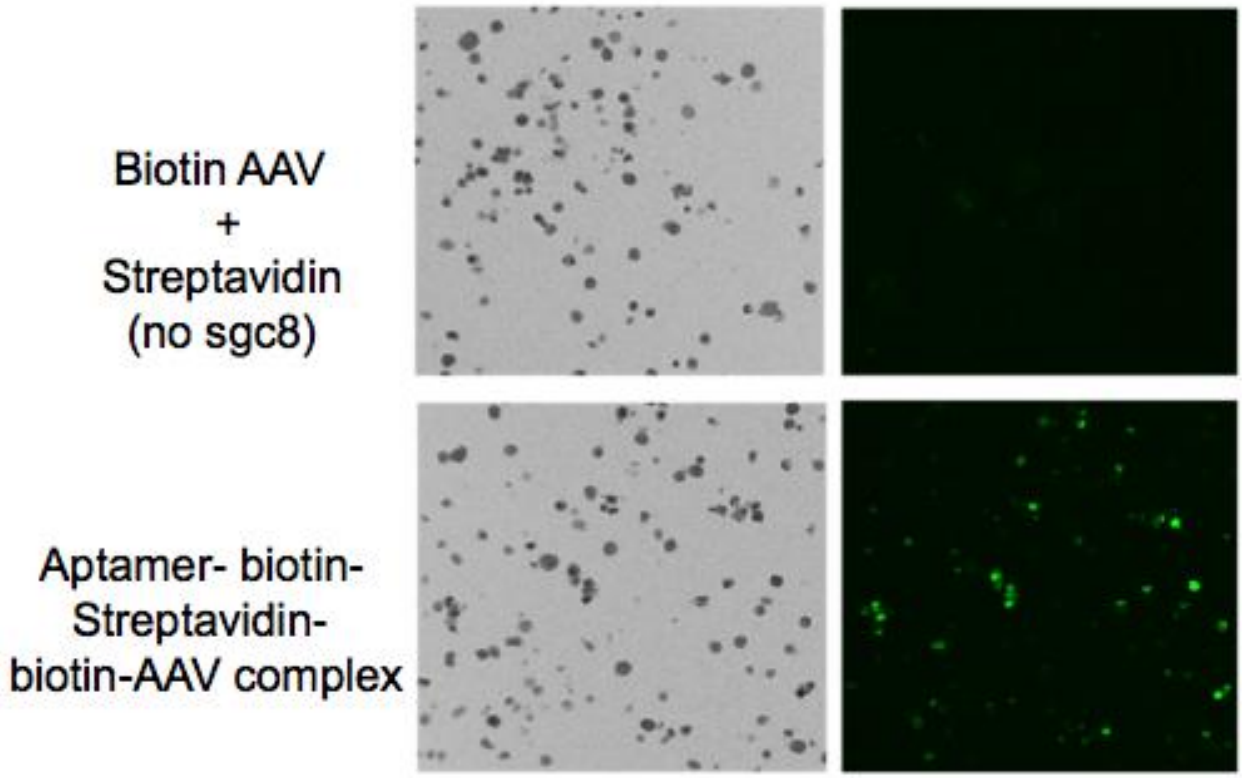

Figure B-4: Transfection of CEM cells using aptamer-labeled AAV. Chemical biotinylation of the AAV capsid proteins.

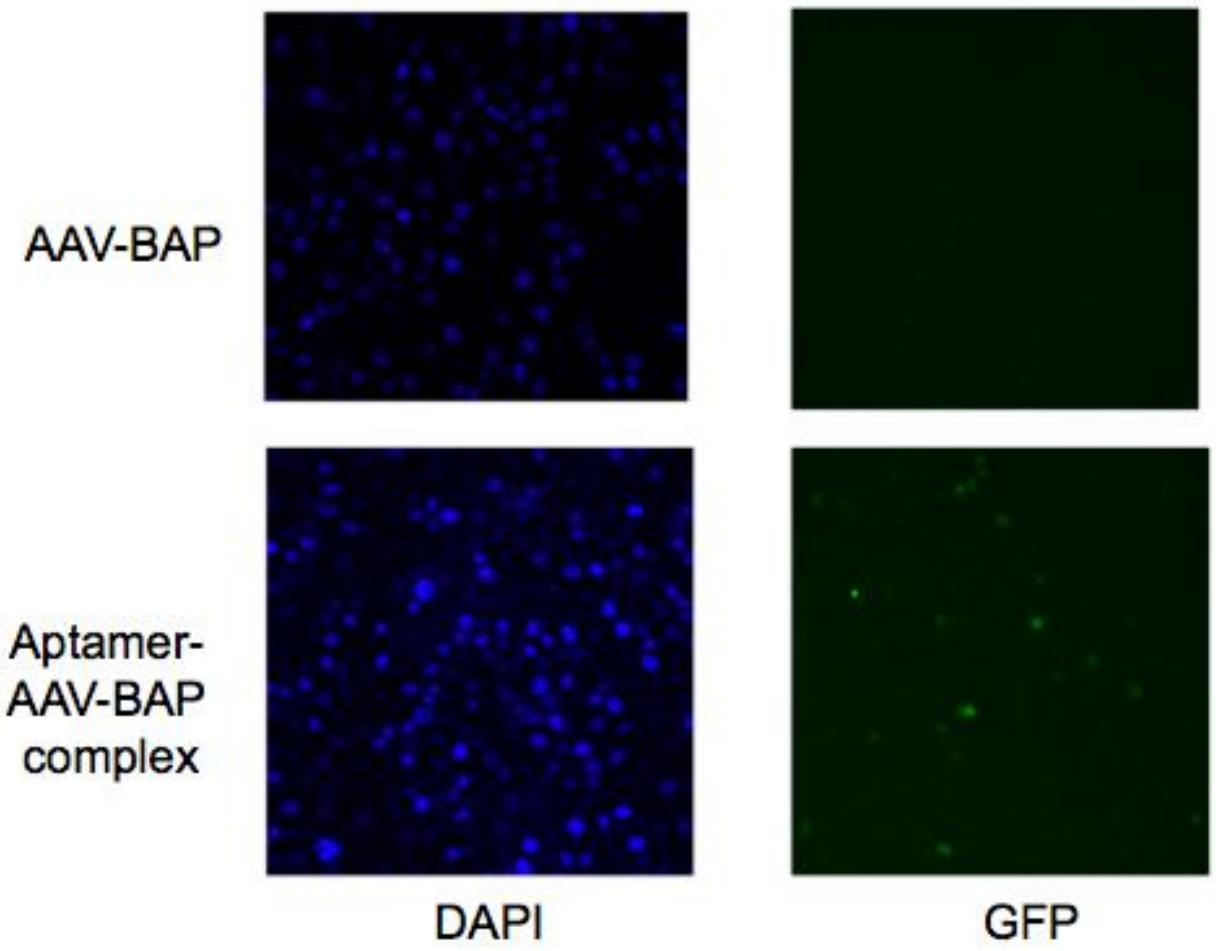

Figure B-5: Transfection of CEM cells using aptamer-labeled AAV. Metabolic biotinylation of the AAV capsid proteins.

LIST OF REFERENCES

1. Williams, T. I., Toups, K. L., Saggese, D. a, Kalli, K. R., Cliby, W. a, and Muddiman, D. C. (2007) Epithelial ovarian cancer: disease etiology, treatment, detection, and investigational gene, metabolite, and protein biomarkers., *Journal of Proteome Research 6*, 2936-62.

2. Zhang, B., Barekati, Z., Kohler, C., Radpour, R., and Asadollahi, R. (2010) Review : Proteomics and Biomarkers for Ovarian Cancer Diagnosis *40*, 218-225.

3. Jemal, A., Siegel, R., Xu, J., and Ward, E. (2010) Cancer Statistics, 2010., *CA: A Cancer Journal for Clinicians*.

4. Colombo, N., Van Gorp, T., Parma, G., Amant, F., Gatta, G., Sessa, C., and Vergote, I. (2006) Ovarian cancer., *Critical Reviews in Oncology/Hematology 60*, 159-79.

5. Hennessy, B. T., Coleman, R. L., and Markman, M. (2009) Ovarian cancer, *The Lancet*, Elsevier Ltd *374*, 1371-1382.

6. Landen, C. N., Birrer, M. J., and Sood, A. K. (2008) Early events in the pathogenesis of epithelial ovarian cancer., *Journal of Clinical Oncology : Official Journal of the American Society of Clinical Oncology 26*, 995-1005.

7. Karst, A. M., and Drapkin, R. (2010) Ovarian cancer pathogenesis: a model in evolution., *Journal of Oncology 2010*, 932371.

8. Husseinzadeh, N. (2010) Status of tumor markers in epithelial ovarian cancer has there been any progress? A review., *GynecologicOoncology*, Elsevier Inc. *120*, 152-157.

9. Moore, R. G., and Maclaughlan, S. (2010) Current clinical use of biomarkers for epithelial ovarian cancer., *Current Opinion in Oncology 22*, 492-7.

10. Karam, A. K., and Karlan, B. Y. (2010) Ovarian cancer: the duplicity of CA125 measurement., *Nature Reviews. Clinical Oncology*, Nature Publishing Group *7*, 335-9.

11. Muller, C. Y. (2010) Doctor, should I get this new ovarian cancer test-OVA1?, *Obstetrics and Gynecology 116*, 246-7.

12. Fung, E. T. (2010) A recipe for proteomics diagnostic test development: the OVA1 test, from biomarker discovery to FDA clearance., *Clinical Chemistry 56*, 327-9.

13. Darcy, K. M., and Birrer, M. J. (2010) Translational research in the Gynecologic Oncology Group: evaluation of ovarian cancer markers, profiles, and novel therapies., *Gynecologic Oncology*, *117*, 429-39.

14. Fleming, J. S., Beaugié, C. R., Haviv, I., Chenevix-Trench, G., and Tan, O. L. (2006) Incessant ovulation, inflammation and epithelial ovarian carcinogenesis: revisiting old hypotheses., *Molecular and Cellular Endocrinology 247*, 4-21.

15. Terry, K. L., Titus-ernstoff, L., Mckolanis, J. R., Welch, W. R., Finn, O. J., and Cramer, D. W. (2007) Incessant Ovulation , Mucin 1 Immunity , and Risk for Ovarian Cancer Ovarian Cancer, *Cancer Research* 30-35.

16. Schorge, J. O., Modesitt, S. C., Coleman, R. L., Cohn, D. E., Kauff, N. D., Duska, L. R., and Herzog, T. J. (2010) SGO White Paper on ovarian cancer: etiology, screening and surveillance., *Gynecologic Oncology*, *119*, 7-17.

17. Chan, J. K., Tian, C., Monk, B. J., Herzog, T., Kapp, D. S., Bell, J., and Young, R. C. (2008) Prognostic factors for high-risk early-stage epithelial ovarian cancer: a Gynecologic Oncology Group study., *Cancer 112*, 2202-10.

18. Pal, T., Permuth-Wey, J., Betts, J. a, Krischer, J. P., Fiorica, J., Arango, H., LaPolla, J., Hoffman, M., Martino, M. a, Wakeley, K., Wilbanks, G., Nicosia, S., Cantor, A., and Sutphen, R. (2005) BRCA1 and BRCA2 mutations account for a large proportion of ovarian carcinoma cases., *Cancer 104*, 2807-16.

19. Lin, C., Sasaki, T., Strumwasser, A., and Harken, A. (2011) The case against BRCA 1 and 2 testing., *Surgery*, Mosby, Inc. *149*, 731-4.

20. Gómez-Raposo, C., Mendiola, M., Barriuso, J., Hardisson, D., and Redondo, a. (2010) Molecular characterization of ovarian cancer by gene-expression profiling., *Gynecologic oncology*, *118*, 88-92.

21. Bell, D. a. (2005) Origins and molecular pathology of ovarian cancer., *Modern pathology : An Official Journal of the United States and Canadian Academy of Pathology,* S19-32.

22. Booth, S. J., Turnbull, L. W., Poole, D. R., and Richmond, I. (2008) The accurate staging of ovarian cancer using 3T magnetic resonance imaging--a realistic option., *BJOG : An International Journal of Obstetrics and Gynecology 115*, 894-901.

23. Malpica, A. (2008) Grading of ovarian cancer: a histotype-specific approach., *International Journal of Gynecological Pathology : Official Journal of the International Society of Gynecological Pathologists 27*, 175-81.

24. Bankhead, C. R., Collins, C., Stokes-Lampard, H., Rose, P., Wilson, S., Clements, a, Mant, D., Kehoe, S. T., and Austoker, J. (2008) Identifying symptoms of ovarian cancer: a qualitative and quantitative study., *BJOG : An International Journal of Obstetrics and Gynecology 115*, 1008-14.

25. Lee, C. J., Ariztia, E. V., and Fishman, D. a. (2007) Conventional and proteomic technologies for the detection of early stage malignancies: markers for ovarian cancer., *Critical Reviews in Clinical Laboratory Sciences 44*, 87-114.

26. Jacobs, I. J., and Menon, U. (2004) Progress and challenges in screening for early detection of ovarian cancer., *Molecular & Cellular Proteomics : MCP 3*, 355-66.

27. Bast, R. C., Jacobs, I., and Berchuck, a. (1992) Malignant transformation of ovarian epithelium., *Journal of the National Cancer Institute 84*, 556-8.

28. Kim, J.-H., Skates, S. J., Uede, T., Wong, K.-kwok, Schorge, J. O., Feltmate, C. M., Berkowitz, R. S., Cramer, D. W., and Mok, S. C. (2002) Osteopontin as a potential diagnostic biomarker for ovarian cancer., *JAMA : the Journal of the American Medical Association 287*, 1671-9.

29. Zhang, L. (2006) Integrative Genomic Analysis of Protein Kinase C (PKC) Family Identifies PKC as a Biomarker and Potential Oncogene in Ovarian Carcinoma, *Cancer Research 66*, 4627-4635.

30. Moore, R. G., MacLaughlan, S., and Bast, R. C. (2010) Current state of biomarker development for clinical application in epithelial ovarian cancer., *Gynecologic Oncology*, *116*, 240-5.

31. Köbel, M., Kalloger, S. E., Boyd, N., McKinney, S., Mehl, E., Palmer, C., Leung, S., Bowen, N. J., Ionescu, D. N., Rajput, A., Prentice, L. M., Miller, D., Santos, J., Swenerton, K., Gilks, C. B., and Huntsman, D. (2008) Ovarian carcinoma subtypes are different diseases: implications for biomarker studies., *PLoS Medicine 5*, e232.

32. Bese, T., Barbaros, M., Baykara, E., Guralp, O., Cengiz, S., Demirkiran, F., Sanioglu, C., and Arvas, M. (2010) Comparison of total plasma lysophosphatidic acid and serum CA-125 as a tumor marker in the diagnosis and follow-up of patients with epithelial ovarian cancer., *Journal of Gynecologic Oncology 21*, 248-54.

33. Baron, A. T., Boardman, C. H., Lafky, J. M., Rademaker, A., Liu, D., Fishman, D. a, Podratz, K. C., and Maihle, N. J. (2005) Soluble epidermal growth factor receptor (sEGFR) [corrected] and cancer antigen 125 (CA125) as screening and diagnostic tests for epithelial ovarian cancer., *Cancer Epidemiology, Biomarkers & Prevention : A Publication of the American Association for Cancer Research, Cosponsored by the American Society of Preventive Oncology 14*, 306-18.

34. Shoji, A., Kuwahara, M., Ozaki, H., and Sawai, H. (2007) Modified DNA aptamer that binds the (R)-isomer of a thalidomide derivative with high enantioselectivity., *Journal of the American Chemical Society 129*, 1456-64.

35. Dey, A. K., Griffiths, C., Lea, S. M., and James, W. (2005) Structural characterization of an anti-gp120 RNA aptamer that neutralizes R5 strains of HIV-1., *RNA 11*, 873-84.

36. Ellington, A. D., and Szostak, J. W. (1992) Selection in vitro of single-stranded DNA molecules that fold into specific ligand-binding structures, *Nature*, *355*, 850–852.

37. Shangguan, D., Cao, Z., Meng, L., Mallikaratchy, P., Sefah, K., Wang, H., Li, Y., and Tan, W. (2008) Cell-Specific Aptamer Probes for Membrane Protein Elucidation in Cancer Cells research articles, *Journal of Proteome Research* 2133-2139.

38. Gopinath, S. C. B., Sakamaki, Y., Kawasaki, K., and Kumar, P. K. R. (2006) An efficient RNA aptamer against human influenza B virus hemagglutinin., *Journal of Biochemistry 139*, 837-46.

39. Townshend, B., Aubry, I., Marcellus, R. C., Gehring, K., and Tremblay, M. L. (2010) An RNA aptamer that selectively inhibits the enzymatic activity of protein tyrosine phosphatase 1B in vitro., *Chembiochem : A European Journal of Chemical Biology 11*, 1583-93.

40. Patel, D. J., Suri, a K., Jiang, F., Jiang, L., Fan, P., Kumar, R. a, and Nonin, S. (1997) Structure, recognition and adaptive binding in RNA aptamer complexes., *Journal of Molecular Biology 272*, 645-64.

41. Wang, K. Y., Krawczyk, S. H., Bischofberger, N., Swaminathan, S., and Boltont, P. H. (1993) The Tertiary Structure of a DNA Aptamer Which Binds to and Inhibits Thrombin Determines Activity, *Biochemistry*. 32, 42, 11285-11292

42. Neves, M. a D., Reinstein, O., Saad, M., and Johnson, P. E. (2010) Defining the secondary structural requirements of a cocaine-binding aptamer by a thermodynamic and mutation study., *Biophysical Chemistry*, *153*, 9-16.

43. Proske, D., Blank, M., Buhmann, R., and Resch, A. (2005) Aptamers--basic research, drug development, and clinical applications., *Applied Microbiology and Biotechnology 69*, 367-74.

44. Hicke, B. J., Stephens, A. W., Gould, T., Chang, Y.-F., Lynott, C. K., Heil, J., Borkowski, S., Hilger, C.-S., Cook, G., Warren, S., and Schmidt, P. G. (2006) Tumor targeting by an aptamer., *Journal of Nuclear Medicine : Official Publication, Society of Nuclear Medicine 47*, 668-78.

45. Chu, T. C., Twu, K. Y., Ellington, A. D., and Levy, M. (2006) Aptamer mediated siRNA delivery., *Nucleic Acids Research 34*, e73.

46. Shangguan, D., Meng, L., Cao, Z. C., Xiao, Z., Fang, X., Li, Y., Cardona, D., Witek, R. P., Liu, C., and Tan, W. (2008) Identification of liver cancer-specific aptamers using whole live cells., *Analytical Chemistry 80*, 721-8.

47. Shangguan, D., Li, Y., Tang, Z., Cao, Z. C., Chen, H. W., Mallikaratchy, P., Sefah, K., Yang, C. J., and Tan, W. (2006) Aptamers evolved from live cells as effective molecular probes for cancer study., *Proceedings of the National Academy of Sciences of the United States of America 103*, 11838-43.

48. Shangguan, D., Tang, Z., Mallikaratchy, P., Xiao, Z., and Tan, W. (2007) Optimization and modifications of aptamers selected from live cancer cell lines., *Chembiochem : A European Journal of Chemical Biology 8*, 603-6.

49. Jeong, Y. Y., Kim, S. H., Jang, S. I., and You, J. C. (2008) Examination of specific binding activity of aptamer RNAs to the HIV-NC by using a cell-based in vivo assay for protein-RNA interaction., *BMB Reports 41*, 511-5.

50. Rusconi, C. P., Roberts, J. D., Pitoc, G. a, Nimjee, S. M., White, R. R., Quick, G., Scardino, E., Fay, W. P., and Sullenger, B. a. (2004) Antidote-mediated control of an anticoagulant aptamer in vivo., *Nature Biotechnology 22*, 1423-8.

51. Sarraf-Yazdi, S., Mi, J., Moeller, B. J., Niu, X., White, R. R., Kontos, C. D., Sullenger, B. a, Dewhirst, M. W., and Clary, B. M. (2008) Inhibition of in vivo tumor angiogenesis and growth via systemic delivery of an angiopoietin 2-specific RNA aptamer., *The Journal of Surgical Research 146*, 16-23.

52. Hoshika, S., Minakawa, N., and Matsuda, A. (2004) Synthesis and physical and physiological properties of 4'-thioRNA: application to post-modification of RNA aptamer toward NF-kappaB., *Nucleic Acids Research 32*, 3815-25.

53. Virno, A., Randazzo, A., Giancola, C., Bucci, M., Cirino, G., and Mayol, L. (2007) A novel thrombin binding aptamer containing a G-LNA residue., *Bioorganic & Medicinal Chemistry 15*, 5710-8.

54. Di Primo, C., Rudloff, I., Reigadas, S., Arzumanov, A. a, Gait, M. J., and Toulmé, J.-J. (2007) Systematic screening of LNA/2'-O-methyl chimeric derivatives of a TAR RNA aptamer., *FEBS Letters 581*, 771-4.

55. Burmeister, P. E., Lewis, S. D., Silva, R. F., Preiss, J. R., Horwitz, L. R., Pendergrast, P. S., McCauley, T. G., Kurz, J. C., Epstein, D. M., Wilson, C., and Keefe, A. D. (2005) Direct in vitro selection of a 2'-O-methyl aptamer to VEGF., *Chemistry & Biology 12*, 25-33.

56. Pestourie, C., Tavitian, B., and Duconge, F. (2005) Aptamers against extracellular targets for in vivo applications., *Biochimie 87*, 921-30.

57. Shamah, S. M., Healy, J. M., and Cload, S. T. (2008) Complex target SELEX., *Accounts of Chemical Research 41*, 130-8.

58. Deissler, H. L., and Lang, G. E. (2008) Effect of VEGF165 and the VEGF aptamer pegaptanib (Macugen) on the protein composition of tight junctions in microvascular endothelial cells of the retina., *Klinische Monatsblätter für Augenheilkunde 225*, 863-7.

59. Lee, J.-H., Jucker, F., and Pardi, A. (2008) Imino proton exchange rates imply an induced-fit binding mechanism for the VEGF165-targeting aptamer, Macugen., *FEBS Letters 582*, 1835-9.

60. Bunka, D. H., Platonova, O., and Stockley, P. G. (2010) Development of aptamer therapeutics., *Current Opinion in Pharmacology*, 1-6.

61. Nicholson, B. P., and Schachat, A. P. (2010) A review of clinical trials of anti-VEGF agents for diabetic retinopathy., *Graefe's Archive for Clinical and Experimental Ophthalmology 248*, 915-30.

62. Trujillo, C. a, Nery, A. a, Alves, J. M., Martins, A. H., and Ulrich, H. (2007) Development of the anti-VEGF aptamer to a therapeutic agent for clinical ophthalmology., *Clinical Ophthalmology 1*, 393-402.

63. Sefah, K., Shangguan, D., Xiong, X., O'Donoghue, M. B., and Tan, W. (2010) Development of DNA aptamers using Cell-SELEX., *Nature Protocols*, *5*, 1169-85.

64. Hermann, T. (2008) Adaptive Recognition by Nucleic Acid, *Science 820*.

65. Macaya, R. F., Schultze, P., Smith, F. W., Roe, J. a, and Feigon, J. (1993) Thrombin-binding DNA aptamer forms a unimolecular quadruplex structure in solution., *Proceedings of the National Academy of Sciences of the United States of America 90*, 3745-9.

66. Bonifacio, L., Church, F. C., and Jarstfer, M. B. (2008) Effect of locked-nucleic acid on a biologically active g-quadruplex. A structure-activity relationship of the thrombin aptamer., *International Journal of Molecular Sciences 9*, 422-33.

67. Xiao, Z., Shangguan, D., Cao, Z., Fang, X., and Tan, W. (2008) Cell-specific internalization study of an aptamer from whole cell selection., *Chemistry 14*, 1769-75.

68. Li, W., Yang, X., Wang, K., Tan, W., He, Y., Guo, Q., Tang, H., and Liu, J. (2008) Real-time imaging of protein internalization using aptamer conjugates., *Analytical Chemistry 80*, 5002-8.

69. Chen, C.-hong B., Dellamaggiore, K. R., Ouellette, C. P., Sedano, C. D., Lizadjohry, M., Chernis, G. a, Gonzales, M., Baltasar, F. E., Fan, A. L., Myerowitz, R., and Neufeld, E. F. (2008) Aptamer-based endocytosis of a lysosomal enzyme., *Proceedings of the National Academy of Sciences of the United States of America 105*, 15908-13.

70. Shangguan, D., Li, Y., Tang, Z., Cao, Z. C., Chen, H. W., Mallikaratchy, P., Sefah, K., Yang, C. J., and Tan, W. (2006) Aptamers evolved from live cells as effective molecular probes for cancer study., *Proceedings of the National Academy of Sciences of the United States of America 103*, 11838-43.

71. Sefah, K., Tang, Z. W., Shangguan, D. H., Chen, H., Lopez-Colon, D., Li, Y., Parekh, P., Martin, J., Meng, L., Phillips, J. a, Kim, Y. M., and Tan, W. H. (2009) Molecular recognition of acute myeloid leukemia using aptamers., *Leukemia : Official Journal of the Leukemia Society of America, Leukemia Research Fund, U.K 23*, 235-44.

72. Tang, Z., Shangguan, D., Wang, K., Shi, H., Sefah, K., Mallikratchy, P., Chen, H. W., Li, Y., and Tan, W. (2007) Selection of aptamers for molecular recognition and characterization of cancer cells., *Analytical Chemistry 79*, 4900-7.

73. Xu, Y., Phillips, J. a, Yan, J., Li, Q., Fan, Z. H., and Tan, W. (2009) Aptamer-based microfluidic device for enrichment, sorting, and detection of multiple cancer cells., *Analytical Chemistry 81*, 7436-42.

74. Shangguan, D., Cao, Z. C., Li, Y., and Tan, W. (2007) Aptamers evolved from cultured cancer cells reveal molecular differences of cancer cells in patient samples, *Clinical Chemistry*, Am Assoc Clin Chem *53*, 1153-1158.

75. Borbas, K. E., Ferreira, C. S. M., Perkins, A., Bruce, J. I., and Missailidis, S. (2007) Design and synthesis of mono- and multimeric targeted radiopharmaceuticals based on novel cyclen ligands coupled to anti-MUC1 aptamers for the diagnostic imaging and targeted radiotherapy of cancer., *Bioconjugate Chemistry 18*, 1205-12.

76. Da, C., Perkins, A. C., and Missailidis, S. (2009) Anti-MUC1 aptamers : radiolabelling with 99m Tc and biodistribution in MCF-7 tumour-bearing mice, *Nuclear Medicine and Biology*, *36*, 703-710.

77. Tong, R., Coyle, V. J., Tang, L., Barger, A. M., Fan, T. M., and Cheng, J. (2010) Polylactide nanoparticles containing stably incorporated cyanine dyes for in vitro and in vivo imaging applications., *Microscopy Research and Technique 909*, 901-909.

78. Farokhzad, O. C., Cheng, J., Teply, B. a, Sherifi, I., Jon, S., Kantoff, P. W., Richie, J. P., and Langer, R. (2006) Targeted nanoparticle-aptamer bioconjugates for cancer chemotherapy in vivo., *Proceedings of the National Academy of Sciences of the United States of America 103*, 6315-20.

79. Shi, H., Tang, Z., Kim, Y., Nie, H., Huang, Y. F., He, X., Deng, K., Wang, K., and Tan, W. (2010) In vivo fluorescence imaging of tumors using molecular aptamers generated by cell-SELEX., *Chemistry, an Asian Journal 5*, 2209-13.

80. Shi, H., He, X., Wang, K., Wu, X., Ye, X., Guo, Q., Tan, W., Qing, Z., Yang, X., and Zhou, B. (2011) Activatable aptamer probe for contrast-enhanced in vivo cancer imaging based on cell membrane protein-triggered conformation alteration., *Proceedings of the National Academy of Sciences of the United States of America 108*, 1-6.

81. Hwang, D. W., Ko, H. Y., Lee, J. H., Kang, H., Ryu, S. H., Song, I. C., Lee, D. S., and Kim, S. (2010) A nucleolin-targeted multimodal nanoparticle imaging probe for tracking cancer cells using an aptamer., *Journal of nuclear medicine : official publication, Society of Nuclear Medicine 51*, 98-105.

82. Van Simaeys, D., López-Colón, D., Sefah, K., Sutphen, R., Jimenez, E., and Tan, W. (2010) Study of the molecular recognition of aptamers selected through ovarian cancer cell-SELEX., *PloS One 5*, e13770.

83. Chen, H. W., Medley, C. D., Sefah, K., Shangguan, D., Tang, Z., Meng, L., Smith, J. E., and Tan, W. (2008) Molecular recognition of small-cell lung cancer cells using aptamers., *ChemMedChem 3*, 991-1001.

84. Zhao, Z., Xu, L., Shi, X., Tan, W., Fang, X., and Shangguan, D. (2009) Recognition of subtype non-small cell lung cancer by DNA aptamers selected from living cells., *The Analyst 134*, 1808-14.

85. Sefah, K., Meng, L., Lopez-Colon, D., Jimenez, E., Liu, C., and Tan, W. (2010) DNA aptamers as molecular probes for colorectal cancer study., *PloS One 5*, e14269.

86. Mallikaratchy, P., Tang, Z., Kwame, S., Meng, L., Shangguan, D., and Tan, W. (2007) Aptamer directly evolved from live cells recognizes membrane bound immunoglobin heavy mu chain in Burkitt's lymphoma cells., *Molecular & Cellular Proteomics : MCP 6*, 2230-8.

87. Mallikaratchy, P. R., Ruggiero, A., Gardner, J. R., Kuryavyi, V., Maguire, W. F., Heaney, M. L., McDevitt, M. R., Patel, D. J., and Scheinberg, D. a. (2010) A multivalent DNA aptamer specific for the B-cell receptor on human lymphoma and leukemia., *Nucleic Acids Research* 1-12.

88. Meng, L., Sefah, K., O'Donoghue, M. B., Zhu, G., Shangguan, D., Noorali, A., Chen, Y., Zhou, L., and Tan, W. (2010) Silencing of PTK7 in colon cancer cells: caspase-10-dependent apoptosis via mitochondrial pathway., *PloS One 5*, e14018.

89. Huang, Y.-fen, Shangguan, D., Liu, H., Phillips, J. A., and Zhang, X. (2009) Molecular Assembly of an Aptamer – Drug Conjugate for Targeted Drug Delivery to Tumor Cells *ChemBioChem* 10, 5, 862 - 868.

90. Smith, J. E., Medley, C. D., Tang, Z., Shangguan, D., Lofton, C., and Tan, W. (2007) Aptamer-conjugated nanoparticles for the collection and detection of multiple cancer cells., *Analytical Chemistry 79*, 3075-82.

91. Zhang, J., Jia, X., Lv, X.-jing, Deng, Y.-lin, and Xie, H.-yan. (2010) Talanta Fluorescent quantum dot-labeled aptamer bioprobes specifically targeting mouse liver cancer cells, *Talanta*, *81*, 505-509.

92. DeWeese, T. L., Ni, X., Zhang, Y., and Lupold, S. (2009) PSMA Aptamer-targeted SiRNAs Selectively Enhance Prostate Cancer Radiation Sensitivity, *International Journal of Radiation Oncology Biology Physics*, *75*, S91-S92.

93. Min, K., Jo, H., Song, K., Cho, M., Chun, Y.-S., Jon, S., Kim, W. J., and Ban, C. (2011) Dual-aptamer-based delivery vehicle of doxorubicin to both PSMA (+) and PSMA (-) prostate cancers., *Biomaterials*, *32*, 2124-32.

94. Min, K., Song, K.-M., Cho, M., Chun, Y.-S., Shim, Y.-B., Ku, J. K., and Ban, C. (2010) Simultaneous electrochemical detection of both PSMA (+) and PSMA (-) prostate cancer cells using an RNA/peptide dual-aptamer probe., *Chemical Communications 46*, 5566-8.

95. Dassie, J. P., Liu, X.-Y., Thomas, G. S., Whitaker, R. M., Thiel, K. W., Stockdale, K. R., Meyerholz, D. K., McCaffrey, A. P., McNamara, J. O., and Giangrande, P. H. (2009) Systemic administration of optimized aptamer-siRNA chimeras promotes regression of PSMA-expressing tumors., *Nature Biotechnology 27*, 839-49.

96. Kim, D., Jeong, Y. Y., and Jon, S. (2010) A drug-loaded aptamer-gold nanoparticle bioconjugate for combined CT imaging and therapy of prostate cancer., *ACS Nano 4*, 3689-96.

97. Chu, T. C., Marks, J. W., Lavery, L. a, Faulkner, S., Rosenblum, M. G., Ellington, A. D., and Levy, M. (2006) Aptamer:toxin conjugates that specifically target prostate tumor cells., *Cancer Research 66*, 5989-92.

98. Tang, Z., Parekh, P., Turner, P., Moyer, R. W., and Tan, W. (2009) Generating aptamers for recognition of virus-infected cells., *Clinical Chemistry 55*, 813-22.

99. Brown, M., and Wittwer, C. (2000) Flow cytometry: principles and clinical applications in hematology., *Clinical Chemistry 46*, 1221-9.

100. Wicker, T., Schlagenhauf, E., Graner, A., Close, T. J., Keller, B., and Stein, N. (2006) 454 Sequencing Put To the Test Using the Complex Genome of Barley., *BMC Genomics 7*, 275.

101. Fan, T., Zhao, Q., Chen, J. J., Chen, W.-T., and Pearl, M. L. (2009) Clinical significance of circulating tumor cells detected by an invasion assay in peripheral blood of patients with ovarian cancer., *Gynecologic Oncology*, *112*, 185-91.

102. Molloy, T. J., Devriese, L. a, Helgason, H. H., Bosma, a J., Hauptmann, M., Voest, E. E., Schellens, J. H. M., and Van't Veer, L. J. (2011) A multimarker QPCR-based platform for the detection of circulating tumour cells in patients with early-stage breast cancer., *British Journal of Cancer* 1 - 7.

103. Martin, J. a, Phillips, J. a, Parekh, P., Sefah, K., and Tan, W. (2011) Capturing cancer cells using aptamer-immobilized square capillary channels, *Molecular BioSystems*.

104. Shen, S., Bryant, K. D., Brown, S. M., Randell, S. H., and Asokan, A. (2011) Terminal N-linked galactose is the primary receptor for adeno-associated virus ., *The Journal of Biological Chemistry*.

105. Parekh, P., Tang, Z., Turner, P., and Moyer, R. (2010) Aptamers Recognizing Glycosylated Hemagglutinin Expressed on the Surface of Vaccinia Virus-Infected Cells, *Analytical 82*, 8790-8797.

106. Chang, P. V., Prescher, J. a, Sletten, E. M., Baskin, J. M., Miller, I. a, Agard, N. J., Lo, A., and Bertozzi, C. R. (2010) Copper-free click chemistry in living animals., *Proceedings of the National Academy of Sciences of the United States of America 107*, 1821-6.

107. Agnew, H. D., Rohde, R. D., Millward, S. W., Nag, A., Yeo, W.-S., Hein, J. E., Pitram, S. M., Tariq, A. A., Burns, V. M., Krom, R. J., Fokin, V. V., Sharpless, K. B., and Heath, J. R. (2009) Iterative in situ click chemistry creates antibody-like protein-capture agents., *Angewandte Chemie 48*, 4944-8.

108. Markoullis, K., Bulian, D., Hölzlwimmer, G., Quintanilla-Martinez, L., Heiliger, K.-J., Zitzelsberger, H., Scherb, H., Mysliwietz, J., Uphoff, C. C., Drexler, H. G., Adler, T., Busch, D. H., Schmidt, J., and Mahabir, E. (2009) Mycoplasma contamination of murine embryonic stem cells affects cell parameters, germline transmission and chimeric progeny., *Transgenic Research 18*, 71-87.

109. Kumar, A., and Yerneni, L. K. (2009) Semi-automated relative quantification of cell culture contamination with mycoplasma by Photoshop-based image analysis on immunofluorescence preparations., *Biologicals : Journal of the International Association of Biological Standardization*, *37*, 55-60.

110. Young, L., Sung, J., Stacey, G., and Masters, J. R. (2010) Detection of Mycoplasma in cell cultures., *Nature Protocols 5*, 929-34.

111. Chung, T. S., and Kim, J. H. (2005) Detection of Mycoplasma Infection in Cultured Cells on the Basis of Molecular Profiling of Host Responses, *Genomics 3*, 63-67.

112. Logunov, D. Y., Scheblyakov, D. V., Zubkova, O. V., Shmarov, M. M., Rakovskaya, I. V., Gurova, K. V., Tararova, N. D., Burdelya, L. G., Naroditsky, B. S., Ginzburg, a L., and Gudkov, a V. (2008) Mycoplasma infection suppresses p53, activates NF-kappaB and cooperates with oncogenic Ras in rodent fibroblast transformation., *Oncogene 27*, 4521-31.

113. Mariotti, E., Mirabelli, P., Di Noto, R., Fortunato, G., and Salvatore, F. (2008) Rapid detection of mycoplasma in continuous cell lines using a selective biochemical test., *Leukemia Research 32*, 323-6.

114. Kumar, A., Ali, A., and Yerneni, L. K. (2008) Tandem use of immunofluorescent and DNA staining assays to validate nested PCR detection of mycoplasma., *In Vitro Cellular & Developmental Biology. Animal 44*, 189-92.

115. Kong, H., Volokhov, D. V., George, J., Ikonomi, P., Chandler, D., Anderson, C., and Chizhikov, V. (2007) Application of cell culture enrichment for improving the sensitivity of mycoplasma detection methods based on nucleic acid amplification technology (NAT)., *Applied Microbiology and Biotechnology 77*, 223-32.

116. Li, W., Wang, K., Tan, W., Ma, C., and Yang, X. (2007) Aptamer-based analysis of angiogenin by fluorescence anisotropy., *The Analyst 132*, 107-13.

117. Uddin, S. N. (2007) Cationic lipids used in non-viral gene delivery systems, *Molecular Biology 2*, 058-067.

118. Sato, Y., Yamauchi, N., Takahashi, M., Sasaki, K., Fukaura, J., Neda, H., Fujii, S., Hirayama, M., Itoh, Y., Koshita, Y., Kogawa, K., Kato, J., Sakamaki, S., and Niitsu, Y. (2000) In vivo gene delivery to tumor cells by transferrin-streptavidin-DNA conjugate., *The FASEB Journal : Official Publication of the Federation of American Societies for Experimental Biology 14*, 2108-18.

119. Jeong, S., Lee, H. K., and Kim, M. Y. (2009) Gene Therapy of Cancer, *Gene Therapy 542*, 363-377.

120. Bloquel, C., Bourges, J. L., Touchard, E., Berdugo, M., BenEzra, D., and Behar-Cohen, F. (2006) Non-viral ocular gene therapy: potential ocular therapeutic avenues., *Advanced Drug Delivery Reviews 58*, 1224-42.

121. Perabo, L. (2003) In vitro selection of viral vectors with modified tropism: the adeno-associated virus display, *Molecular Therapy 8*, 151-157.

122. Perabo, L., Endell, J., King, S., Lux, K., Goldnau, D., Hallek, M., and Büning, H. (2006) Combinatorial engineering of a gene therapy vector: directed evolution of adeno-associated virus., *The Journal of Gene Medicine 8*, 155-62.

123. Choi, V. W., McCarty, D. M., and Samulski, R. J. (2005) AAV hybrid serotypes: improved vectors for gene delivery., *Current Gene Therapy 5*, 299-310.

124. Xie, Q., Bu, W., Bhatia, S., Hare, J., Somasundaram, T., Azzi, A., and Chapman, M. S. (2002) The atomic structure of adeno-associated virus (AAV-2), a vector for human gene therapy., *Proceedings of the National Academy of Sciences of the United States of America 99*, 10405-10.

125. Arnold, G. S., Sasser, a K., Stachler, M. D., and Bartlett, J. S. (2006) Metabolic biotinylation provides a unique platform for the purification and targeting of multiple AAV vector serotypes., *Molecular Therapy : the Journal of the American Society of Gene Therapy 14*, 97-106.

BIOGRAPHICAL SKETCH

Dalia López-Colón was born in San Juan Puerto Rico. She obtained her bachelor's degree in science (2005) in industrial chemistry from the University of Puerto Rico, Humacao campus. During her undergraduate studies, Dalia performed research on the synergistic effect of ultrasound and antitumor quinones for four years under the supervision of Dr. Antonio E. Alegría. Furthermore, she participated in the University of Florida's Research Experience for Undergraduates (REU) program in 2003, when she worked in Charles Martin's lab on the development of protein nanotubes using gold-coated silica membranes as templates. The following year, she participated in the REU study abroad program at the Université Louis Pasteur, where she worked with Dr. Laurence Sabatier to study of *Drosophila mellanogaster*'s immune response. She joined the University of Florida in 2005 and received her Ph.D. in Biochemistry in 2011 under the tutorage of Dr. Weihong Tan.